



University of Kentucky
UKnowledge

University of Kentucky Master's Theses

Graduate School

2005

EXERGY BASED METHOD FOR SUSTAINABLE ENERGY UTILIZATION ANALYSIS OF A NET SHAPE MANUFACTURING SYSTEM

JAYASANKAR SANKARA

University of Kentucky, sankara@uky.edu

[Right click to open a feedback form in a new tab to let us know how this document benefits you.](#)

Recommended Citation

SANKARA, JAYASANKAR, "EXERGY BASED METHOD FOR SUSTAINABLE ENERGY UTILIZATION ANALYSIS OF A NET SHAPE MANUFACTURING SYSTEM" (2005). *University of Kentucky Master's Theses*. 351.

https://uknowledge.uky.edu/gradschool_theses/351

This Thesis is brought to you for free and open access by the Graduate School at UKnowledge. It has been accepted for inclusion in University of Kentucky Master's Theses by an authorized administrator of UKnowledge. For more information, please contact UKnowledge@lsv.uky.edu.

ABSTRACT OF THESIS

EXERGY BASED METHOD FOR SUSTAINABLE ENERGY UTILIZATION ANALYSIS OF A NET SHAPE MANUFACTURING SYSTEM

The approach advocated in this work implements energy/exergy analysis and indirectly an irreversibility evaluation to a continuous manufacturing process involving discrete net shape production of compact heat exchangers through a complex controlled atmosphere brazing (CAB) process. The system under consideration involves fifteen cells of a continuous ramp-up heating, melting, reactive flow, isothermal dwell, and rapid quench solidification processing sequence during a controlled atmosphere brazing of aluminum compact heat exchangers. Detailed mass, energy, and exergy balances were performed. The irreversibility sources were identified and the quality of energy utilization at different processing steps determined.

It is demonstrated that advanced thermodynamics metrics based on entropy generation may indicate the level of sustainable energy utilization of transient open systems, such as in manufacturing. This indicator may be related to particular property uniformity during materials processing. In such a case, the property uniformity would indicate systems' distance from equilibrium, i.e., from the process sustainable energy utilization level. This idea is applied to net shape manufacturing process considered. A metric based on exergy destruction is devised to relate the heat exchanger temperature uniformity and the quality. The idea advocated in this thesis will represent the coherent framework for developing energy efficient, economically affordable and environmentally friendly manufacturing technology.

KEYWORDS: Materials Processing-Controlled Atmospheric Brazing, Sustainable Manufacturing, Thermodynamics Metrics, Energy-Exergy Analysis.

JAYASANKAR SANKARA
December 1st, 2005

**EXERGY BASED METHOD FOR SUSTAINABLE ENERGY
UTILIZATION ANALYSIS OF A NET SHAPE MANUFACTURING
SYSTEM**

By

Jayasankar Sankara

Dr. Dusan P. Sekulic

(Director of Thesis)

Dr. George Huang

(Director of Graduate Studies)

Date: December 1st, 2005

RULES FOR THE USE OF THESES

Unpublished theses submitted for the Master's degree and deposited in the University of Kentucky Library are a rule open for inspection, but are to be used only with due regard to the rights of the authors. Bibliographical references may be noted, but quotations or summaries of parts may be published only with the permission of the author, and with the usual scholarly acknowledgements.

Extensive copying or publication of the theses in whole or in part also requires the consent of the Dean of the Graduate School of the University of Kentucky.

THESIS

Jayasankar Sankara

**The Graduate School
University of Kentucky**

2005

**EXERGY BASED METHOD FOR SUSTAINABLE ENERGY
UTILIZATION ANALYSIS OF A NET SHAPE MANUFACTURING
SYSTEM**

THESIS

A thesis submitted in partial fulfillment of the requirements for the degree of Master of Science in Mechanical Engineering from the College of Engineering at the University of Kentucky

By

Jayasankar Sankara

Lexington, Kentucky

**Director: Dr. D.P. Sekulic, Professor
Center for Manufacturing, Department of Mechanical Engineering
Lexington, Kentucky**

2005

MASTER'S THESIS RELEASE

I authorize the University of Kentucky
libraries to reproduce this thesis in whole or in part for purposes of research.

Signed: Jayasankar Sankara

Date: December 1st, 2005

Dedicated To My Parents

(Mrs. Achutamba and Dr. Tulasiram Sankara)

ACKNOWLEDGEMENTS

This thesis work is the fruit of guidance and inspiration, by several individuals. First and foremost, I would like to thank my thesis director and advisor Dr. Dusan P. Sekulic, an epitome of perfection, for providing me the opportunity and mentoring relentlessly throughout my course of study. I have been extremely humbled by his intellect and motivated by his encouragement and I am thankful that he was a major influence in my Masters' experience. This research work was supported by Kentucky Science and Engineering Foundation through the grant KSEF-395-RDE-003 and 005. I would like to acknowledge the Research Assistantship obtained from the University of Kentucky, Center for Manufacturing.

I would then like to extend my thankfulness to Dr. I. S. Jawahir, for his encouragement and insights on sustainability engineering, and also for agreeing to be on my advisory committee. I would also like to thank Dr. K. Saito, for agreeing to be on my advisory committee. I would like to thank my D.G.S, Dr. Huang, for giving me an opportunity to pursue my Master's at University of Kentucky. I express my gratitude to Mr. M. Irish and Mr. J. Rosen for providing relevant data about industrial CAB systems. I acknowledge the assistance of Mr. F. Bryan who was responsible for data collection in the early stages of the study. I also acknowledge the help of my research team, friends and roommates whose support has made my life in US comfortable and also helped me in achieving my tasks with ease. Ms. R. Itharaju and Mr. N.V. Thuramalla helped me in writing the thesis.

Above all, I would like to thank my parents Dr. Tulasiram and Mrs. Achutamba Sankara for their unconditional support and making me believe that I could reach the pinnacle of success. I am ever indebted for their motivation and encouragement, which made every hurdle surmountable and every task achievable. I dedicate each and every achievement to them and consider myself blessed to have such a family.

Jayasankar Sankara

Table of Contents

ACKNOWLEDGEMENTS	iii
List of Figures.....	vi
List of Tables.....	ix
Nomenclature.....	x
List of files.....	xiv
Chapter 1 INTRODUCTION.....	1
1.1 Environmentally benign manufacturing	1
1.2 Controlled Atmospheric Brazing (CAB)	3
1.3 Problem definition and significance	6
1.4 Research objectives.....	11
1.5 Thesis layout	14
Chapter 2 LITERATURE REVIEW	16
2.1 Present state of knowledge in the field	16
2.2 Exergy and sustainable development.....	18
2.3 General idea of the exergy analysis	20
2.4 Summary	23
Chapter 3 NET-SHAPE MANUFACTURING SYSTEM.....	24
3.1 System description	24
3.2 Sequence of phenomena during CAB.....	28
3.3 Time-temperature history of the materials processing.....	30
3.4 System integration	33
3.5 Generalized system cell	37
Chapter 4 ENERGY-EXERGY BALANCE	40
4.1 Mass balance-flow rate calculation.....	41
4.2 Energy balance.....	43
4.3 Exergy analysis.....	51
4.4 Energy utilization for the net shape effect	59
Chapter 5 SUSTAINABILITY METRICS AND IRREVERSIBILITY MODELS	61
5.1 Quality of energy utilization at different processing stages.....	61

5.2 Sources of irreversibility.....	64
5.3 Sustainability metrics and irreversibilities.....	65
5.4 Temperature - entropy plots.....	70
5.5 Non-uniform temperature, product quality and sustainability metric.....	74
5.5.1 Temperature non-uniformity across the heat exchanger core.....	74
5.5.2 Prolegomena for a sustainability metric, uniform core temperature and product quality	79
Chapter 6 CONCLUSIONS AND FUTURE WORK.....	83
6.1 Conclusions.....	83
6.2 Future work.....	85
References.....	87
Appendix A System integration.....	93
Appendix B Reduced temperature, temperature and mass flow rate calculations.....	94
Appendix C Enthalpy and energy balance calculation	96
Appendix D Entropy and exergy balance calculation.....	99
Appendix E Derivation of entropy generation equation.....	103
Appendix F Entropy generation calculation	106
VITA.....	113

List of Figures

Figure 1-1	Braze sheet configuration and typical braze joint.....	4
Figure 1-2	Typical system configuration.....	5
Figure 1-3	A sequence of operations during CAB manufacturing [9]	6
Figure 1-4	Furnace hot zone settings (presented as liner segments at different temperature levels) vs. temperature profiles of a heat exchanger.....	7
Figure 1-5	A complex joint assembly manufactured by a CAB process [8].....	8
Figure 1-6	An exergy flow along the manufacturing process materials flow line	13
Figure 2-1	The interdisciplinary triangle of exergy [37].....	19
Figure 2-2	Qualitative illustration of the relations between the environmental impact and sustainability of a process, and its exergy efficiency [38].....	20
Figure 2-3	Model of the system exergy analysis. [55]	22
Figure 3-1	CAB system under Consideration.....	25
Figure 3-2	Heat exchanger core with braze tray and fixtures.....	26
Figure 3-3	A typical ramp-up/dwell/quench temperature history of a CAB brazing process [59].....	29
Figure 3-3	Temperature history of a heat exchanger core during processing [27].....	30
Figure 3-4	Water quench in Cells 11, 12 and 13	32
Figure 3-5	Air blast in Cell 15.....	33
Figure 3-6	A generalized system cell [60].....	38
Figure 4-1	Mass inflows and outflows for a generic cell	41
Figure 4-2	Energy (Sankey) flow diagram for a CAB system [27].....	50
Figure 4-3	Exergy (Grassman) flow diagram for a CAB system [27]	58
Figure 4-4	A heat exchanger design. Compact heat exchanger – flat webbed tube and multilouver fin automotive condenser [57].....	60

Figure 5-1	The First & Second Law of Thermodynamics efficiencies of energy utilization within the continuous CAB razing furnace (Processing stages, 2 through 10, indicate the heating cells).....	63
Figure 5-2	A symbolic representation of a simplified model of materials processing. Two particular cases correspond to lumped and to spatially distributed heating accomplished through two heating strategies, with either single or multiple heating stages (in time). (a) lumped transient heating with constant heating source temperature throughout (at any instant of time material has uniform but different temperature), (b) the same as (a) but the heating accomplished by using a series of heaters, each at a different, increasing temperature, (c) Spatially distributed heating with constant heat source, (d) the same as (c) but with a series of heaters, each at a different, increasing temperature [28]......	69
Figure 5-3	Various temperature distributions. Case (a) corresponds to the pair: Constant $T_m = T_s$ and Constant T_{hr} ; Case (c) Variable T_m and Constant T_{hr} ; (d) Variable T_m and variable T_{hr} . For the sake of comparison, the actual material temperature distribution, if the material were exposed to the same variable heater distribution as for (d), is included as well. [28]	71
Figure 5-4	Entropy generation for theoretical model [ideal (lumped) case, and spatially distributed cases (constant and variable heating sources)], and experimental data [28].....	73
Figure 5-5	Cross sectional view of brazing furnace muffle	75
Figure 5-6	Thermocouple locations on traversing Heat exchanger core.....	75
Figure 5-7	Temperature Non-Uniformity measured by thermocouples at points across the 2 nd diagonal @ peak brazing temperature 875K.....	76
Figure 5-8	Temperature Non-Uniformity measured by thermocouples at points across the 2 nd diagonal @ peak brazing temperature 875K.....	77
Figure 5-9	Temperature differences history across different locations on the processed material.....	78

Figure 5-10 Temperature difference between Heater (T_s) and processed material (T_{core}).
Zones 2-8, indicate the heating stages of the process of the furnace79

Figure 5-11 Exergy inefficiency of the different processing stages.81

Figure 5-12 Temperature differences history across the processed material. The difference
measured across the top surface diagonal of a heat exchanger unit during
processing in a continuous controlled atmosphere-brazing furnace [28].82

List of Tables

Table 3.1	Temperature set-points of furnace	32
Table 3.2	Input process parameters.....	36
Table 4.1	Formulae for calculating interaction rates.	42
Table 4.2	Values of coefficients in Eq 4.2 from NIST database[63].....	44
Table 4.3	Values of coefficients in Eq(4.9) from NIST database[63]	53
Table 4.4	A heat exchanger mass distribution [27]	59
Table 5.1	First and Second Law efficiency.....	62
Table 5.2	Temperature differences between source and core effecting energy utilization quality.....	70
Table 5.3	Total entropy generated for material processing models B1 and B2.....	73
Table 5.4	Exergy inefficiency of the different processing stages.....	80

Nomenclature

a) Symbol

$A, B, \dots H$	Coefficients in eqs. (2) and (9)
A	Total cross sectional area of the core, [m ²]
Bi	Biot number, [dimensionless]
h_{eff}	Heat transfer coefficient (with radiative effect), [W/m ² .K]
c_p	Specific heat of the materials [J/kg K]
C_1	Coefficient in the one-term approximation to the series of solutions for transient 1D conduction, [dimensionless]
d	Diameter of airflow ducts in/out, [m]
dt	Change in time, [sec]
DT	Change in temperature, [K]
D	Distance between the cores, [m]
Fo	Fourier number, [dimensionless]
$\dot{E}x_i$	Exergy flow rate, [kJ/sec]
$\dot{E}x_D$	Exergy loss rate, [kJ/sec]
$\dot{E}x_{RH,i}^{in}$	Heater draw, [W]
Δh_f	Specific enthalpy of phase change, [kJ/kg]
\bar{h}	Specific enthalpy of the products, [kJ/kg]
\dot{H}_i	Enthalpy rate, [kJ/sec]
k_o	Thermal conductivity of aluminum alloy, [W/m.K]

k_l	Thermal conductivity of air, [W/m.K]
$k = k_{\text{eff}}$	Effective thermal conductivity of the porous core, [W/m.K]
L	Core length in the direction of flow, [m]
\dot{m}	Mass flow rate of bulk materials passing through the system, [kg/sec]
m	Mass of bulk materials passing through the system, [kg]
\dot{Q}_k	Heat transfer rate (absolute value), [kJ/sec]
s	Specific entropy, [kJ/kg K]
S	Entropy, [kJ/ K]
t	Reduced temperature = $T(\text{K})/1000$ -{Eq.'s (4.2) & (4.9)}, [K] and Time to heating to peak brazing temperature- {Eq.'s (5.3)- (5.12)}, [sec]
T	Inlet/outlet temperature of the bulk flows, [K]
T_o	Mid-plane temperature of the brazed object, [K]
L_c	Characteristic length of the brazed object, [m]
u_1	Speed of conveyer 1, [m/s]
u_2	Speed of conveyer 2, [m/s]
$\dot{V}_{N_2,i}^{\text{out}}$	Volumetric flow rate of the bulk flows at the inlet/outlet, [m ³ /s]
V	Volume of the core, [m ³]
W	Belt (conveyer) effective width, [m]
\dot{W}_j	Work flow rate (absolute value), [kJ/sec]
$\dot{W}_{\text{AUX},i}^{\text{in}}$	Auxiliary power, [W]

x^*	Dimensionless spatial coordinate ($\equiv \frac{x}{L}$)
α	Thermal diffusivity, [m^2/s]
Δ	Residue (heat losses, imbalance, error in calculation)
ξ	Liquid fraction of clad of a brazing sheet material, Eq. (1.1), [dimensionless]
ξ'	Percent of heater draw, [%]
ε^*	Energy utilization for the net shape effect, defined by Eq (1.1) & (4.13)
ε	First law efficiency, defined by Eq. (5.1), [dimensionless]
η	Second law efficiency, defined by Eq. (5.2), [dimensionless]
ν_{Ex}	Exergy Inefficiency Eq. (5.12), [dimensionless]
$\rho_{L,CON}^{in}$	Belt (conveyer) area mass (L) density, [Kg/m^2]
$\rho_{N_2,i}^{in}$	Mass density of N_2 gas at inlet, [Kg/m^3]
ζ_1	Coefficient in the one-term approximation to the series of solutions for transient 1D conduction, [dimensionless]
τ_t	Thermal time constant, [dimensionless]
ε	Emissivity, [dimensionless]
σ	Boltzman constant, [$\text{W}/\text{m}^2\text{K}^4$]
Φ	Volume fraction of the porous structure, [dimensionless]
$\Delta, \dots, 0$	Thermocouple locations, [dimensionless]

b) Superscript:

In State point at the inlet of system/ sub-system.

Out State point at the outlet of system/sub-system.

C) Subscript:

<i>AUX</i>	Auxiliary power
<i>RH</i>	Heater draw
<i>o</i>	Reference state
$\infty/Surr$	Surroundings
<i>s/htr</i>	Source/Heater
<i>eff</i>	Effective
<i>gen</i>	Generation
<i>i,j</i>	Processing segments (i,j=1 to15)
<i>initial/1</i>	Initial state point
<i>final/2</i>	Final state point
<i>Clad</i>	Clad material of the brazing sheet/object
<i>Core/HEX</i>	Core material of the sheet/object
<i>Expt</i>	Experimental
<i>Fixt</i>	Fixture holding the braze material
<i>Flx</i>	Flux for braze joint formation
<i>Con1</i>	Conveyor 1, circulating the heating zones , water cool and exit
<i>Con2</i>	Conveyor 2, circulating the airblast
<i>N₂</i>	Nitrogen (atmosphere)
<i>H₂O</i>	Water (quench)

List of files

1. SANKARA.pdf
2. Energy-Exergy Balance.xls
3. Entropy Generation.xls

Chapter 1 INTRODUCTION

1.1 Environmentally benign manufacturing

Environmentally conscious design and manufacturing approaches are gaining increasing importance for sustainable development and industrial ecology. Environmentally benign manufacturing enables economic progress while minimizing pollution, waste and conserving resources. It protects the environment for next generations. It has become a paramount concern for engineers, economists and policy makers to incorporate the sustainability metrics in the design and development of new and existing processes/systems. Clean production is necessary, that is, the effective use of resources, and the preservation of the ecological environment must be taken into consideration during the whole production process from the designing stage onwards. Product characteristics like functionality, performance, cost, time to market and design/manufacturing aspects of the product for its functional life are typical aspects of consideration for traditional manufacturing methods and product design. Sustainability consideration is not a major decisive factor. *Product design and manufacture in the 21st century will require greater knowledge and integration of life cycle, sustainable product/process designs and their implementation in the manufacture of engineered products* [1]. A change from traditional approaches to include sustainability concerns including life-cycle considerations in the design and manufacturing practices for next-generation products is warranted. Optimized methodologies like environmentally conscious, energy-efficient, hazard-free, lean manufacturing methods involving human interfaces with product maintenance, disassembly, recycling and re-manufacturing should be incorporated in the modus operandi of current and future product design and manufacturing methods [2].

Energy plays a central role in the development of world and is a major challenge for sustainable development. Fossil fuels bare 80% of the primary energy consumption today and this share is like to remain high in the future [3]. Consumption of resources, including the utilization of energy and present environmental problem are directly linked with each

other and will be so in the future. Energy & material efficiency and the integration of the renewable resources will therefore have to play a major role for sustainable development [56]. Energy is the lifeblood of manufacturing. Industry converts fuels to thermal, electric or motive energy to manufacture all the products of daily life. American industry's energy demand is one-third of total U.S. energy consumption [4]. Energy allows manufacturers to transform raw materials into final consumer goods. Raw materials pass through a number of intermediate stages, with these intermediates representing the bulk of industrial energy consumption. In economic sense energy performs work that adds value to intermediate products as they are progressively transformed into final consumer goods [5]. The opportunities to improve energy efficiency at each step of a manufacturing process must be explored. The price of final product absorbs the wastage of energy at each layer of the whole process. Any waste of energy at different steps of manufacture, disguised in the cost of inputs, eats up profit margins and in effect is 'taxed' on the consumers at the end.

A variety of materials processing in modern manufacturing processes, such as advanced metal bonding, laser cutting, processing involving rapid solidification, etc., require physical transformations that lead to interactions at nano-, micro- and/or mezzoscales, and often a large volume productions at the macro-scale. Some of the processes involved are, as a rule, non-traditional (when compared with traditional, say, metal forming or machining manufacturing processes), and a good control of energy efficiency and/or environmental capability of the process and/or specific targeted objectives imposed by design requirements are needed. "Energy efficiency" refers to technologies and standard operating procedures that reduce the volume of energy per unit of industrial production. Energy efficiency provides better control over plant assets and inputs. For example, energy efficient practices ensure that thermal resources are applied at the right temperature, for the right duration and in correct proportion to raw materials. This control reduces a facility's scrap rates as well as energy consumed per unit of production. A product's *energy lifecycle* should be considered in evaluating the overall energy efficiency of the system. Here energy life cycle describes its total energy impact, including all stages of its manufacture through the end of its operating life and includes its eventual disposal [5]. The lifecycle energy concept outlines the opportunities to create superior product value—beginning with the

elimination of energy waste in manufacturing, and continuing through energy efficiency benefits conveyed to the consumer.

Development of a non-traditional or an entirely new advanced manufacturing process, in particular in the first stages, is, as a rule not thoroughly optimized from the point of view of energy efficiency and environmental impact [9]. On the contrary, these processes, although rightly considered as state-of-the-art, are often not optimized at all. For example, the energy consumption for a realization of a process (or its environmental impact) may be surprisingly unfavorable. This can even be the case for some widely utilized process, worth billions of dollars in annual production! One such process will be considered in this thesis from the energy utilization point of view within the context of sustainable development. This process involves mass production of heat exchangers by net shape brazing. It is known under the term controlled atmospheric brazing.

1.2 Controlled Atmospheric Brazing (CAB)

A state-of-art process known under the term Controlled Atmosphere Brazing was developed by Alcan, under their trade name NOCOLOK[®], as a non-corrosive flux brazing process and is now established as the most widely accepted process for brazing of aluminum heat exchangers. Aluminum brazing involves joining of components with a brazing clad alloy whose melting point is appreciably lower than that of the base alloy material. The cladding is typically placed adjacent to or in between the components to be joined and the assembly is heated to a temperature where the cladding material melts and the parent material does not. Upon cooling the cladding forms a metallurgical bond between the joining surfaces of the component. The aluminum brazing process under controlled atmosphere occurs in a furnace under the following process parameters: [6]

- Operating Temperature 853K to 893K
- Part Temperature Uniformity of $\pm 3^*$ degrees K

* Accomplished under ideal conditions. A part temperature uniformity of $\pm 12^{\circ}\text{K}$ is more pragmatical.

- Oxygen free, Nitrogen Atmosphere with dew point $< -233\text{K}$ and <100 PPM of O_2 content

In automotive heat exchanger applications, the cladding is supplied via a thin layer, metallurgically attached to the base alloy in form of the brazing sheets. The base alloy provides the structural integrity while the low melting point cladding melts to form the brazed joints. A typical joint from an aluminum heat exchanger as shown in Fig 1-1; may be manufactured using a base aluminum alloy such as AA 3003 with a cladding of AA 4343, 4045, or 4047. While the base alloy melts at about 630°C , the clad material melts between 577°C and 613°C . Therefore, the ideal furnace temperature is somewhere in the middle of the melting range of the cladding material. A basic non-corrosive flux such as potassium fluoro aluminate, a KAlF_4 compound, must be used to break down the oxide layer of aluminum and provide a surface for capillary action to draw the molten cladding into the joints. A controlled atmosphere that has an oxygen content of less than 100 ppm and a dewpoint of less than -40°C must be provided [6]. These atmospheric conditions are accomplished through the use of nitrogen, which is readily available.

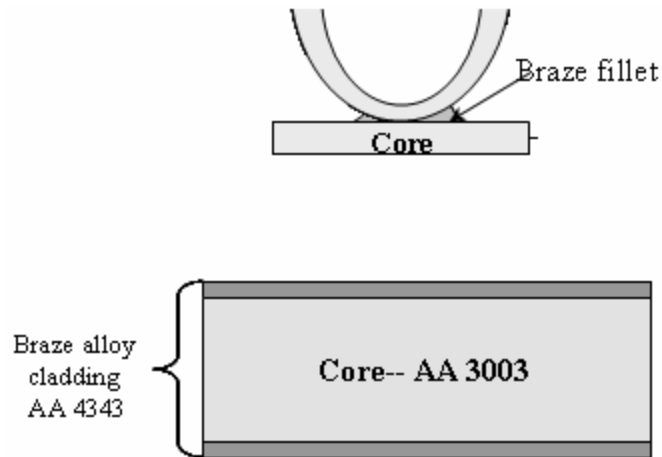


Figure 1-1 Braze sheet configuration and typical braze joint

A radiation CAB furnace, as shown in Fig 1-2, is an ideal facility for brazing similar size products in a continuous flow environment. If one intends to produce a single type or only a few variations of a product in large numbers, a radiation furnace system

makes sense. For example: 60 radiators/hr or 60 condensers/hr. The furnace is designed to use a stainless steel muffle to contain the nitrogen atmosphere and provide uniform heating of the products. The heat input into the furnace chamber is controlled through electric heating elements or natural gas fired burners to heat muffle which in turn heats the products.

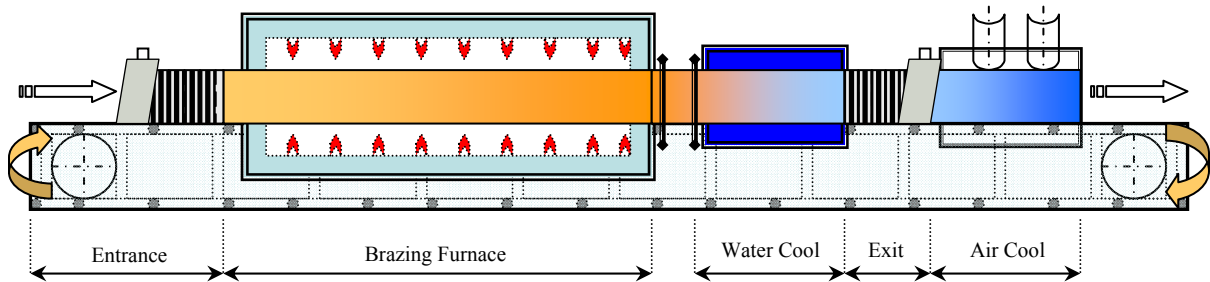


Figure 1-2 Typical system configuration

Today, more than 400 CAB furnaces are in operation throughout the world using the NOCOLOK process [6]. This technology offers the benefits of a flux utilization for successful oxide removal and operation at atmospheric pressure while avoiding the disadvantages of post braze treatments and corrosion susceptibility.

The process in most brazing operations includes the following steps [7]:

- Component forming and assembly
- Cleaning and flux application
- Brazing

The process sequence in brazing operations is depending on:

- Heat exchanger design
- Cleaning method

- Flux Application method

Success or Failure in CAB production relies on several factors [7]. The starting point is good product fit-up. Parts to be metallurgically joined must have intimate contact at some point along the joint. An adequate quantity of filler metal, but not an excessive amount must be available to fill the joints. Intimate contact is recommended, when clad products are used. Another essential basis for reliable brazing results is a uniform flux coating on all surfaces involved in the joint formation. The main focus for achieving this task is cleaning and fluxing procedure. Equally important are the furnace conditions, i.e. temperature profile, temperature uniformity, and atmosphere conditions.

A series of operations during CAB manufacturing with a schematic of main energy and materials interactions is presented in Fig 1-3. The steps (not all presented) involve headers/tanks/manifolds manufacturing, fabrication of extruded tubes with micro channels, fabrication of fin foils, washing, fluxing, drying, controlled atmosphere brazing, induction brazing of terminal ports, post brazing procedures (painting, curing, pack assemblies, test, repair).

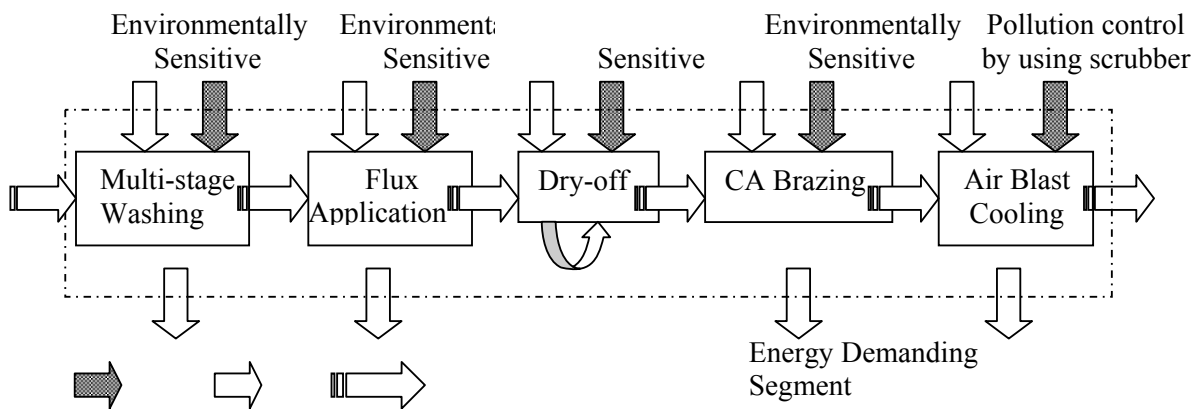


Figure 1-3 A sequence of operations during CAB manufacturing [9]

1.3 Problem definition and significance

Before stating the research objectives, the problem and concerns that this work addresses are explained here. The evolution of ideas and the motivation of taking up this problem are explained in this section. The system under study is a Continuous Net-shape Manufacturing process; Net shape processing refers to any manufacturing process which creates an object in its finished form *without* the need for finish machining or other actions. Examples of net shape manufacturing operations include casting, stamping, injection molding, sheet metal working etc. The heat exchangers manufactured in the continuous brazing furnace are held together with fixtures in a desired frame, and successions of them are mass produced. As described in previous section, brazed joints are formed by clad melting and its flow governed by surface tension along the complex mating surfaces shaped by using a series of a metal forming processes. The heat exchanger cores are exposed to a peak brazing temperature, time dwell at the peak, under conditions controlled by a series of process and material parameters. A record of time-temperature history to which each unit is exposed (along with a mezzo scale unit segments) is illustrated in Fig. 1-4. To achieve the profiles, distinct heating zones were used, each with a different temperature level. Different

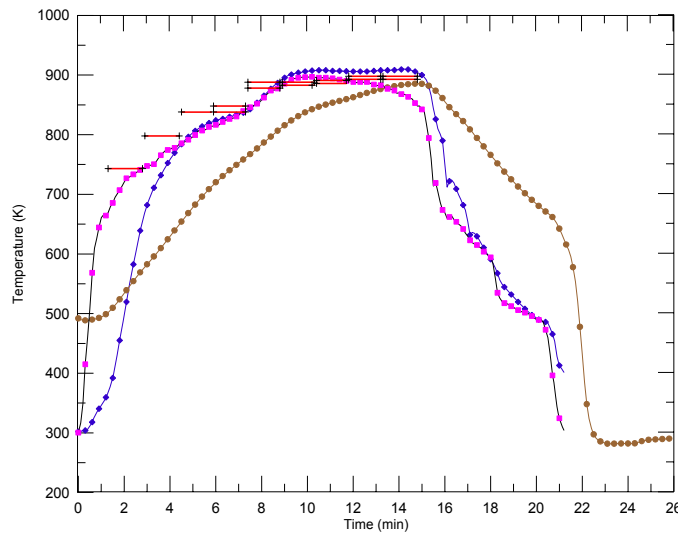


Figure 1-4 Furnace hot zone settings (presented as liner segments at different temperature levels) vs. temperature profiles of a heat exchanger.

curves represent the temperature profile for core, conveyor and nitrogen flows. This way, the heat exchanger assembly is brought into the brazing furnace system as shown in Fig. 1-

2; from room to a required temperature level for brazing of the whole assembly. It is very important to notice that a long sequence of distinct temperature levels must be imposed, and that each level is characterized by different quality of energy transformation involved, with materials processing at that level.

A composite view of a post braze state of a compact heat exchanger manifold shell is presented in the Fig. 1-5. (The segment of the exchanger construction presented is only a small portion of the manufactured macro object). Thickness of the clad residue in microns, formed during continuous brazing on exposed surfaces upon formation of joints is indicated along the perimeter. This material processing is highly energy intensive and is operated at a certain energy efficiency. It is pertinent to know whether, such a state-of-art system is operated at high or low efficiency. Also, it is to be researched if such information would give some insights in possible venues for improving the current process or a new and more efficient one.

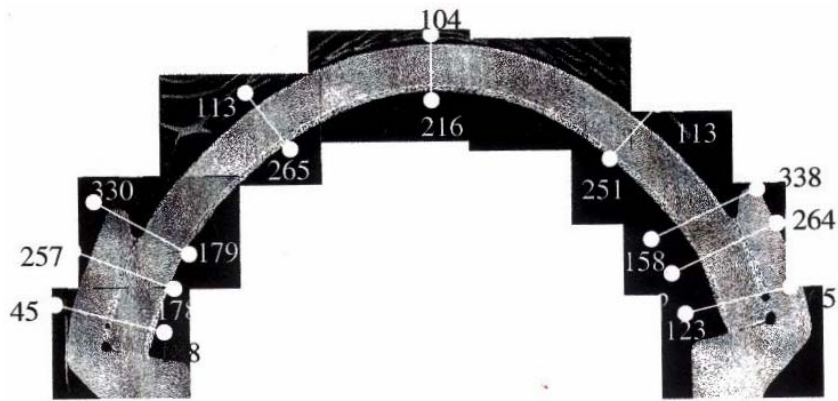


Figure 1-5 A complex joint assembly manufactured by a CAB process [8]

Assuming that brazed-joint formation is an ultimate objective of this net-shape manufacturing process, the energy efficiency of the materials processing sequence is calculated, and an alarming result is obtained. The energy utilization efficiency of the current process is formulated as follows:

$$\text{Efficiency} = \varepsilon^* = \frac{\text{Energy needed to form all the joints of a brazed object}}{\text{Total energy invested to change enthalpy of a brazed object}} \quad (1.1)$$

By calculating the efficiency as per the above formulation, it is found out (see Section § 4.4) that, 94% of excess energy is supplied than what is required for achieving the desired net shape manufacturing effect under ideal conditions (neglecting the energy losses and assuming perfect energy usage); i.e., only 6% of total electrical work/thermal energy inputs provided into the system to change the enthalpy of the heat exchanger core, is utilized to form the joints in the heat exchanger. The 6% fraction of total energy used for the net shape manufacturing effect indicates a fraction of energy involved under ideal conditions (the percentage of energy spent for heating and melting the clad to form brazed joints). This result is inherent to this manufacturing process. Hence it is not a consequence of a system imperfection.

In an industrial operation, the brazing furnace with no pre-heating consumes 7.8×10^6 J/unit for producing 160 units per hour. It is known that, under ideal conditions the energy required to accomplish the same effect would be 1.2×10^6 J/unit [9]. Consequently, the energy utilization would be at the level of only 15%. However, if the energy needed for producing the net shape result only (heating and melting cladding) is considered as defined in Eq.(1.1), utilization of energy would be at the 1% level! This means, only one percent of total energy invested into the process is effectively utilized for net shape result in a state-of-the art manufacturing process! The above analysis shows that the situation in reality, in a state-of- the-art facility, is even worse. This research addresses the energy utilization efficiency improvement between 1 and 6% levels, and also an eventual margin of improvement above the 15% level mentioned above.

The significance of this effort can be identified in the realm of aluminum industry efficiency improvements and automotive and process industries compact heat exchanger manufacturing processes developments. More generally, the methodology proposed could be applied to any manufacturing process for which the component materials transformation exergy evaluation is defined.

The significance of energy efficiency improvements achieved through mapping of exergy flows and through determining monetary values of these flows can be illustrated by: (1) referring to current energy requirements for related manufacturing processes and pollutants present, and (2) determining energy efficiency margins in a state-of-the-art manufacturing process.

Yearly energy utilization for aluminum rolled products, including brazing sheets, incurred by one of the largest manufacturers is at the level of 10^9 kWh, which has a dollar value of approximately US $\$2 \times 10^7$ (for 2001) [9]. One percent of reduction in that expense would lead to savings of US $\$ 2 \times 10^5$ – for only one manufacturer. On the other side, in a CAB brazing facility, one production line (CAB only), the electrical power utilization may reach 6×10^4 kWh a day. The total number of heat exchangers manufactured per day may reach 3×10^4 units, what leads to more than 11 million heat exchangers per year [9]. Without any further economic analysis, one may conclude that energy utilization and its management for these processes are of paramount importance.

The proposed method would reveal that there is great potential for improvement in even the most widespread state-of-the-art manufacturing processes, such as CAB brazing. The proposed method identifies the extremely low efficiency of the manufacturing process under consideration. This improvement indicates the significance and potential impact of the approach. But more importantly the proposed study of individual processes during materials processing (by using concept of exergy and irreversibility analysis) has a capacity to identify the venues for developing completely new processes. For example, in the existing process of CAB brazing, mass production is conducted using a non-localized energy flux. That means that the whole object must be heated and subsequently cooled-not only the joint zones. This indicates an inherent problem with the existing technology. The level of importance of that problem can be quantified using the proposed method. Study of possible options can be well organized within the framework of such new approaches.

1.4 Research objectives

An approach to solving the above defined problem (improvement of energy utilization of a manufacturing process or uncovering a need for devising a new one) needs to be carried out in a systematic and general manner. The research objective is to define a theoretical approach based on identification of inherent irreversibilities in materials processing first, and then to identify, trace and eventually optimize the materials and energy flows in a manufacturing process as a whole. In this thesis, the objective is focused on the first three tasks (i.e., optimization will be addressed only marginally). It is profoundly important to recognize that use of an entropy generation (e.g., exergy) based approach has an advantage over the old fashioned energy savings approach because the former compounds several important state variables and, in addition, measures the level of irreversibility. The measure of irreversibility based effectiveness becomes a pragmatically justified figure of merit of the analyzed process.

The idea of analyzing a manufacturing system by considering it as an open thermodynamic system is employed in this work. The system is analyzed in terms of exergy flows that can be determined from energy and mass flow inputs and outputs, including pollutants. In principle a multivariable objective function with a given set of constraints related to the design, cost and environmental perspectives, is hypothesized to be able to minimize exergy loss, and at the same time conform to sustainable/green manufacturing objectives. Considering the environmental concerns in a similar fashion as used in a thermo-economic analysis, a given manufacturing system can be evaluated more comprehensively based on the Second Law Thermodynamics. Such an engineering tool for optimizing energy systems, where energy conversion *per se* is primary objective, has been under development for some time [10]. For a continuous net-shape manufacturing system, where the objective is to make a quality product, to the best knowledge of this researcher, the analysis offered here is the first ever proposed. Non-energy related outcomes of a manufacturing process (involving materials transformations) may also be the sites of energy conversion and environmental pollution, and can be examined by a non-conserved property like ‘exergy’.

To identify the areas of improvement or the areas operating with lowest energy efficiency, a specialized analysis tool will be developed. This showcases the sites of activity where the subsequent R&D efforts must be focused and explored. Such a study will identify the locations of exergy destruction (in energy terms) or irreversibility generations (in entropy production terms) and possibly lead to economic/process optimization through process design that may take into account monetary costs of the environmental impact, along with the costs of energy. Design characteristics and product quality of the elements of the product flow (i.e, the “stream” of heat exchanger assemblies as a material flow in the manufacturing process of aluminum compact heat exchangers, for example) enter the analysis as the imposed constraints and will affect the outcome of the optimization. Hence a fully integrated analysis of the design and process operations would become possible. *“Once developed, the value of this approach far exceeds its utility for a particular manufacturing process (i.e. CAB process), and would be of a great relevance for any other manufacturing process if a rigorous identification of its interaction with the surroundings (energy, materials, economic) can be fully defined. It will represent the coherent framework for developing energy efficient, economically affordable and environmentally friendly manufacturing technology”* [9]

The key element of such a methodological tool to be developed for the energy/environmental aspects of the analysis is the concept of exergy [11]. A pivotal role in the approach has the exergy flow “balance”, written for a control volume defined around a segment or a whole manufacturing line, Fig.1-6; that interacts with the environment through mass (materials, auxiliary fluids, pollutants), energy and ultimately exergy flows [11],

$$\frac{dEx}{dt} = \sum \left(1 - \frac{T_0}{T_i} \right) \dot{Q} + \sum (\dot{m}e)_j^{net} - \sum \dot{W}_k - \Delta \dot{E}x_D \quad (1.2)$$

Where $(\dot{m}e)_j^{net} = (\dot{m}e)_{j,in} - (\dot{m}e)_{j,out}$, represents net exergy rate of a material flow j with respect to the environmental reference system. (T_0 , h_0 , s_0 , i.e., temperature, specific

enthalpy, and specific entropy of the material flow with reference to the surrounding environment).

$$\dot{E}x = \dot{m}e = \dot{m}[(h - h_o) - T_o(s - s_o)] \quad (1.3)$$

Equation (1.3) takes into account only physical (thermal) exergy (i.e., chemical exergy is not considered). The system being considered exchanges heat transfer rate \dot{Q} , is exposed to work interactions, and material flows (products, fluids, pollutants) with the surroundings, while at the same time it features internal irreversibilities (inherent to process imperfections). These irreversibilities lead to exergy (available energy) loss $\Delta\dot{E}x_D$ [11].

$$\Delta\dot{E}x_D = T_o\Delta\dot{S}_{gen} \quad (1.4)$$

Where $\Delta\dot{S}_{gen}$ represents the entropy generation rate, manifested within the system boundaries

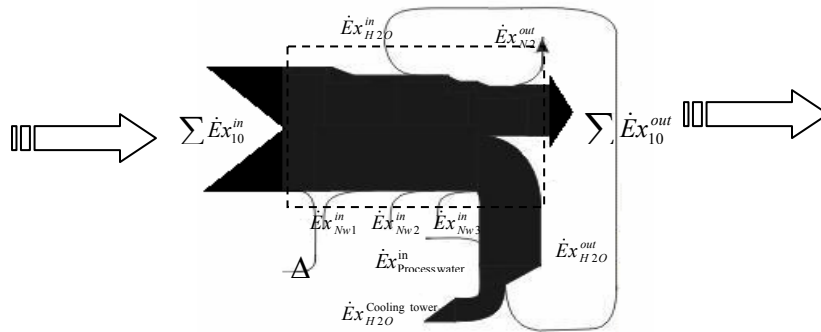


Figure 1-6 An exergy flow along the manufacturing process materials flow line

To summarize, the following points are the major steps to be accomplished to perform a thorough and rigorous study of energy usage in the considered manufacturing system.

- 1) Controlled Atmospheric Brazing (CAB) system description, data acquisition and building a data matrix of process parameters, zone/cell wise that are needed for an overall system analysis.
- 2) Computing the zonal Energy and Exergy balances and summing them together for the overall system.
- 3) Building corresponding “Sankey” and “Grassman” plots for a given product flow through the manufacturing process (Product: compact heat exchanger for automotive applications; Process: Controlled Atmosphere Brazing (CAB) process).
- 4) Perform a detailed study of energy/exergy flows, including effluents and identify the irreversibilities associated with the process.
- 5) Devise a metric that correlates product quality with energy resource utilization along the path of materials processing, and develop a simplified heat exchanger core quality vs. energy utilization model.

1.5 Thesis layout

The thesis is organized into six chapters; first chapter gives a brief introduction to the present work i.e., the significance of the effort, applicability in the aluminum industry, motivation and objectives to be accomplished. It lays out the fundamentals and basic description of the manufacturing process under consideration. The grounds of improvement and scope of energy efficiency analysis to such a state-of-the-art system are identified. The second chapter would deal with sustainability footprint for manufacturing and use of exergy based methodologies in the past for such an analysis. It elucidates current state of knowledge in using Thermodynamic based metrics like entropy generation and exergy destruction as indicators for establishing how far from equilibrium a given system will be. A detailed literature review on the concept of exergy analysis and its role in performing a sustainability analysis of a manufacturing system is presented in chapter two. Third chapter explicates the manufacturing system under study, the material processing stages, physics of

the phenomena and the product-outcome of the system. It gives a prelude about the whole system being integrated as a collection of generic cells, and the data assembled at the industrial site are restructured into a data matrix. The fourth chapter details the procedure of energy and exergy analysis and respective flow patterns with respect to the system operation. The fifth chapter briefly describes the simplified model developed to assess the energy utilization's in idealized and realistic situations and compares them to assess the energy utilization in the system. Identification of sources of irreversibilities and the quality of energy utilization at different processing stages are also presented in this chapter. Finally in chapter six, the results and plots obtained from the work are analyzed and their inferences are presented. The last chapter concludes the work presented in previous chapters and suggests some areas of further exploration, which might give an insightful path to carry this work further.

Chapter 2 LITERATURE REVIEW

2.1 Present state of knowledge in the field

A very little research is published that encompasses sustainability analysis, (i.e., using entropy generation levels) to evaluate materials processing (in particular a state-of-art manufacturing process under consideration in this thesis, i.e., CAB). Systems whose sole purpose is to efficiently deliver energy for a given task are widely subjected to analysis of energy resources utilization using traditional tools of engineering thermodynamics [12], [13], [14], [15]. An extensive study of closed, steady state or quasi-steady-state systems, such as large energy systems, is conducted using such tools [16]. Environmic modeling involving the same concepts, but for energy systems, has been recently summarized [10]. Thermodynamic irreversibility approaches, in particular exergy (i.e., availability) [17], [18], and/or entropy generation studies [19] have gained popularity among all. An early work which considers materials processing thermo-mechanical exergy can be traced in open literature [20]. The approach to thermo-economy is well documented when dealing with conventional energy and process systems [11].

Since the late eighties, the ASME Advanced Energy System Division has devoted numerous conferences to thermo-economic analysis and the use of exergy concepts in energy systems, for example ASME AES-33, 1994 [21], and ASME AES-36, 1996 [22], but no significant efforts have been attempted in the field of materials processing for manufacturing. A selection of reviews regarding more recent efforts in traditional areas of application is given in [23]. Manufacturing/materials processing exergy analysis was rarely undertaken, except possibly for large metallurgical and/or petrochemical systems [24]. This lack of analysis holds true especially for continuous manufacturing systems related to advanced materials processing. A significant boost the manufacturing disciplines have experienced by investing in new efforts related to non traditional processing clearly uncovered a lack of approaches that address the emphasized issues in a systematic and scientifically sound manner. Nevertheless, in the light of the importance of sustainability

assessments across all facets of societal development [25], in particular within the context of green engineering [26], the necessity to perform such a study becomes more critical. Moreover, regardless of being notoriously energy inefficient and environmentally unfriendly, large scale industrial operations divert the importance of ultimate goal, to product quality [27]. These systems (and the related processes) are, as a rule, open & transient (for example, joining technologies, such as mass production brazing in automotive industry,) [28].

Applying advanced thermodynamics tools to analyze such systems (in the chemical industry) is already explored [29], but not very much for sustainability analysis of manufacturing systems' in general. A change in a property of a material under processing in any open manufacturing system contributes to a certain degree to an overall outcome of all the interactions between material flows and surroundings, considered as a *closed* system. The fact that each material flow must be in equilibrium with its surroundings, both at the location of its extraction from the surroundings and at the moment of its ultimate return to the environment (which would be considered as closed path), assists this analysis. Any advanced thermodynamics approach identifies rigorously how far from equilibrium (vs. surroundings) a process and/or its outcomes are. By definition, the exergy and/or entropy generation approaches identify the points of equilibrium vs. relevant surroundings as points where driving potentials diminish (equilibrium would constitute, in terms of sustainability, a desired but never achieved goal) [28]. Hence any material flow involved in a manufacturing process begins initially from the equilibrium point with surroundings, and finally reaches the same point, after undergoing a departure. That is, it starts at a point where any possible exergy destruction would be zero and eventually returns to the same point. In a similar way, if the boundaries of the system are extended to include the whole life cycle, any sequence of an open manufacturing process, becomes a segment of a rigorously defined closed cycle [28].

In this thesis, the possibility of using advanced thermodynamics for sustainable energy utilization assessment of continuous manufacturing system featuring a series of transient materials processing segments is considered. A near-net-shape mass production of

compact heat exchangers accomplished by utilization of controlled atmosphere brazing (CAB) is the system/process under study.

2.2 Exergy and sustainable development

Numerous descriptions of sustainable development have been given, including the following popular one: ‘development that meets the needs of the present without compromising the ability of future generations to meet their own needs’ [30]. In all the factors that contribute to achieving sustainable development the most important is the requirement for a supply of energy resources that is fully sustainable [31][32][33]. Societal sustainable development is intimately related to energy resources and their utilization. Focus should not only be on discovering sustainable energy resources, but also to increasing the energy efficiencies of processes utilizing these resources. Many energy conservation and efficiency improvement programs have been and are being developed to reduce present levels of energy use. [34] A society seeking sustainable development ideally must utilize only energy resources which cause no environmental impact (e.g. which release no emissions to the environment). However, since all energy resources lead to some environmental impact, it is reasonable to suggest that some (not all) of the concerns regarding the limitations imposed on sustainable development by environmental emissions and their negative impacts can be in part overcome through increased energy efficiency [34]. A strong relation clearly exists between energy efficiency and environmental impact since, for the same services or products, less resource utilization and pollution is normally associated with higher efficiency processes. Today, for example, it is known –maybe to everyone- that between two processes: one with high equipment cost and low energy consumption and one with lower equipment cost but higher energy consumption, the latter is opposite to the aims of sustainable development. It has been suggested by that entropy generation /exergy destruction is the indicator to identify activities that are opposite to sustainable development [35].

The exergy idea is just old as thermodynamics and is based on both the first and second law of thermodynamics. Exergy is defined as the maximum (theoretical) work that

can be extracted (or the minimum work that is required) from the entity (e.g. stream, amount of matter) as an entity passes from a given state to one of equilibrium with the environment. As such, exergy is a measure of the departure of the given state from the environmental state—the larger the departure, the greater the potential for doing work. Exergy analyses are performed more and more now a days to show where energy inefficiencies occur within processes, denoted as exergy losses [36].

Environmental problems associated with energy utilization span a growing spectrum of environmental issues and natural ecosystem [38]. The second law of thermodynamics is considered to be instrumental in providing insights into environmental impact. In conjunction with this, exergy appears to be an effective measure of the potential of a substance to impact the environment. Dincer, et. al [37], suggested that the study of exergy balances is a distinct discipline, because of its interdisciplinary character as the confluence of energy, environment and sustainable development as shown in Fig. 2-1.

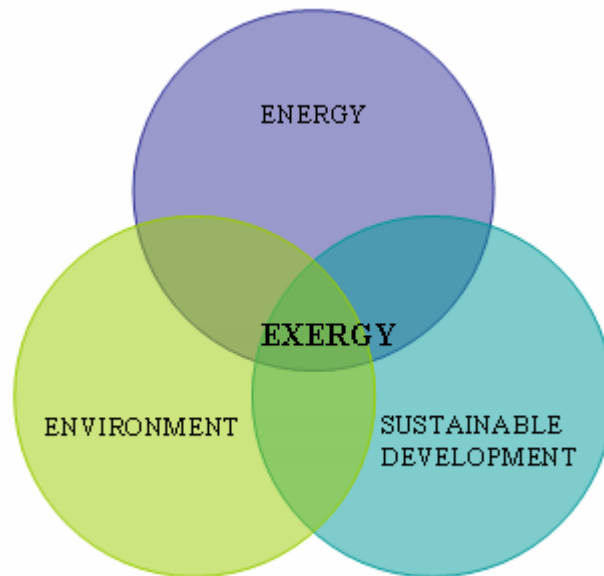


Figure 2-1 The interdisciplinary triangle of exergy [37]

The relation between exergy, sustainability and environmental impact is illustrated by Dincer, I., *et.al* in 2005 [38] as shown in Fig 2-2. Sustainability is seen to increase and

environmental impact to decrease as the exergy efficiency of a process increases. The two limiting efficient cases in Fig 2-2 are significant: [38]

- As exergy efficiency approaches 100%, the environmental impact associated with process operation approaches zero, since exergy is only converted from one form to another without loss (either through, say, internal combustion or waste emissions). Also sustainability approaches infinity because the process approaches reversibility.
- As exergy efficiency approaches 0%, sustainability approaches zero because exergy-containing resources (fuel ores, steam etc) are used but nothing is accomplished. Also, environmental impact approaches maximum because, to provide a fixed service, an ever-increasing quantity of resources must be used and a correspondingly increasing amount of exergy-containing wastes are emitted.

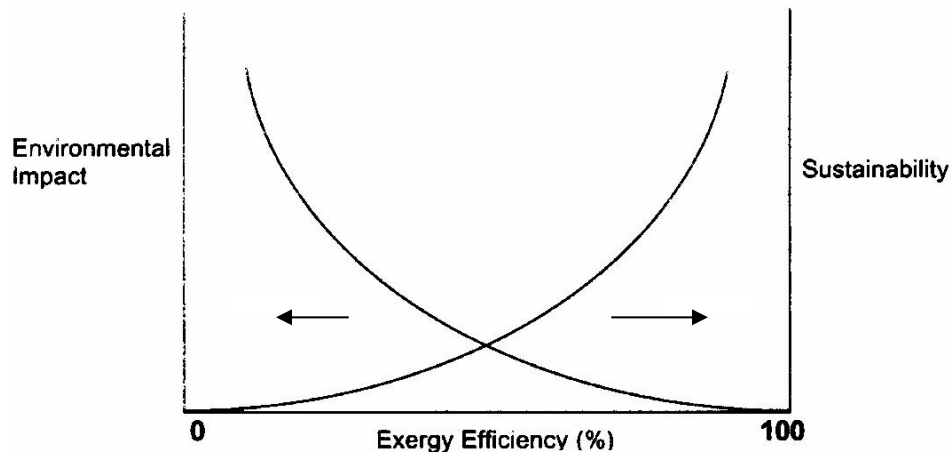


Figure 2-2 Qualitative illustration of the relations between the environmental impact and sustainability of a process, and its exergy efficiency [38]

2.3 General idea of the exergy analysis

The term exergy (Ger. exergie) was proposed by Z. Rant as late as 1956 [17]. A brief but complete definition was given by H. D. Baehr in 1965[39]: “*Die Exergie ist der unbeschränkt, d.h. in jede andere Energieform umwandelbare Teil der Energie*” (Exergy is

the totally convertible part of the energy, i.e. that part which may be converted into any other energy form.) After several decades of development, the exergy analysis has become the basic theory and a useful tool in analyzing energy system and has obtained world-wide attention and applications. Taking the environmental state as its “dead” state, the concept of exergy can be used to measure the difference between a system/ stream in a given state and in the state of equilibrium with the environment. Therefore, if an appropriate reference environment state is chosen, it can measure not only the energy or resources use in a system, but also the pollution of the discharged waste to the environment.

The traditional method of assessing the energy disposition of an operation involving the physical or chemical processing of materials and products with accompanying transfer and/or transformation of energy is by the completion of an energy balance. This balance is apparently based on the First Law of Thermodynamics (FLT). In this balance, information on the system is employed to attempt to reduce energy losses or enhance energy recovery. However, from such a balance no information is available on the degradation of energy, occurring in the process and to quantify the usefulness or quality of the heat/energy content in various streams leaving the process as products, wastes, or coolants. The exergy method of analysis overcomes the limitations of the FLT. The concept of exergy is based on simultaneous application of both first law and second law in analysis and design [36][40][41][42][43][44][45]. In the 1990s it has become the premier method of thermodynamic analysis in engineering education [19,46,47,48,49,50,65] and it is now sweeping every aspect of engineering practice [23,51,52,53,54].

Energy flows into and out of a system via mass flow, heat transfer, and work (i.e., bulk flow through pipes, heat exchangers, energy transfer via shafts, piston rods). Energy is conserved, not destroyed: this is a statement made by the FLT. Exergy is entirely different concept from energy. It represents quantitatively the ‘useful’ energy or the ability to do or receive work-the work content-of the great variety of interactions (mass, heat, work) that flow through the system. Fig 2-2 shows the physical model of an exergy analysis.

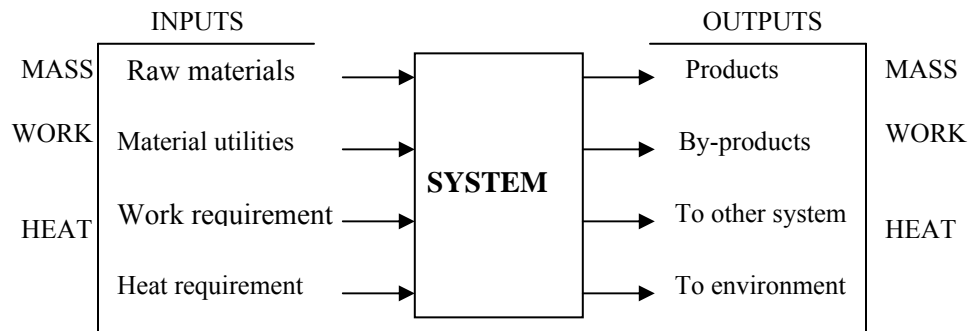


Figure 2-3 Model of the system exergy analysis. [55]

Mass transfer accompanies the input of raw and other materials (steam, chemical, products and catalysts etc) and all the output products, by-products and waste, etc. Work transfer and heat transfer are represented by the energy input (electricity, mechanical work, solar energy, steam, etc) and the energy output and losses [56]. The first attribute of the property ‘exergy’ is that it makes it possible to compare on a common basis different interactions (inputs, outputs) that are quite different in physical sense (e.g. work and heat). Another benefit is that unlike energy, exergy is not conserved; rather it is consumed or destroyed to a certain extent in any real process. Therefore by accounting for all the exergy streams of the system it is possible to determine the extent to which the system destroys exergy. The destroyed exergy is proportional to the generated entropy. In actual systems, exergy is always destroyed, partially or totally: This statement is a consequence of the Second Law of Thermodynamics (SLT). The destroyed exergy, or the generated entropy, is responsible for the less-than-theoretical efficiency of the system.

Exergy analysis is a method of analysis that uses the conservation of mass and conservation of energy principles together with the SLT for the analysis, design and improvement of energy intensive systems [36]. By performing the exergy accounting in subsystems, we should be able to draw a map of how the destruction of exergy is distributed over the manufacturing system of interest as far any other engineering system. In this way, we are able to pinpoint the components and the mechanisms (processes) that

destroy exergy the most. This is a real advantage in the search for improving efficiency (always by finite means), because it tells us from the start how to allocate engineering effort and resources. Therefore, exergy analysis can reveal whether or not and by how much it is possible to design more efficient energy intensive systems by reducing the inefficiencies in existing systems. It is important to highlight that exergy analysis can lead to a substantially reduced rate in the use of natural resources and the environmental pollution by reducing the rate of discharge of waste products.

2.4 Summary

From the above literature review it is evident that there is a potential for exergy based sustainability analysis in various manufacturing systems. As this approach is new for assessing manufacturing processes and systems, a thorough and rigorous study should be carried out and a standard procedure should be established. While energy and environmental optimizations based on exergy concept of thermo-economics have been under intense development within the realm of energy applications, basic exergy theory for manufacturing processes does not exist yet. Understanding of exergy interactions, especially of losses related to such diverse phenomena as metal forming, rapid solidification, transient radiation-conduction-convection heat treatments, chemical flux interactions during oxide removal, and variety of other complex materials processing phenomena important for advanced manufacturing, regardless of whether they are energy intensive (as in some net shape and metal joining processes) or energy non-intensive (such as nano manufacturing), is as yet virtually nonexistent. Hence this makes the present chosen topic for the research significant. The literature clearly shows that exergy destruction / entropy production can be established as the “*indicator*” for sustainable development.

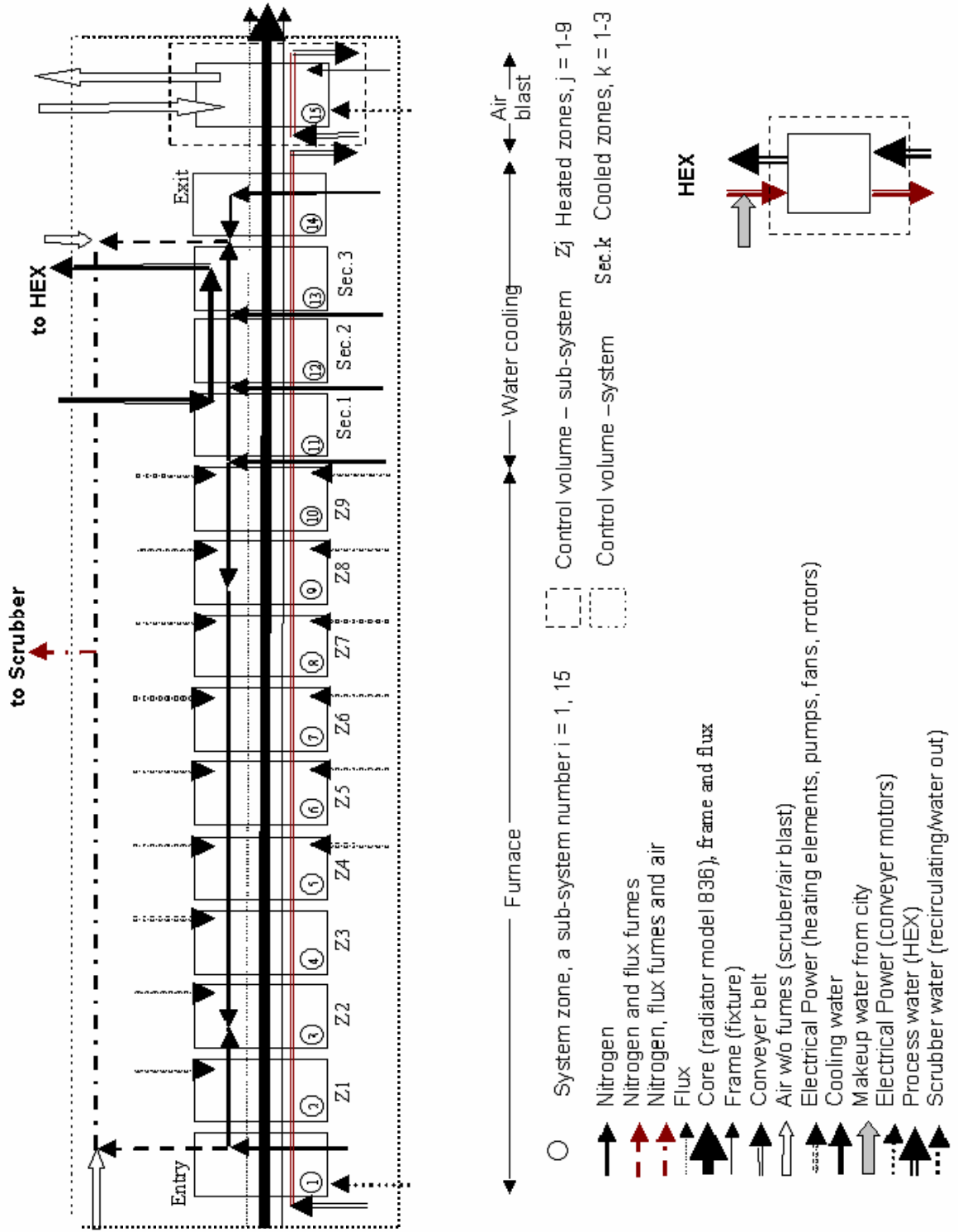
Chapter 3 NET-SHAPE MANUFACTURING SYSTEM

3.1 System description

The system under study involves a state-of-the-art continuous furnace for mass production of aluminum compact heat exchangers, for automotive applications. The process used is controlled atmospheric brazing, one of the possible choices. This is the system responsible for production of over 11 million heat exchangers per year [9]. In manufacturing aluminum compact heat exchangers, controlled atmosphere brazing (CAB) has been the process of choice. There exist 15 sub-system cells in the particular system to be considered, starting with the entrance zone into the furnace ‘Entry’, Fig (3.1) nine heating zones (Z1-Z9, cells 2-10), three water cooling zones (Sec. 1 – Sec. 3, cells 11-13), the ‘Exit’ chamber from the furnace (cell 14), and the air blast-cooling zone (Air blast, cell 15). As indicated in Fig. 3-1, a number of materials and fluid flows are directed through some or all of the cells. These flows involve pure nitrogen, processed nitrogen including pollutants, water and air flows, as well as semi-discrete “flows” of processed material (heat exchanger cores and associated flux and fixture materials, including conveyor belt).

The furnace provides inert atmosphere within its hot zone. The atmosphere is sustained by nitrogen entering the furnace at room temperature in to the cells 1, 11, 12, 13, 14 and exiting through the two duct ports at cells 2 and 14; mixed with emitted and exhaust gases generated during the brazing process. Nitrogen flows predominantly in the reverse direction to the movement of conveyor belts and flow of processed material. Any mass/energy balancing of such a system must involve one or more conveyor belts, energy inputs in form of electrical supply for heating elements and auxiliary energy resources (such as fans, pumps, motors, etc). There are two conveyor belts involved with known belt speeds, one that circulates the processed materials in the cells 1-13 and a dedicated conveyor for the exit and air blast. The control volume is crossed by mass and energy flows as depicted in the schematic presented in the Fig 3-1. Proper system definition is of crucial importance for the analysis. The system is schematically marked by the

Figure 3.1 CAB system under consideration [9]



system control volume (see the schematic of the system Fig 3-1) and each cell by the cell control volume. In addition, the proper system definition includes each of the system constituents and interactions. A set of assumptions is introduced to define system component property characterization. These definitions are carefully considered, but will not be explicitly listed here (The calculation of property data and state changes during materials processing will be provided in the next chapter and all the other data from this list will be given in Appendices B, C and D). The system as a whole and each sub-system are all open systems/sub-systems. That means that each system/sub-systems in addition to identified interactions, exchanges bulk mass flow rates of processed material, auxiliary materials flows, and process fluid flows.

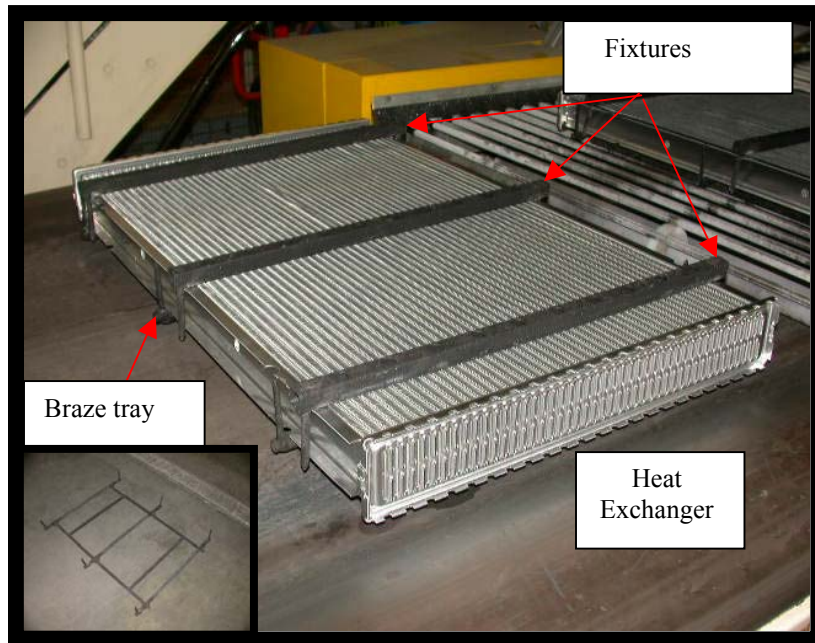


Figure 3-2 Heat exchanger core with braze tray and fixtures

The process consists of a sequence of steps to which a non-brazed assembly of a heat exchanger is exposed. This sequence of events is as follows: *fluxing-degreasing-CAB furnace heating-indirect water cooling-air blast*. As shown in Fig 3-2, the heat exchanger cores with the flux deposited are positioned on the conveyor, held together by the braze

tray and braze bars. The series of cores enters the furnace at an elevated temperature of 491 K from the degreaser. They are subsequently heated using electric heaters. To a lesser degree heated/cooled by convective heating/cooling by nitrogen flowing in opposite direction as they progress from cell 2 to 10. In cells 11 to 13, they are cooled from peak brazing temperature to room temperature by heavy stream of water jacketed around the heat exchanger cores and in cell 15 they are cooled down even more, so that the operator at the end port can pick a heat exchanger up safely. Air is blown down onto the stream of cores by a fan positioned above the conveyer belt within the air blast chamber, and then the air is sucked out by other fans. It is blown out of the building through outlet ducts.

It is important to notice that the purpose of the system is to process the discrete material flow (manufactured products–heat exchanger cores) in order to accomplish the manufacturing task. Note that such system is not a traditional energy and/or process industry system that has been subject to standard energy optimizations. This fact distinguishes such a system from most of the systems for which traditional energy, exergy, or generally thermo-economics and/or energo-environomics approaches have been developed. This difference is primarily due to [27]:

- a. System objective
- b. Discrete material flows
- c. Transient operation
- d. Variable mass flows
- e. Open system.

Still, such a system must clearly be characterized with both energy utilization efficiency and an assessment of its environmental impact. Since the objective of the system is to execute a manufacturing process, i.e. to obtain a good quality product, one may suspect that the energy efficiency of such a system may be far from an optimal in the traditional sense. It should be noted that at present there is virtually no available criteria what these optima may be, and how to be defined.

3.2 Sequence of phenomena during CAB

The objective of the materials processing procedure accomplished in a continuous brazing furnace for manufacturing aluminum compact heat exchangers [57], is to melt the micro layers of Si - Al alloy of composite brazing sheets, and to allow for the induced surface-tension-driven flows to drag the molten clad into the joint areas. Hence, the energy demands for a useful net shape effect in this manufacturing task is related to heating and melting of the clad layer. To accomplish this task, the existing brazing technology requires heating of the whole complex structure and a subsequent damping of most of that energy into the auxiliary coolant flows (water and air) during the cool-down process.

The main purpose of such a system is to bring a continuous sequence of heat exchanger cores to the peak brazing temperature (878 K), followed by a quench and joint formation, [58]. A typical ramp-up/dwell/quench temperature history of a CAB brazing process is shown in Fig 3-3. The temperature history of materials processing must be tightly controlled due to a need to achieve series of materials processing steps, [59]. These steps involve:

- 1) Achievement of as uniform as possible spatial temperature distributions within the brazed parts.
- 2) Control of diffusion processes in the solid and liquid metal states.
- 3) Selective melting of the composite alloy brazing sheets.
- 4) Control of a reactive flow of molten clad into the joints (up to 10,000 joints per unit).
- 5) Formation of the joints, and
- 6) Solidification of clad material throughout the complex heat exchanger structure.

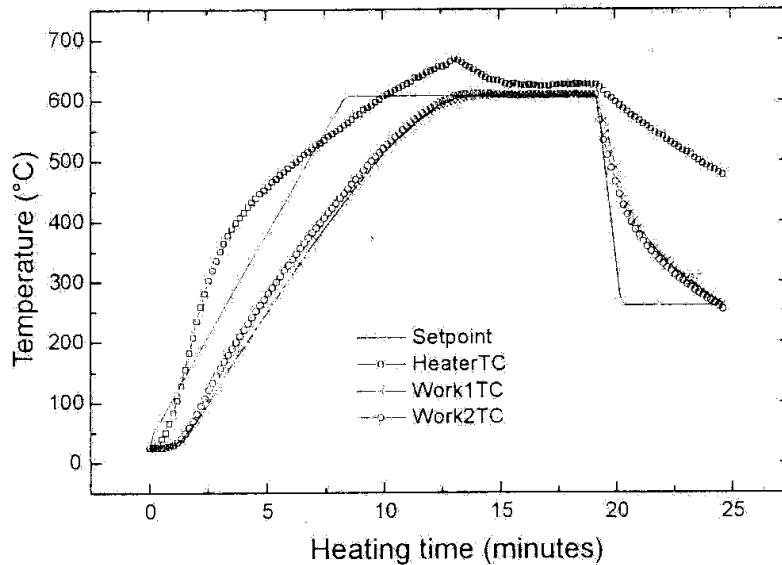


Figure 3-3 A typical ramp-up/dwell/quench temperature history of a CAB brazing process [59]

Heat transfer mechanisms during the described sequence of a brazing cycle involve the following phenomena [59]. “The heat exchanger core is exposed to a transient radiation heating, with a less pronounced simultaneous heat convection due to nitrogen flow required to maintain the background atmosphere with as little oxygen as possible. The presence of an inert atmosphere is important in particular in the range of temperatures between 670 K and 770 K when an action of the added flux starts (the flux is a fluoride eutectic water slurry of potassium fluoroaluminate $K_xAlF_y \cdot xH_2O \rightarrow KAlF_4 + K_3AlF_6 + H_2O$ with an average particle size of 8 μm and with the liquidus temperature either within or above the range between 835 K and 848 K). The dominant heat transfer mechanism in the ramp-up segment of brazing cycle is a conjugate radiation-conduction heat transfer involving complex geometry of the heat transfer surface and the radiation shield.” The complexity of the process is related to both [59]:

- (1) Radiation interaction between the heater that surrounds the core and the intricate collection of core surfaces, and

- (2) The conduction through the solid core composite structure that consists of multiple layers of thin fin foils and more massive extruded tubes. In addition, a complex temperature fields are formed in header areas.

3.3 Time-temperature history of the materials processing

In Fig. 3-3, a representative temperature history of a processing for brazing of a compact heat exchanger along its passage through the system (Fig. 3-1) is presented. This cycle is executed in an industrial setting under actual operating conditions [60]. The first three heating stages of the process have one heating source at the top of the furnace muffle, while the remaining have two, at the bottom and also at the top of the muffle (represented by red horizontal line segments in Fig. 3-3). The red/blue arrows indicate energy transfer interactions between the respective heater/coolant and the product in the given zone. [27]

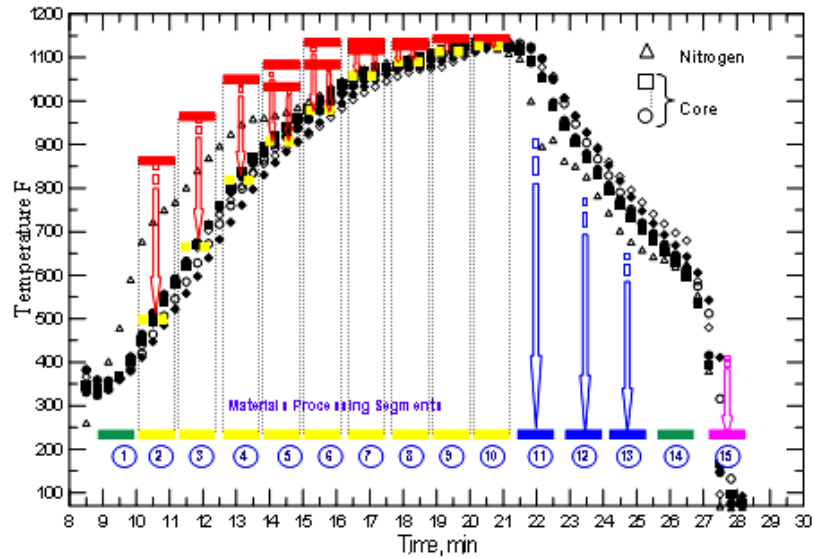


Figure 3-3 Temperature history of a heat exchanger core during processing [27]

The materials' processing segments are indicated at the bottom along the abscissa. Temperatures of the heat exchanger core during processing were collected in real time (data logger travels through the furnace). At a given instant of time, it is measured at 8 locations by thermocouples attached to the traveling core. These are represented on the

time-temperature history plot above as a collection of points with their respective symbols ($\square, \diamond, \dots, \circ$). Temperatures of the conveyor belt (noload conditions) at one location and the Nitrogen flow (Δ) that travels in the opposite direction of core processing are also monitored in the real time and with respect to time, as cores progress from the entry towards the exit. (See Appendix B (a) *Temperatures of each cell* for measured values of temperature at the entry and exit ports of each cell). In Airblast (Cell 15), air is sucked from the plant roof and is forced through the jacketed passages enclosing traveling cores. The temperatures of air at the intake and exhaust are measured. Similarly, in the water cooling segment (Cells 11, 12, 13); water enters the water jackets at room temperature and exits at elevated temperatures (309, 311, 307 K respectively). The uncertainty level of temperature measurements is determined to be less than 0.5 deg. The main characteristic of such a system is that its spatially distributed heating zones must be tuned to various temperature levels characterized by various associated energy ratings (variable in time as well). This energy is delivered by thermal radiation. This is so because the exact amounts of thermal energy must be directed to the traveling cores to achieve the exact enthalpy rate change of the manufactured structures, following the requested temperature profile dictated by the uniformity of the temperature field in the core. Hence, thermal energy flows into the cores (for each core these energy flows represent heat transfer flows, while for the system as a whole (and for the respective cell) each heating element represents a work interaction driven by an electrical input of a given rating). Note that these energy inputs are not only spatially distributed, but a transient activation of a series of electrical heat sources at different power levels is required. The temperature levels of energy sources as indicated earlier are presented in Fig. 3-3, by thick line segments (either single or multiple for each of the heating stages of the process) positioned above the core temperature profile.

Temperature set points for furnace-heating zones are as follows:

	T (K)	
Cell 2	743	
Cell 3	798	
Cell 4	838	
	Top	Bottom
Cell 5	838	848
Cell 6	878	888
Cell 7	883	888
Cell 8	886	891
Cell 9	893	898
Cell 10	893	898

Table 3.1 Temperature set-points of furnace

Cooling during the quench is accomplished by:

1) Water flow that is jacketed within the cooling sections and around the heat exchanger cores (the heat transfer between the cores and the jacket walls is accomplished by thermal radiation). The hot water coming out of the water jacket as shown in the following schematic Fig. 3-4, goes to an auxiliary heat exchanger, which cools it down with a separate flow of process water coming from the cooling water tower.

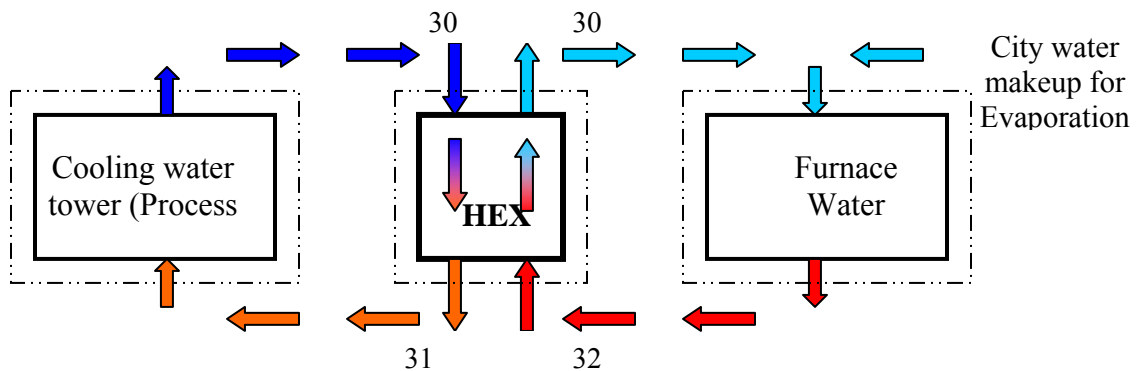


Figure 3-4 Water quench in Cells 11, 12 and 13

2) Convective cooling through utilization of the air blast:

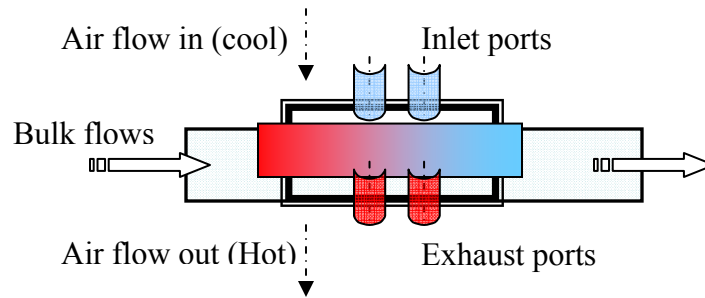


Figure 3-5 Air blast in Cell 15

It should be noticed that the temperature non-uniformity within the core was most pronounced between 10-17 min after initiation of radiation heating (during the ramp-up segment of the brazing cycle). However, the most critical segment starts later, approximately 18 min after the ramp-up initiation when the temperature approaches the peak brazing temperature. It must be clear that a very elaborate, hence complex energy management spatially distributed and time dependent control is needed. However, the key question is how efficient such an intensive energy utilization process may be - even if fine-tuned. In chapter 4, it will be demonstrated that such a system operates with very low energy efficiency. Subsequently, a detailed energy and exergy balancing will be conducted, and ultimately the First and Second Laws of Thermodynamics figures of merit of energy conversions along materials processing paths will be determined.

3.4 System integration

A detailed study of a real industrial process and inherent materials processing of the selected system is done. A member in the research group* conducted a detailed process monitoring and system analysis of the material processing sequence at an industrial site. The raw data from this data acquisition is utilized in this work. The segments of the process involving heating, brazing and rapid quench are included into analysis. Thermal degreasing and fluxing are excluded. This effort was completed within the scope of a emerging idea project grant sponsored by KSEF [60]. All the relevant information about process features like materials flows, energy utilization and other auxiliary data was collected during data

collection. These data include temperature vs. time data for processed materials (spatially and temporally distributed), mass flow rates of various fluids, pressures of all involved fluids and effluents. Also, energy ratings and energy utilization rates/fractions were measured in real time. In this study, the integrated system is identical to the system under consideration (including only the set of options selected for a particular heat exchanger processing). That means that some of the interaction options (in particular the locations for nitrogen flow inlet/outlets ports) were not utilized. Only the interactions active in the particular run (that depends on the manufactured heat exchanger core unit) are explicitly mentioned in the data set. The following table summarizes the process parameters which are measured and/or calculated respectively to perform the mass, energy and exergy accounting, and are given in chapter 4.

Table 3.2 Input Process Parameters (Measured)

Symbol	Variable	Units	Comment
u_1	Conveyer 1 speed	m/s	“Recipe list” specific
u_2	Conveyer 2 speed	m/s	“Recipe list” specific
L	Core length in the direction of flow	m	Core specific
D	Distance between the cores	m	Variable
w	Belt (conveyer) effective width	m	Fixed
$\rho_{L,CON}^{in}$	Belt (conveyer) area mass (L) density	kg/m ²	Conveyer’s material property (inlet conditions)
$\rho_{L,CON}^{out}$	Belt (conveyer) area mass (L) density	kg/m ²	Assumed to be identical to $\rho_{L,CON}^{in}$
$\rho_{N_2,i}^{in}$	Mass density of N ₂ gas at inlet	kg/m ³	$\rho_{N_2,i}^{in} = f(T,p)$ at the inlet port (ideal gas)
$\dot{V}_{N_2,i}^{in}$	Volumetric flow rate of N ₂ gas at inlet	m ³ /s	Value is known (measured)
$\rho_{N_2,i}^{out}$	Mass density of N ₂ gas at outlet	kg/m ³	$\rho_{N_2,i}^{in} = f(T,p)$ at the outlet port (ideal gas)
$\dot{V}_{N_2,i}^{out}$	Volumetric flow rate of N ₂ gas at outlet	m ³ /s	value is known (measured) for each cell at in/outlet
$\rho_{H_2O,i}^{in}$	Coolant (H ₂ O) mass density	kg/m ³	Assumed as fixed

* Franklin Bryan completed the data acquisition at an industrial site.

	(inlet)		
$\rho_{H_2O, i}^{out}$	Coolant (H ₂ O) mass density (outlet)	kg/m ³	Equal to $\rho_{H_2O, i}^{in}$
$\dot{V}_{H_2O, i}^{in}$	Coolant (H ₂ O) volumetric flow rate (in)	m ³ /s	Value is known (measured)
$\dot{V}_{H_2O, i}^{out}$	Coolant (H ₂ O) volumetric flow rate (in)	m ³ /s	Value is known (measured)
d	Diameter of air flow ducts in/out	m	Value is known (measured)
$v_{Air, i}^{in/out}$	Velocity of air flow	m/s	Value is known (measured)
$\rho_{Air, i}^{in/out}$	Air mass density (in/outlet)	kg/m ³	Assumed as fixed
ξ^1	Percent of heater draw	%	Measured in time *
$\dot{E}_{RH, i}^{in}$	Heater draw	W	Assumed to be equal to heater rating
$\dot{W}_{AUX, i}^{in}$	Auxiliary power in	W	Power for electric motors, pumps, fans, etc
$T_{core/flux/fix}^{in}$	Inlet temperature of core, flux and fixture	K	Value is known (measured)
$T_{core/flux/fix}^{out}$	Outlet temperature of core, flux and fixture	K	Value is known (measured)
T_{CON}^{out}	Inlet temperature of conveyor	K	Value is known (measured)
T_{CON}^{out}	Outlet temperature of conveyor	K	Value is known (measured)
T_{air}^{in}	Inlet temperature of air	K	Value is known (measured)
T_{air}^{out}	Outlet temperature of air	K	Value is known (measured)
$T_{N_2}^{in}$	Inlet temperature of N ₂	K	Value is known (measured)
$T_{N_2}^{out}$	Outlet temperature of N ₂	K	Value is known (measured)
$T_{H_2O}^{in}$	Inlet temperature of water	K	Value is known (measured)
$m_{Core, i}^{in}$	Core mass at the inlet of a zone	kg	Value is known (measured)
$m_{HEX, i}^{out}$	Core mass at the outlet of a zone	kg	To be assumed equal to the vale of $m_{HEX, i}^{in}$
$m_{FLUX, i}^{in/out}$	Mass of flux (on core & frame)	kg	Value is known (measured)
$m_{FIX, i}^{in}$	Mass of fixture (in)	kg	Measured as weight

* An average value of the heater (top/bottom) draw is considered for a measured span of 30 min for establishing heater temperature for a given heating zone

$m_{FIX,i}^{out}$	Mass of fixture (out)	kg	Equal to $m_{FIX,i}^{in}$
d	Diameter of air flow ducts in/out	m	Value is known (measured)

Table 3.2 Input process parameters

Notes and Assumptions

- 1) The masses of the core, flux, fixture and water are assumed to remain constant (no losses) and hence the mass flow rates at the inlet and outlet are equal.
- 2) The temperature of the mixture of nitrogen and obnoxious gases (like HF) emitted from the furnace are measured before they are ducted out to scrubber. The volumetric flow rate of nitrogen entering the furnace is different at various points along the flow of the material and is measured accordingly.
- 3) The percent of time of the operation of the heaters is assessed from partially incomplete set of data gathered (i.e., only a representative short period of monitoring time (30 min) is registered). The power levels of the heaters are assumed to be equal to “power ratings” as defined in Appendix A. The pairs of values (when present) indicate the ratings for top and bottom heaters, respectively.
- 4) Auxiliary energy use is defined for the following uses:
 - i. Conveyer power is assigned to the first cell
 - ii. Water pump for water-cooling is assigned to Cell 11.
 - iii. The Cell 15 includes power needed for air blast fans.
- 5) The last cell is an air blast zone and does not feature any protective atmosphere flow.
- 6) All the losses from the walls of the furnace are assumed to be convected with a heat transfer coefficient of 20 W/m²K.

- 7) The individual heat transfer surface areas exposed to convective heat loss from the furnace associated with each cell are not known exactly. It can be assumed these values to be equal to the outside surfaces of the furnace that are associated with each cell segment.
- 8) The temperature of the ambient is assumed to be 300 K.
- 9) The state properties of the materials being processed like temperature, enthalpy and entropy at the exit of a given cell are assumed to be equal to those at the entry of the successive cell (coupling conditions).
- 10) To determine the exact temperature of core/fixture/flux at cell terminal points it's very pertinent to know the exact location of inlet/outlet cross-section of each zone and instant of time at which the core passes them. The determination of these locations is performed from a drawing of the furnace (i.e. the axial dimensions of each zone) and the given velocity of the conveyor.

3.5 Generalized system cell

Each cell, Fig.3.1, along the path of the materials processing sequence is a site of materials and energy conversions, and a possible emitter of effluents that may lead to environmental concerns. In terms of energy efficiency, such a cell features various sources of irreversibilities depending on the materials processing sequence. Depending the manufacturing process in question, they may in general include but not restricted to: (1) material forming, (2) material removal processes, (3) heat treatments, (4) joining (adhesive bonding, soldering, brazing, diffusion bonding or welding), and (5) various steps of material assembly and handling. Each of these processes is inherently irreversible. The level of irreversibility influences the sustainability of the product/process as a whole.

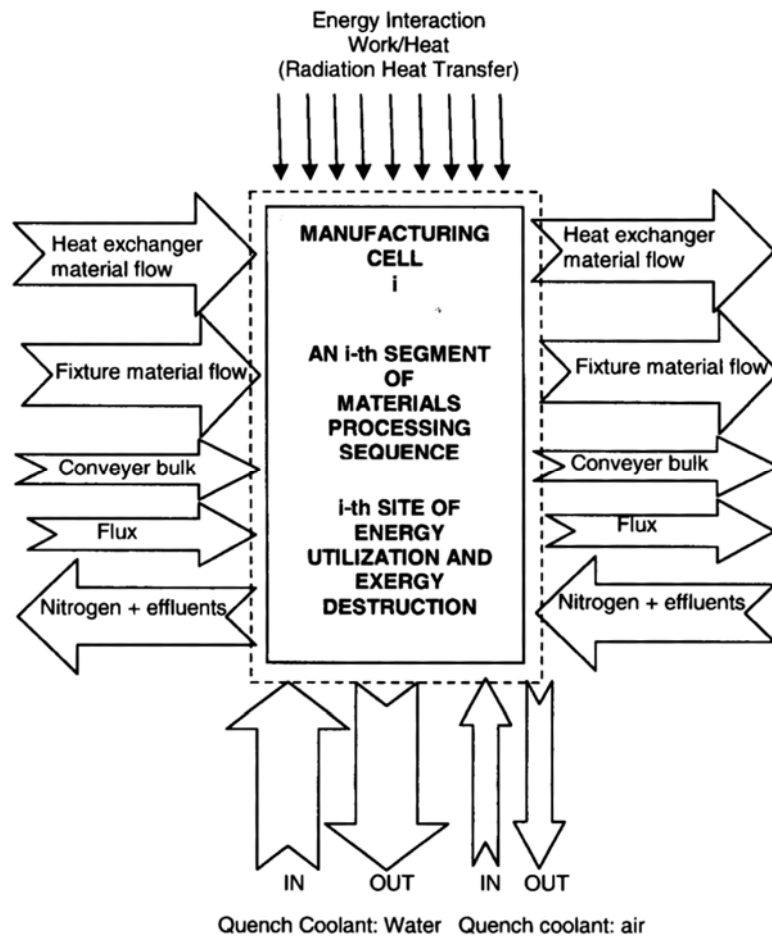


Figure 3-6 A generalized system cell [60]

To be able to analyze and ultimately optimize (optimization would not be the objective of this work) such a complex system (both at the cell and at the system of cells' level), two important steps of the analyses are needed: (1) balancing of relevant entities involved (such as mass, energy, exergy, etc) and (2) analysis of materials/energy conversions at the individual materials' processing levels.

To perform an analysis that will involve proper accounting for all the interactions for a system as a whole and/or any sub-system cell, a "generic zone cell" is defined as shown in Fig 3-6. This cell represents a generic multi port cell that features all identified

interactions (bulk flows of materials and process fluids), energy flows (as heat transfer or work transfers-electrical power involving interactions through heaters, and auxiliary devices such as pumps, fans motors etc). Detailed list of all interactions and corresponding definitions including the algorithm for calculations of each bulk, work and heat flows are provided in the next chapter.

Chapter 4 ENERGY-EXERGY BALANCE

An exploration of a research approach to the energy efficient synthesis of an advanced materials processing for novel manufacturing technologies by identifying, tracing and optimizing energy flows and entropy generation of all materials transformation processes involved, i.e., tracing the exergy flows and their destruction, is done for the considered CAB system. A hypothesis explored, and subsequently verified in this project, is that an “exergo–environmental analysis approach” can be formulated for various materials processing segments of a manufacturing process and for the process as a whole and that such formulation can provide insight into both quantity and quality of energy utilization and environmental impact of the system. The main prerequisite for such an analysis is a confirmation of plausibility of exergy modeling of system’s interactions by [60]:

- 1) Pondering mass and energy flows and/or interactions manifested within the materials processing sequence with corresponding exergy content, and
- 2) Identifying irreversibilities of the related materials processing phenomena.

Synthesis of the analysis at the cell level was conducted first, and is described in the following sections by building the Sankey energy flow diagram and Grassman exergy flow diagram for the CAB furnace system [61]. Individual, complex, materials modification processes considered involve solid state diffusion of composites, non-equilibrium melting of thin metal films, and solidification of metal during brazing process.

Within the scope of this work, both tasks are investigated. Energy and exergy flows analysis uncovers facts for an identification of astonishingly low energy efficiency, and also identifies locations of very low energy quality conversion. The modeling of processes (as a pre-requisite to identify the irreversibility level of a process) will ultimately lead to the determination of the entropy generation as a cause of efficiency deterioration – a necessary tool for defining the means for improvements.

4.1 Mass balance-flow rate calculation

To be able to construct the energy and subsequently exergy flow diagram for the materials processing executed within the integrated system, a corresponding mass flow rate balance calculations should be performed. The mass inflows and outflows of different processed materials are indicated in the following schematic Fig. 4-1, for a generic cell of Fig. 3-6. The numerical values of the mass flow rate for each of them are calculated from the formulae shown in the following table (see next page) and are listed in *Appendix-B (b)-Mass flow rate calculation* spreadsheet. By knowing the various process parameters that are measured (summarized in the System integration section of previous chapter) and calculating the respective mass flow rates, mass balance of the overall system is devised. See Appendix B for detailed calculation routine of mass flow rates, performed using spreadsheets.

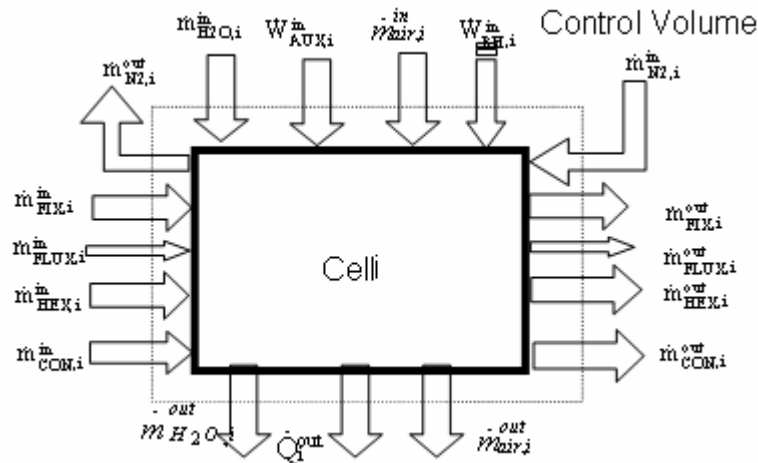


Figure 4-1 Mass inflows and outflows for a generic cell

Notes and Assumptions

1. As there is a variation in the volumetric flow rate of Nitrogen entering the furnace at different ports, the respective mass flow rates are calculated from the measured volumetric rates measured at “normal condition” defined as $T=293.15\text{ K}$, $P=1\text{ atm}$.

2. The air intake and exhaust ducts are different in a corresponding cell cross-section, therefore the velocity of suction and also pressure of air is different at those ports, hence the mass flow rate values are different at entry and exit ports.
3. Except for Air, the entering and leaving mass flow rates are constant and are equal for all the cells of the furnace.
4. In order to obtain the mass flow rates of the bulk flows (core, flux and fixture) as per unit time (1/t)-sec⁻¹, measured mass of the core, flux and fixture is multiplied with a ration of the ‘conveyor speed’(u_{1/2}) to the ‘distance between the two successive cores on the conveyor belt’ (L+D).
5. In order to obtain the mass flow rates of the bulk flows (conveyor) as per unit time (1/t)-sec⁻¹, its mass area density (kg/m²) is determined and multiplied with the given velocity and width of the conveyor
6. The Inlet volumetric flow of water is connected in parallel to the cells 14, 15 at 2.275 Nm³/hr and for cell 13 at 3.8 Nm³/hr. Volumetric flow rates at inlet and outlet ports are assumed to be constant for all the water cooling cells.
7. An average value of the heater (top/bottom) draw-ξ¹; is considered for a measured span of 30 min for establishing heater temperature for a given heating zone.

Interaction	Entity	Symbol	Units	Comment
Bulk flow	Core mass flow rate at the in/outlet	$\dot{m}_{HEX,i}^{in/out}$	kg/s	$\dot{m}_{HEX,i}^{in/out} = \frac{u}{L+D} \sum_{j=1}^k m_j^{in/out} = \frac{u}{L+D} m_{HEX,i}^{in/out}$
Bulk flow	Conveyor mass flow rate at the in/outlet	$\dot{m}_{CON,i}^{in/out}$	kg/s	$\dot{m}_{CON,i}^{in/out} = u \cdot w \cdot \rho_{L,CON}^{in/out}$
Bulk flow	Flux mass flow rate at the in/outlet	$\dot{m}_{FLUX,i}^{in/out}$	kg/s	$\dot{m}_{FLUX,i}^{in/out} = \frac{u}{L+D} m_{FLUX,i}^{in/out}$
Bulk flow	Fixture mass flow rate at in/outlet	$\dot{m}_{FIX,i}^{in/out}$	kg/s	$\dot{m}_{FIX,i}^{in/out} = \frac{u}{L+D} m_{FIX,i}^{in/out}$
Bulk flow	Nitrogen mass flow rate at the inlet	$\dot{m}_{N2,i}^{in}$	kg/s	$\dot{m}_{N2,i}^{in} = \rho_{N2,i}^{in} \dot{V}_{N2,i}^{in}$
Bulk flow	Nitrogen mass flow rate at the outlet	$\dot{m}_{N2,i}^{out}$	kg/s	$\dot{m}_{N2,i}^{out} = \rho_{N2,i}^{out} \dot{V}_{N2,i}^{out}$
Bulk flow	water mass flow rate at the in/outlet	$\dot{m}_{H2O,i}^{in/out}$	kg/s	$\dot{m}_{H2O,i}^{in/out} = \rho_{H2O,i}^{in/out} \dot{V}_{H2O,i}^{in/out}$
Bulk flow	Air mass flow rate at in/outlet	$\dot{m}_{Air,i}^{in/out}$	kg/s	$\dot{m}_{Air,i}^{in/out} = \rho_{air,i}^{in/out} \cdot v_{Air,i}^{in/out} A_{air,i}^{in/out}$
Work flow	Electrical heater power in	$\dot{W}_{RH,i}^{in}$	W	$\dot{W}_{RH,i}^{in} = \xi^1 \dot{E}_{RH,i}^{in}$

Table 4.1 Formulae for calculating interaction rates.

4.2 Energy balance

With a well-defined system and an established mass flow rate diagram and specified interaction, the construction of the energy flow diagram (Sankey diagram) can be initiated. A word of caution would be in place here. A practice of presenting energy utilization within a process through a construction of the related Sankey diagram has been defined long ago for many energy and process (chemical, cryogenic, etc) systems [62]. However, a manufacturing system may feature some peculiarities that may require a series of additional assumptions. For example, in our continuous net-shape manufacturing of compact heat exchangers process, in addition to the bulk flows of various fluids and energy transfers (in form of electrical energy inputs, heat losses, work etc.), a continuous flow of discrete objects to be manufactured must be defined. In our approach as presented in section § 4.1, we will model such a flow as a continuous bulk flow for which a state is assumed in a same manner as the one used for a traditional bulk flow of an open system.

Any energy flow will be presented by an arrow in the energy diagram. The width of an energy flow arrow is proportional to the involved energy “content of a material flow and/or energy interaction”. An energy balance for any control volume of an open system with bulk material’s flow and energy interactions (work, heat) can, in general, be written (for a steady state conditions of an open system) as follows: (note, the sign convention has already been incorporated and all energy flow quantities should be taken into account at their absolute values). This balance is valid for each cell and for the entire system [64].

$$\sum_{i=1}^n \dot{H}_i^{in} + \sum_j^m \dot{W}_j^{in} + \sum_{k=1}^p \dot{Q}_k^{in} = \sum_{i=1}^n \dot{H}_i^{out} + \sum_j^m \dot{W}_j^{out} + \sum_{k=1}^p \dot{Q}_k^{out} \quad (4.1)$$

Where \dot{H} terms denote enthalpy rates of materials flows (including the “flows” of heat exchanger cores, fixtures, and conveyer material), and \dot{W} and \dot{Q} terms indicate “work” inputs for the conveyer belt movement and heat losses associated with cooling of both heat exchanger cores, and fixtures.

Calculation of enthalpies of materials' flows deserves an additional comment. In a traditional analysis of thermal systems, the bulk flows represent well-defined fluid flows. In a manufacturing process, the bulk flows of materials are represented by motion of distinct material masses, which may not necessarily be a continuous material flow (such as flow of distinct heat exchanger units on the conveyer belt material). In case of discrete flows of materials, a kinetic equation averaged in time is taken into consideration (a number of core units having distinct spatial characteristics move in time with a given speed of motion). An additional issue is involved with the determination of thermodynamic properties (such as enthalpy) of material flows of the alloys and/or chemical compounds. In this analysis, materials' properties are assumed to be idealized by the properties of a dominant (and/or similar) element/compound in a given material (aluminum for AA3003 and AA4343 etc, Fe for steel, potassium hexa-fluoro-aluminate for flux etc). The specific enthalpies of materials are determined following the NIST database [63] and can be calculated using the correlation as follows:

$$\bar{h}^0 - \bar{h}_{298.15}^0 = At + B \frac{t^2}{2} + C \frac{t^3}{3} + D \frac{t^4}{4} - \frac{E}{t} + F - H \quad (4.2)$$

In Eq. (2), the letters A, B, C etc represent the coefficients (real numbers) shown in Table 4.1 below, taken from the NIST database [63] (also see *Appendix C* for a detailed calculation routine using Eq 4.2, of the enthalpies for each cell), and t is the scaled temperature in SI units $T(K)/1000$.

Material \ Coefficient	A	B	C	D	E	F	H
Conveyor & Fixture	18.43	24.64	-8.91	9.66	-0.01	-6.57	0
Heat Exchanger	28.09	-5.41	8.56	3.43	-0.28	-9.15	0
Flux	162.93	238.52	-115.99	19.87	-0.11	-3384.82	-3326.28
Nitrogen	26.09	8.22	-1.98	0.16	0.04	-7.99	0
Air	28.11	0.001967	0.000005	0.000000	-	-	-
Water	-203.61	1523.29	-3196.41	2474.46	3.86	-256.55	-285.83

Table 4.2 Values of Coefficients in Eq 4.2 from NIST database

The distribution of the energy flow cell wise leads to the following balance

$$\sum \dot{H}_i^{\text{in}} = \dot{H}_{\text{Core},i}^{\text{in}} + \dot{H}_{\text{Flx},i}^{\text{in}} + \dot{H}_{\text{Fixt},i}^{\text{in}} + \dot{H}_{\text{Con1},i}^{\text{in}} + \dot{H}_{\text{Con2},i}^{\text{in}} + \dot{H}_{\text{H2O},i}^{\text{in}} + \dot{H}_{\text{Air},i}^{\text{in}} + \dot{H}_{\text{N2},i}^{\text{in}} \quad (4.3)$$

$$\sum \dot{H}_i^{\text{out}} = \dot{H}_{\text{Core},i}^{\text{out}} + \dot{H}_{\text{Flx},i}^{\text{out}} + \dot{H}_{\text{Fixt},i}^{\text{out}} + \dot{H}_{\text{Con1},i}^{\text{out}} + \dot{H}_{\text{Con2},i}^{\text{out}} + \dot{H}_{\text{H2O},i}^{\text{out}} + \dot{H}_{\text{Air},i}^{\text{out}} + \dot{H}_{\text{N2},i}^{\text{out}} \quad (4.4)$$

$$\sum \dot{W}_i^{\text{in}} = \dot{W}_1 + \dot{W}_2 + \dot{W}_3 + \dot{W}_4 + \dot{W}_5 + \dot{W}_6 + \dot{W}_7 + \dot{W}_8 + \dot{W}_9 \quad (4.5)$$

Therefore, Eq (4.1) can be written as:

$$\sum \dot{H}_i^{\text{in}} + \sum \dot{W}_i^{\text{in}} = \sum \dot{H}_i^{\text{out}} + \Delta \quad (4.6)$$

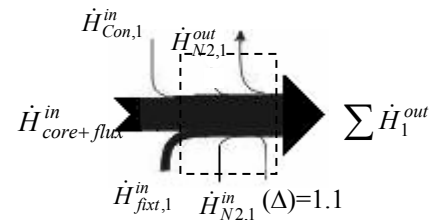
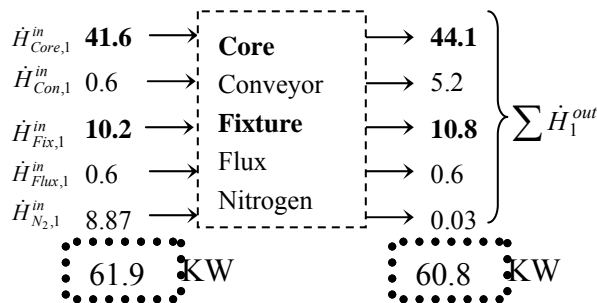
Where Δ indicates the energy balance residues at the cell level (includes heat losses). The energy flow diagram is constructed starting from the inlet into the continuous sequence of cells. The energy flows should be determined by marching from one cell to the other. As far as the main objective of the manufacturing process is concerned, the first cell takes the role as follows:

- To provide an initial “nitrogen barrier” for building a controlled atmosphere.
- To support materials motion function (through a conveyer belt movement)

As can be seen from the energy flow diagram in its final form (see later), a possible misleading impression regarding the relative importance of inlet enthalpy levels of materials' flows requires an additional caution. Since Cell 1 – as well as the system as a whole - represent an open system, energy flows of bulk materials flows must be represented by enthalpy rates. Therefore, the enthalpy rate of the conveyer belt mass rate, for example, may become significant if its absolute value is considered because of the given mass and specific heat values multiplied with the related temperature. But, as it will be clearly seen from the exergy diagram later, its contribution to the overall available

energy flow is virtually zero (it is assumed that the conveyor belt enters the first cell at the temperature of the surroundings)! The change in enthalpy rates of the material streams involving heat exchanger cores, flux and fixture frames from the entrance to the exit of the considered first cell is due to heat transfer indicated as the “leak/residue of the balance” to the surroundings (i.e., in this cell not due to heating-no heating in this cell is involved). Even though this segment of processing is not so “eventful” (i.e., the process involving Cell 1 only), the significant energy flow indicates how a conventional energy flow balance may provide a misleading impression regarding the relative importance of various energy flows associated with materials’ flow in a manufacturing process (as opposed to an energy system). An exergy flow diagram (to be discussed next) indicates this fact much more clearly. The detailed calculation of the enthalpies of each bulk flow indicated in the following illustrations are shown in *Appendix C* and the dominant function (mostly being the core enthalpies) of each cell is indicated in bold letters.

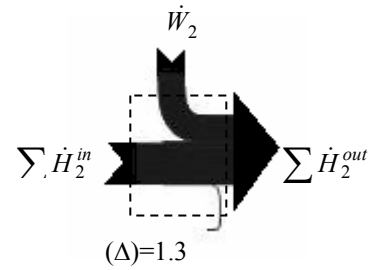
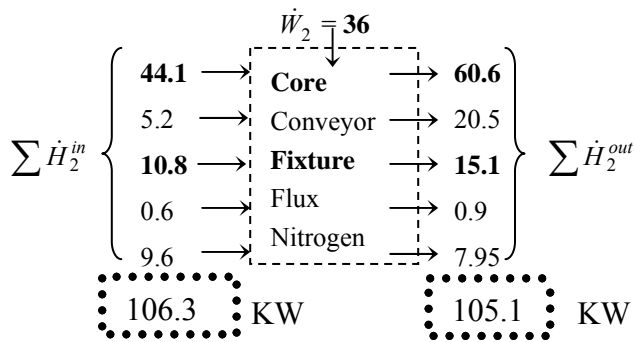
Cell 1:



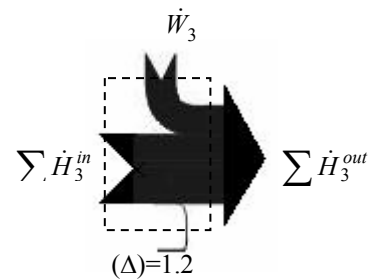
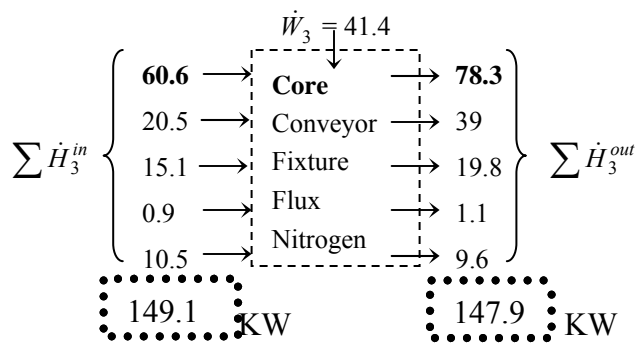
Cell Wise Energy Balances 2-15

Following the initial cell, energy flow diagrams are constructed for each subsequent cell in this section as described above for CELL 1 and an integration of these zonal balances into a system as a whole will be followed. The construction routine/methodology used to devise the Sankey diagram for each processing zone of the CAB furnace will be shown here. To easily decipher the energy interactions for each cell and to make the plot look less intricate, the arrows are drawn as consolidated sum of enthalpies of all bulk flows at entry and exit.

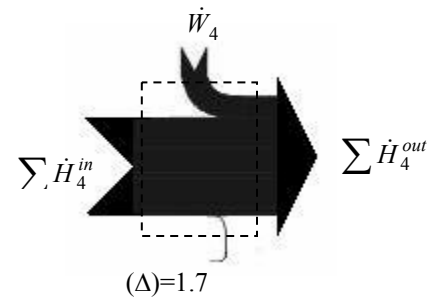
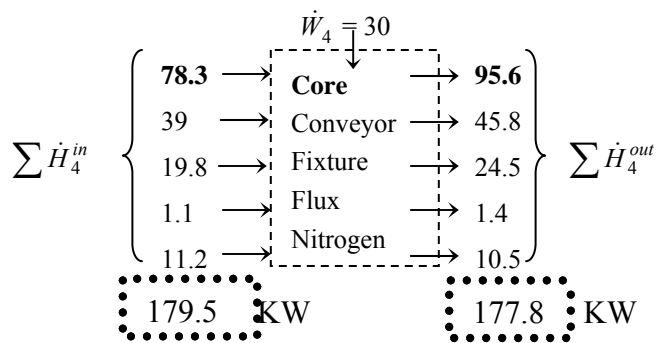
Cell 2:



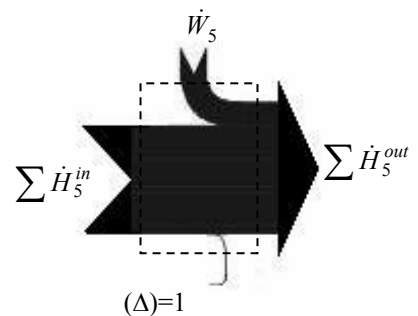
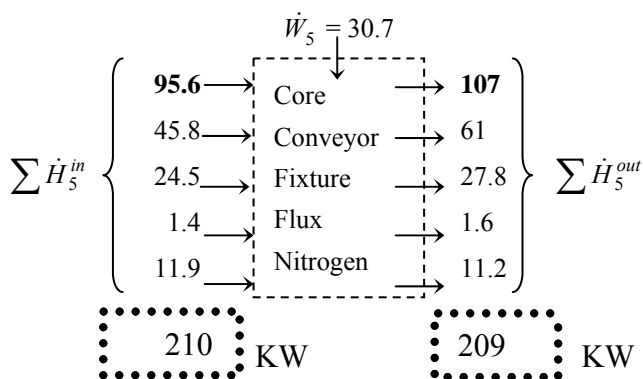
Cell 3:



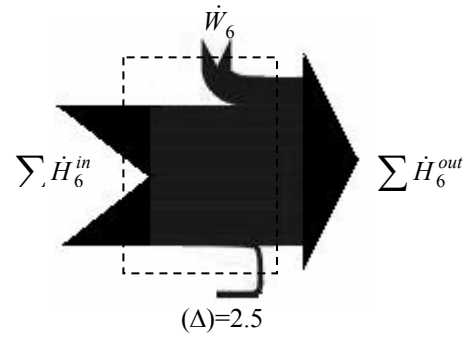
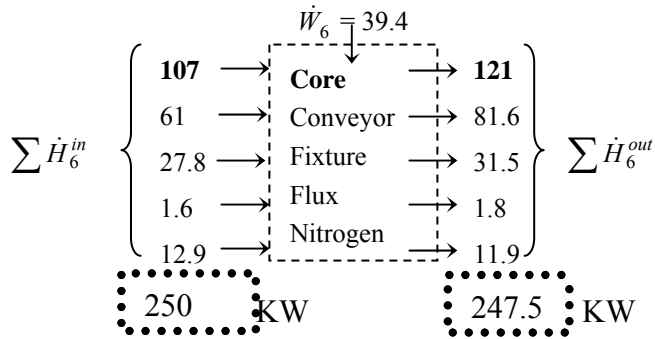
Cell 4:



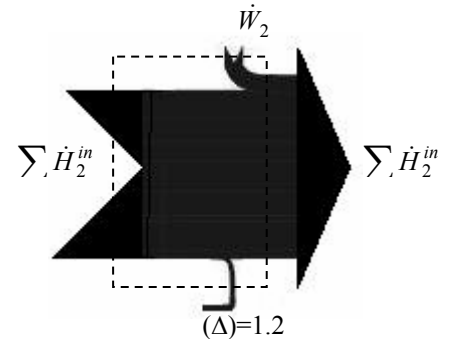
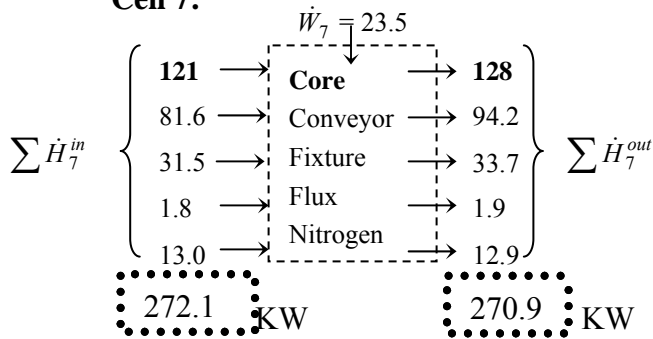
Cell 5:



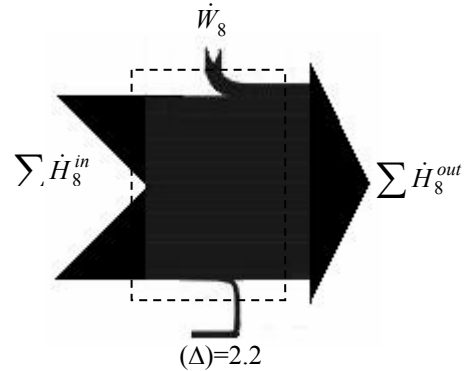
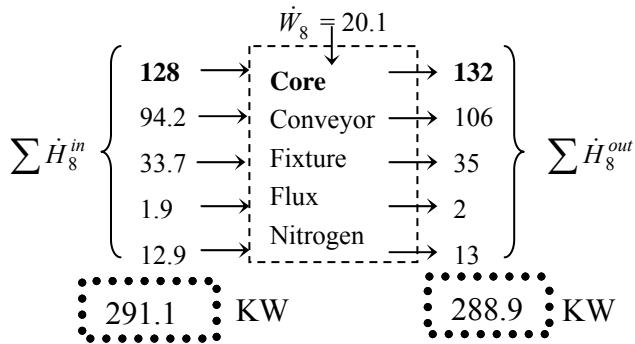
Cell 6:



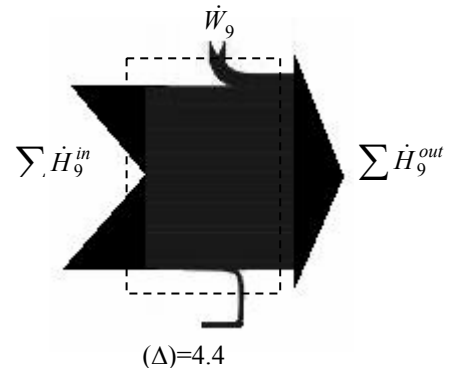
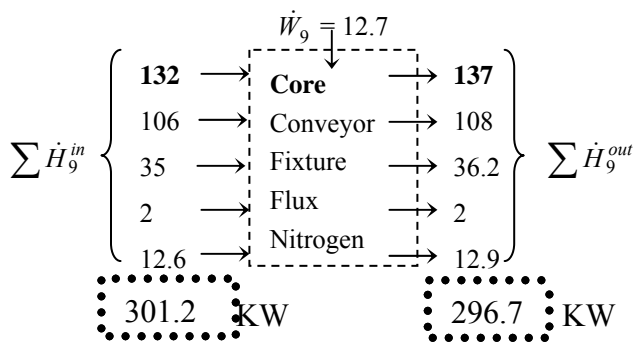
Cell 7:



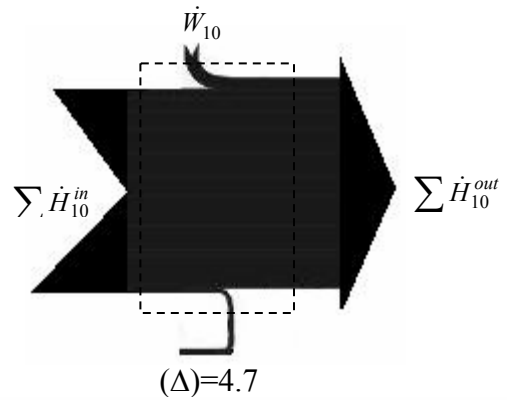
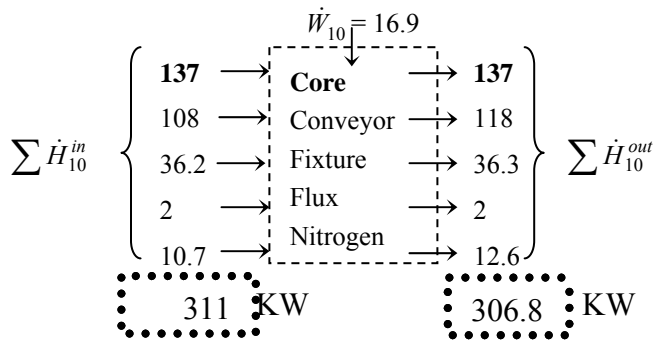
Cell 8:



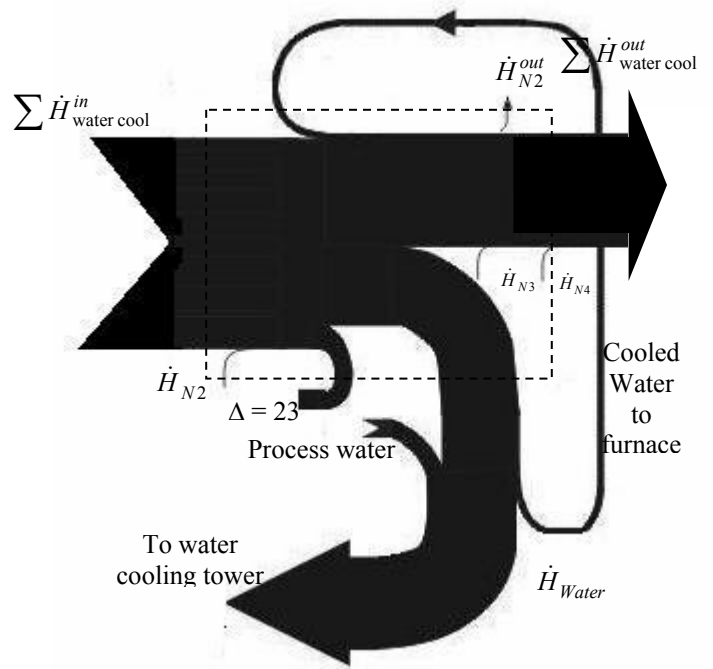
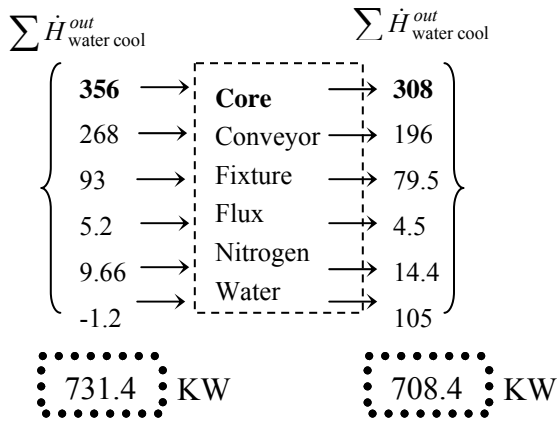
Cell 9:



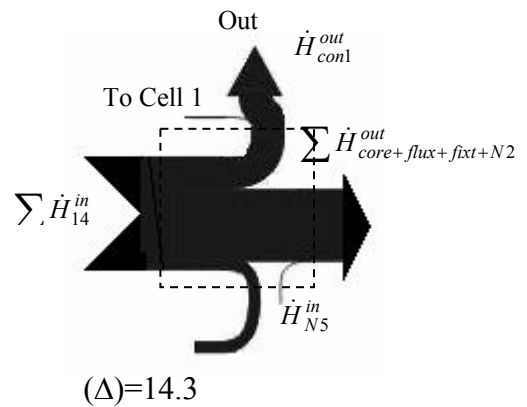
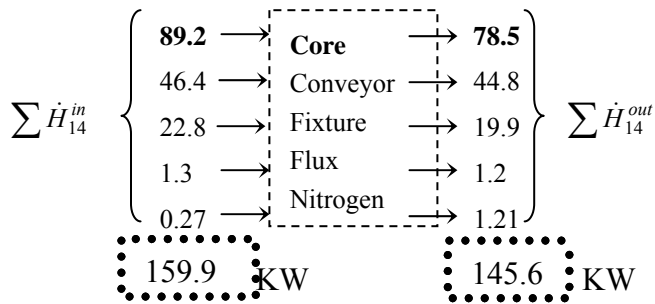
Cell 10:



Cell 11-12-13:



Cell 14:



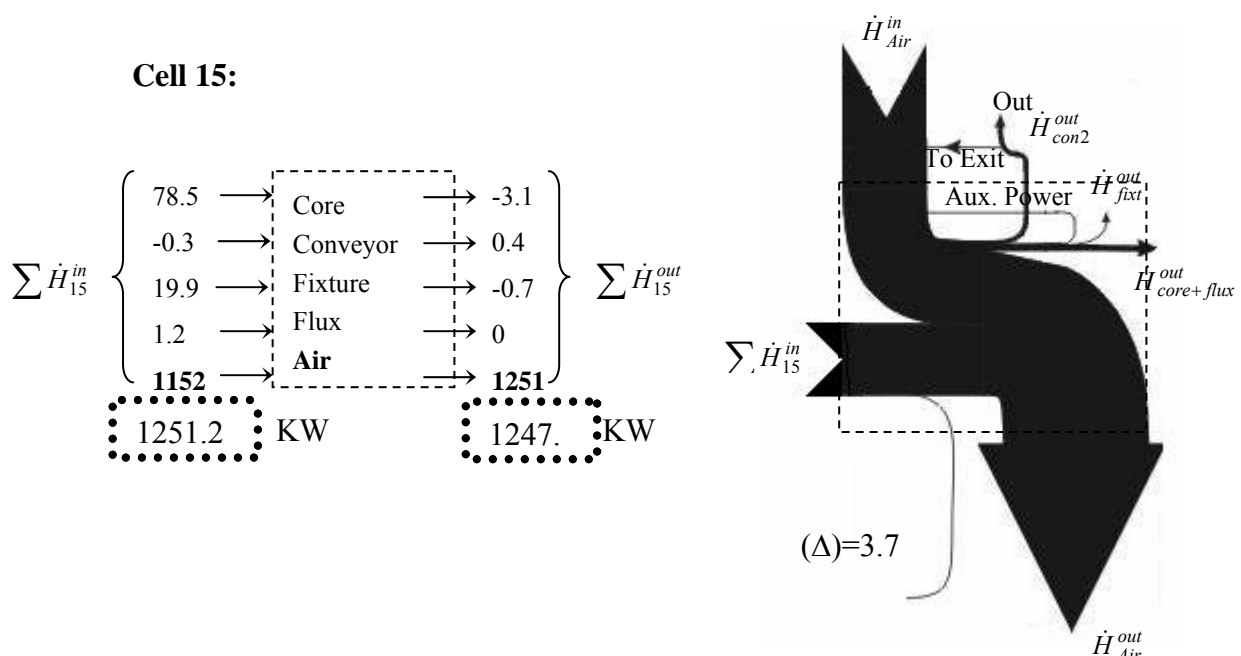


Fig. 4-2 presents the integrated energy flow (Sankey) diagram for the the whole system. As can be concluded from the energy balance, Fig. 4-2, the heat exchanger cores enter the system at an elevated temperature (due to a thermal degreasing process located upstream of the processing sequence considered in this study). A succession of energy (work) interactions (i.e., electrical heaters), after a conversion into the Joule heating inputs, increases the enthalpy rate of all the materials' flows in the direction of materials processing (except for the nitrogen flow that is facilitated in an opposite direction).

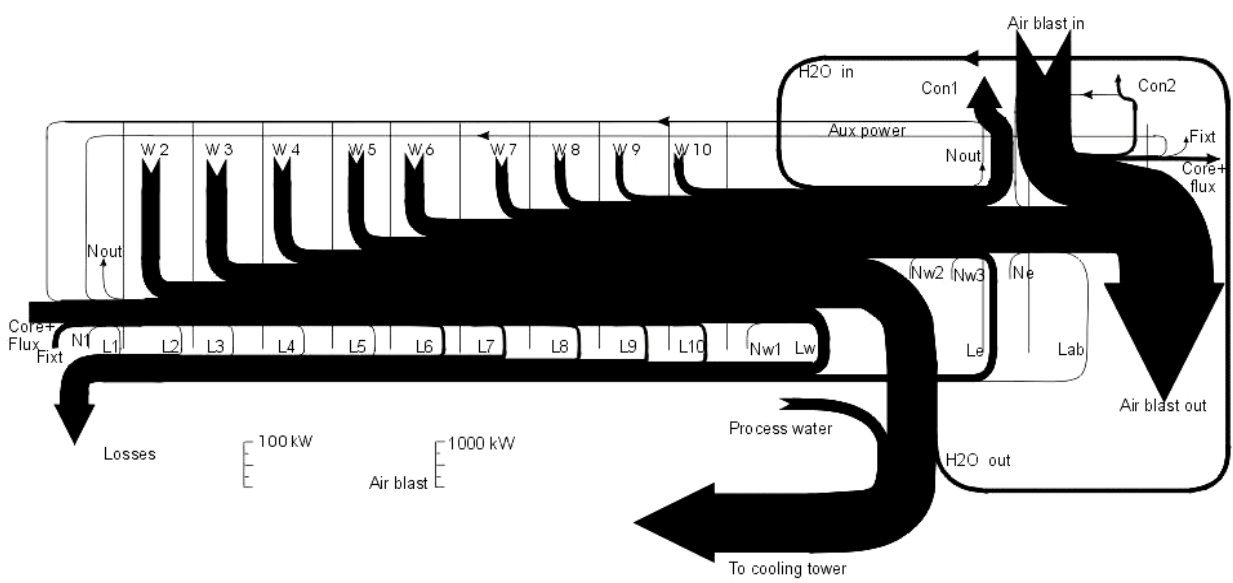


Figure 4-2 Energy (Sankey) flow diagram for a CAB system [27]

However, what becomes even more obvious from this energy flow tree (i.e., a Sankey diagram), is that most of that energy is ultimately destined to be removed by the enthalpy rates of cooling water and air blast, and dumped into the environment (or, eventually recycled in various ways – this important aspect would not be considered in this study). Note the different scales for the air blast and the rest of the system. It is obvious that energy flow diagram of a materials processing sequence may be very misleading, in particular if traditionally different referent values for the zero values of enthalpies are imposed (like for air in this case). W's represent electrical work energy inputs converted in Joule heating, and L's represent the energy balance residues at the cell level (include heat losses and/or uncertainties in data determination). Multiple Nitrogen flows' ports are denoted by N's designators.

4.3 Exergy analysis

Before we get into the details of exergy flow and its analysis, a few additional explanations are needed. Exergy represents an “available energy” magnitude of a considered system/subsystem (say a bulk fluid flow) at a given point along the flow path (i.e., change of state), in this case, materials processing sequence in a net-shape manufacturing process (CAB furnace processing of a steady stream of heat exchanger cores)*. A traditional definition of exergy (for thermal processes) of a manufacturing system's bulk flow for example, refers to an energy-related quantity that carries with its magnitude not only the energy quantity but its quality. As is the case with the energy rate, the exergy rate is expressed in units of energy power, i.e., (in W in the SI system of units). However, exergy indicates with its magnitude the quality of energy flow as well. In simplest terms: the same amount of energy rate (say 1 kW) may have different quality under different conditions of delivery. For an energy flow representing a thermal interaction (heat flow), the quality of 1 kW delivered at 1000K and alternately at 500K and subsequently used at, say 400K is far from being the same - the quality of energy rate delivered at higher temperature level is much higher and using it at the low temperature level (of 400 K) would be wasteful if the same energy can be delivered from a lower

* Note that the terms system/subsystem are used here in their thermodynamic sense, not as a system as perceived in manufacturing system analysis.

temperature level (for accomplishing the same task)! The quality level of the work (say, electrical power) is the same regardless of the temperature level involved, as long as it is delivered as work, i.e., not as heat. So the quality of thermal energy for materials' processing deteriorates along the path of the processing. Each process imperfection contributes to that deterioration through the creation of “irreversibilities” along the processing path. The irreversibility is a measure of how far a given actual process resides from an ideal one in terms of associated entropy generation in the system. These irreversibilities are the cause of exergy destruction, therefore it is important to identify each of them. Note that in our case (a brazing furnace processing of heat exchanger cores) thermal energy interactions are dominant! So, it is to be expected that the study of irreversibilities in these processes may provide an insight into the energy quality use! This is the primary motivation behind the idea to utilize the concept of exergy in a study of a manufacturing system like a CAB furnace.

Exergy, like energy, can be transferred to or from a system in three forms: heat, work, and mass flow exergies [64]. Exergy transfer is recognized at the system boundary as exergy crosses it, and it represents the exergy gained or lost by a system during a process. For an open system in a steady state, an exergy balance (analogously to the energy balance) can be written as follows: [64]

$$\sum_{i=1}^n \dot{E}x_i^{in} + \sum_{j=1}^m \dot{W}_j^{in} + \sum_{k=1}^p \left(1 - \frac{T_o}{T_k}\right) \dot{Q}_k^{in} = \sum_{i=1}^r \dot{E}x_i^{out} + \sum_{j=1}^s \dot{W}_j^{out} + \sum_{k=1}^t \left(1 - \frac{T_o}{T_k}\right) \dot{Q}_k^{out} + \Delta \dot{E}x \quad (4.7)$$

Here, the left-hand side of the equality corresponds to the inlets into the control volume, i.e. exergy transfer into the system by mass, work and heat transfer respectively. And the terms on the right hand side represent exergy transfer out of the system by mass, work and heat transfer respectively through the outlets. The outlet's exergy rates balance side must include the *exergy destruction rate* $\Delta \dot{E}x$ (due to irreversible – read this attribute as a “non ideal”-processes within the control volume)*. Each exergy rate associated with mass flow rate $\dot{E}x_i$ can be represented as:

* This destruction rate is inherent to any real process due to irreversibilities ($\Delta \dot{E}x = T_o \Delta \dot{S}_{irr}$)

$$\dot{Ex}_{in/out} = \dot{m}e_x = \dot{m} \left[h_{in/out}(T, p) - h_o(T_o, p_o) - T_o \left\{ s(T, p) - s_o(T_o, p_o) \right\} + \frac{v^2}{2} + gz \right] \quad (4.8)$$

$$s = A \ln(t) + Bt + C \frac{t^2}{2} + D \frac{t^3}{3} - \frac{E}{2t^2} + G \quad (4.9)$$

In Eq.(4.8), no chemical exergy is included. The letters *A*, *B*, *C* etc represent the coefficients (real numbers - Table 4.2), taken from the NIST database [63] and *t* is the scaled temperature in SI units (T/1000). Equation (4.8) describes the net exergy transfer by mass flow rate through the system boundary.

Material \ Coefficient	A	B	C	D	E	F	H	G
Conveyor, Fixture	18.43	24.64	-8.91	9.66	-0.01	-6.57	0	42.51
Flux	162.93	238.52	-115.99	19.87	-0.11	-3384.82	-3326.28	415.01
Core	28.09	-5.41	8.56	3.43	-0.28	-9.15	0	61.90
Nitrogen	26.09	8.22	-1.98	0.16	0.04	-7.99	0	221.02
Air	28.11	0.00197	0.0	0.0	-	-	-	-
Water	-203.61	1523.29	-3196.41	2474.46	3.86	-256.55	-285.83	-488.71

Table 4.3 Values of Coefficients in Eq(4.9) from NIST database

The exergy flows at the ports of a cell are:

$$\sum \dot{Ex}_i^{in} = \dot{Ex}_{core,i}^{in} + \dot{Ex}_{Flx,i}^{in} + \dot{Ex}_{Fixt,i}^{in} + \dot{Ex}_{con1,i}^{in} + \dot{Ex}_{con2,i}^{in} + \dot{Ex}_{H2O,i}^{in} + \dot{Ex}_{Air,i}^{in} + \dot{Ex}_{N2,i}^{in} \quad (4.10)$$

$$\sum \dot{Ex}_i^{out} = \dot{Ex}_{core,i}^{out} + \dot{Ex}_{Flx,i}^{out} + \dot{Ex}_{Fixt,i}^{out} + \dot{Ex}_{con1,i}^{out} + \dot{Ex}_{con2,i}^{out} + \dot{Ex}_{H2O,i}^{out} + \dot{Ex}_{Air,i}^{out} + \dot{Ex}_{N2,i}^{out} \quad (4.11)$$

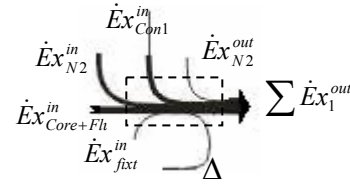
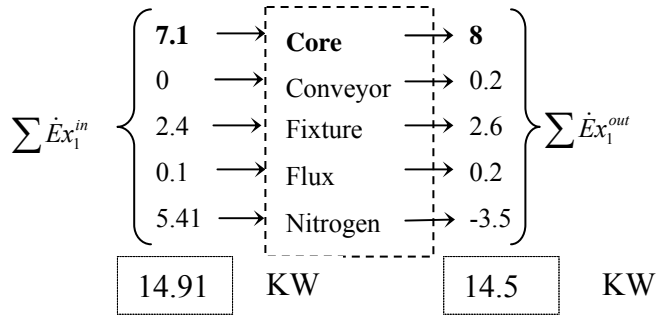
The electrical exergy (work) enters the system as Joule heating; the work and heat terms in Eq. (4.7) reduce to $\sum_{i=1}^n \left(1 - \frac{T_0}{T_{htr}} \right) Q_k^{in}$ at the heater temperature level, T_{htr} . Upon entry into the system, at the contact of the bulk flows at their surface temperature level, T_k

reduce to $\sum_{i=1}^n \left(1 - \frac{T_0}{T_k}\right) Q_k^{out}$. The detailed calculation routine for each cell using is given in *Appendix D (b)-Exergy destruction calculation spreadsheet*. Therefore, and Eq (4.7) transforms as below:

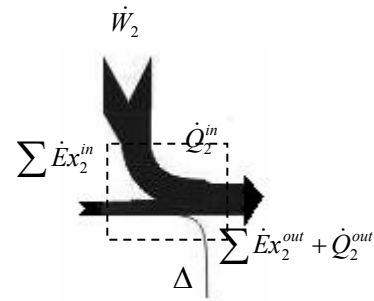
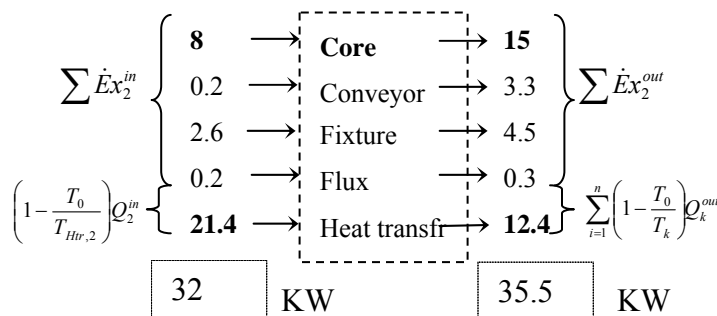
$$\sum_{i=1}^n \dot{E}x_i^{in} + \sum_{i=1}^n \left(1 - \frac{T_0}{T_{hr,i}}\right) Q_k^{in} = \sum_{i=1}^n \dot{E}x_i^{out} + \sum_{i=1}^n \left(1 - \frac{T_0}{T_k}\right) Q_k^{out} + \Delta Ex \quad (4.12)$$

Where Δ indicates the exergy balance residues at the cell level (include heat losses). (Refer *Appendix D (c)-Exergy balance spreadsheet* for a detailed calculation routine using Eq 4.12, of the exergies for each cell). The exergy flow diagram is constructed starting from the inlet into the continuous sequence of cells. The exergy flows should be assessed by marching from one cell to the other. Entropy flows for each bulk flow (for each cell) calculated using Eq. (4.9)-(4.11) are given in *Appendix D (a)-Entropy calculation spreadsheet*.

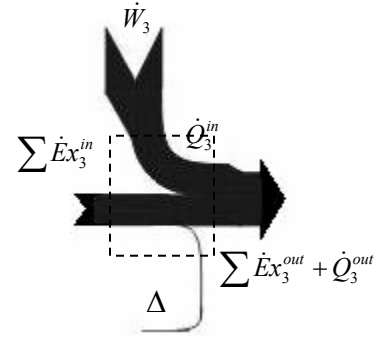
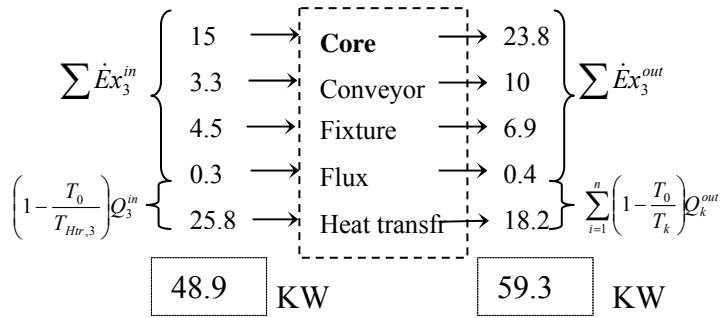
Cell 1



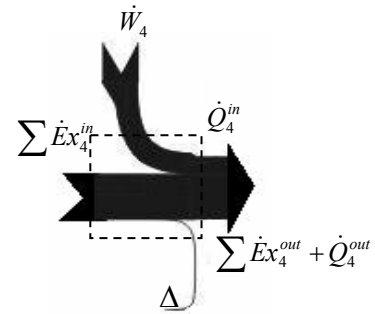
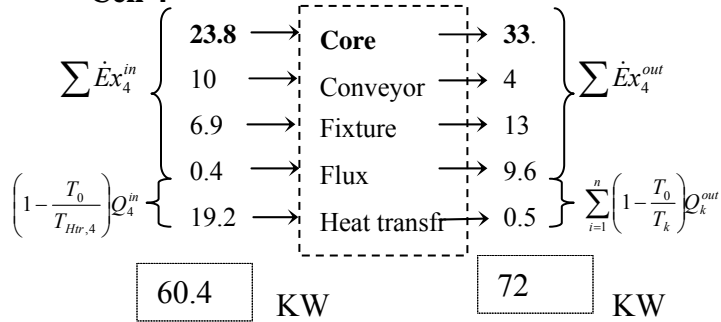
Cell 2



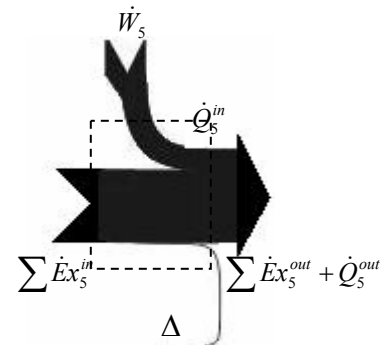
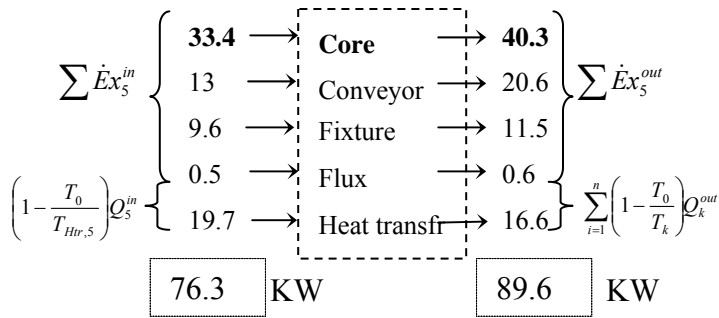
Cell 3



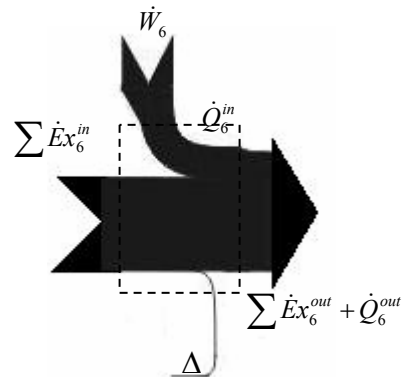
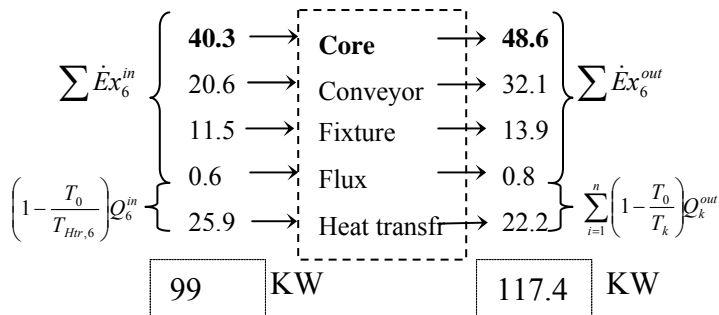
Cell 4



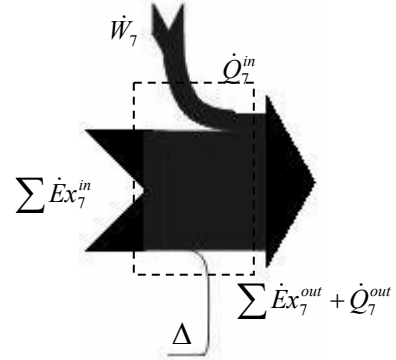
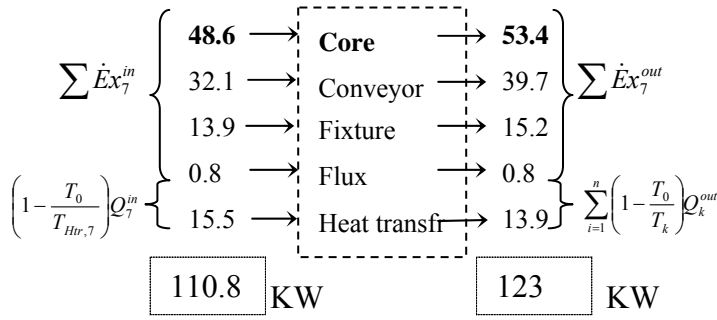
Cell 5



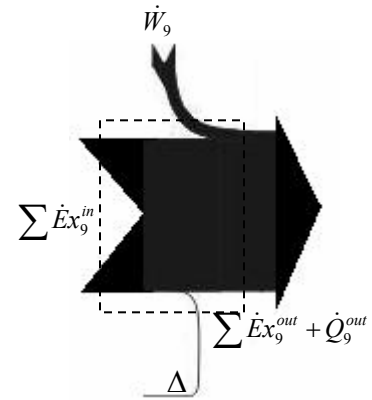
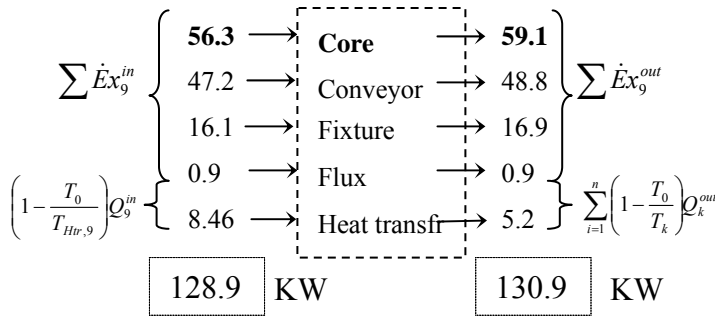
Cell 6



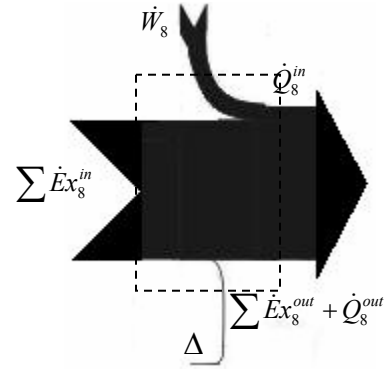
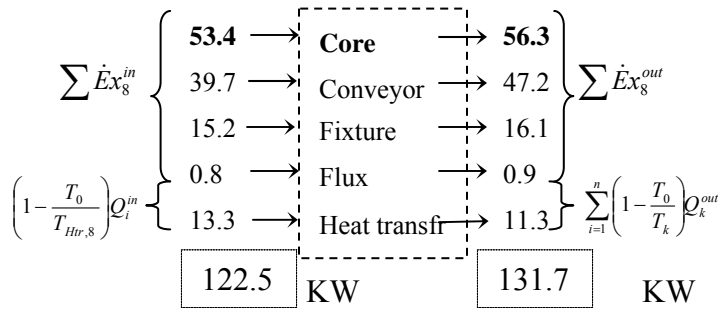
Cell 7



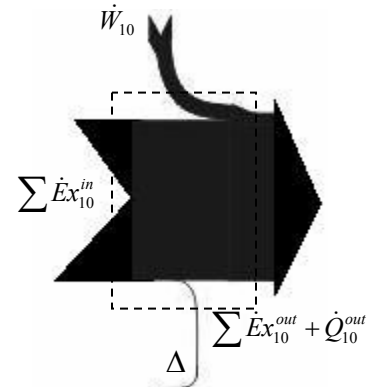
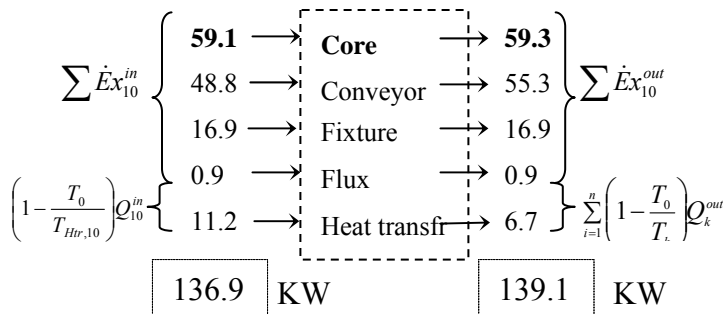
Cell 8



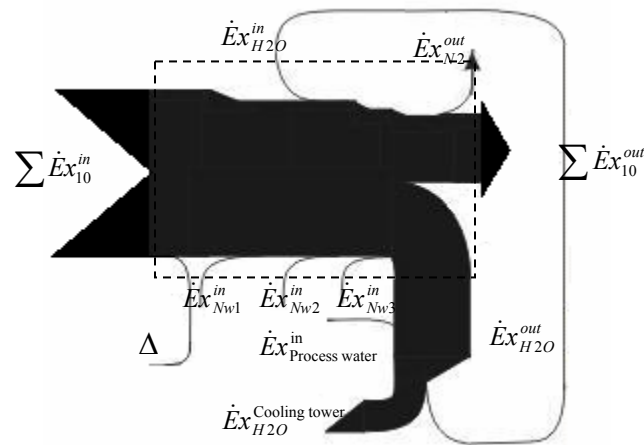
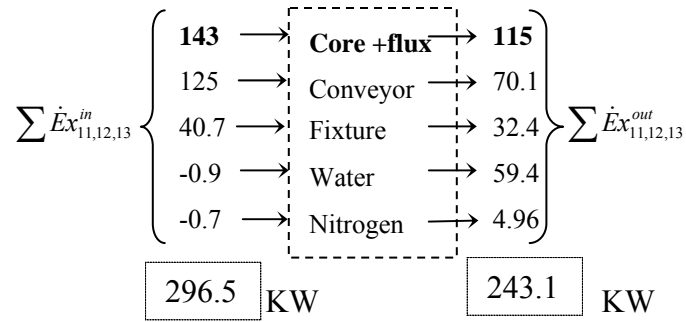
Cell 9



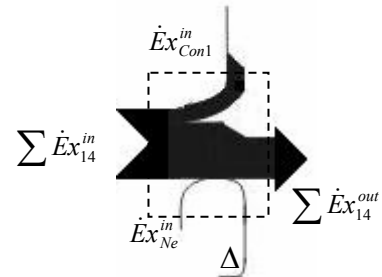
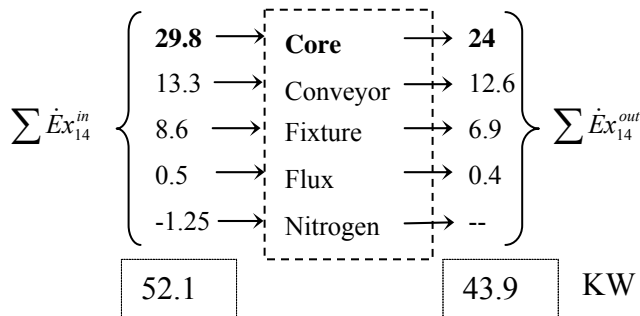
Cell 10



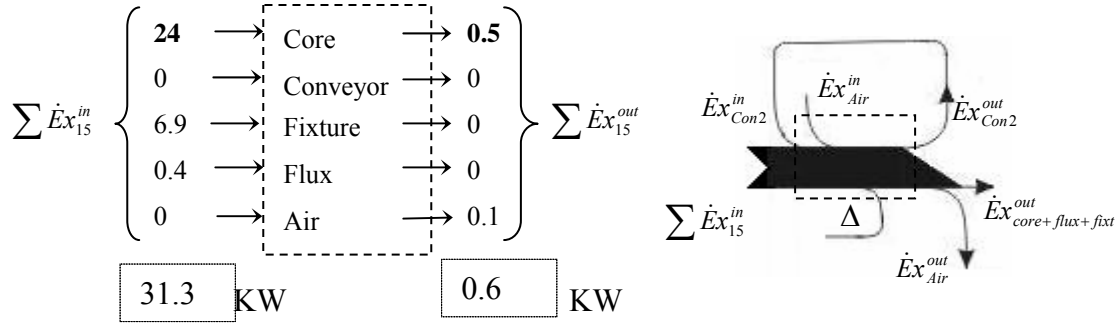
Cell 11-12-13 (Water cooling)



Cell 14 (Exit)



Cell 15 (Air blast)



The overall exergy flow of all the materials, the electrical energies and the coolants flowing across the system is represented in Fig. 4-3 below (flow from left to right indicates the direction of the material processing sequence). It should be noted that as opposed to difference in scales being used in Energy flow diagram, Exergy diagram needs only one scale to represent all the flows even if traditional reference values are used. This diagram gives insight on location, and magnitude of Second Law losses. Electrical exergy entering each heating zone is transferred into the system in the form of Joule heating accompanied with inevitable exergy destruction. An additional exergy is further destroyed inside each cell due to the heat transfer across the finite temperature difference between the heating source and product being processed. It can be clearly observed from the exergy diagram that the air and water cooling zones contribute to a destruction of significant amount of exergy during quenching.

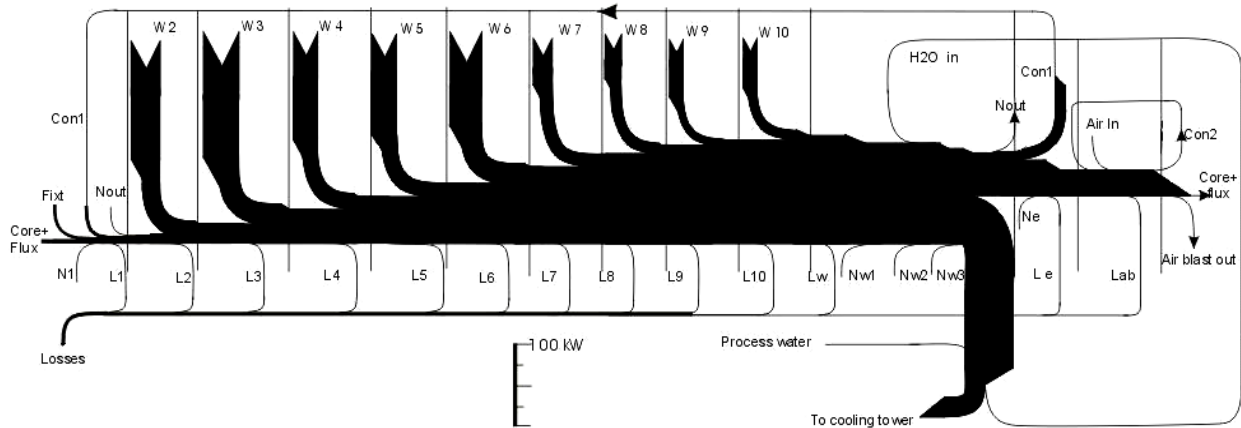


Figure 4-3 Exergy (Grassman) flow diagram for a CAB system [27]

4.4 Energy utilization for the net shape effect [27]

To determine the amount of energy for the net shape effect, one must determine the fraction of energy needed to bring cladding (throughout the heat exchanger) to the melting range and to melt this alloy during the joint formation phase (vs. the total thermal energy used to change the enthalpy of the unit) .

Table 1 A Heat Ex changer mass distribution						
Heat ex changer component	Al alloy	Density [kg/m ³]	Volume × 10 ⁶ m ³	No of pieces	Mass × 10 ³ , kg	
Fins	Core	3003	2740	362.12	49	992
	Clad	4343	2685	40.24		108
Header	Core	3003	2740	34.36	2	94
	Clad	4045	2657	8.59		23
Tank partition	Core	3003	2740	2.19	5	6
	Clad	4047	2657	0.55		1.5
Tube	No clad	Al	2710	536.31	50	1453
Tank	No clad	3003	2740	146.6	2	402
Reinforcement	No clad	3003	2740	34.42	2	94
Fittings	No clad	6061-T6	2712	16.87	2	46
Heat ex changer as a whole					Clad	132 (4%)
					Core	3088 (96%)
					Total	3220 (100%)

Table 4.4 A Heat exchanger mass distribution [27]

“This calculation is performed by taking into account: (1) design characteristics of a particular heat exchanger (see Fig. 4-4 and Table 4.2 for main features of the design), (2) related thermo-physical properties of the materials involved, and (3) temperature history of the processing (such as given in Fig. 3-3). The ultimate result of this analysis in form of energy efficiency of the net shape effect is defined as follows” [27]:

$$\text{Efficiency} = \varepsilon^* = \frac{\text{Energy needed to form the joints (to heat and melt clad)}}{\text{Total energy invested to change enthalpy of a brazed exchanger}}$$

$$\varepsilon = \frac{\sum_{i=1}^n \left(m_{clad} \int_{20}^{577} c_{p,s}(T) dT \right) + \sum_{i=1}^n [m_{clad} (c_{p,l} \Delta T + \xi \Delta h_f)]}{\sum_{j=1}^m \left(m_{core} \int_{20}^{605} c_{p,s}(T) dT \right) + \sum_{i=1}^n \left(m_{clad} \int_{20}^{577} c_{p,s}(T) dT \right) + \sum_{i=1}^n [m_{clad} (c_{p,l} \Delta T + \xi \Delta h_f)]} \approx 0.06 \quad (4.13)$$

An astonishing but expected result is obtained! Even under ideal conditions (i.e., perfect energy utilization of the furnace system with zero energy losses), only 6% of total thermal energy needed to form the joints in a heat exchanger is actually used to achieve the required net shape manufacturing effect. In manufacturing terms, only 6% of the effort is energy value added. This *is not* a consequence of a system imperfection – it is *inherent to the manufacturing process!*

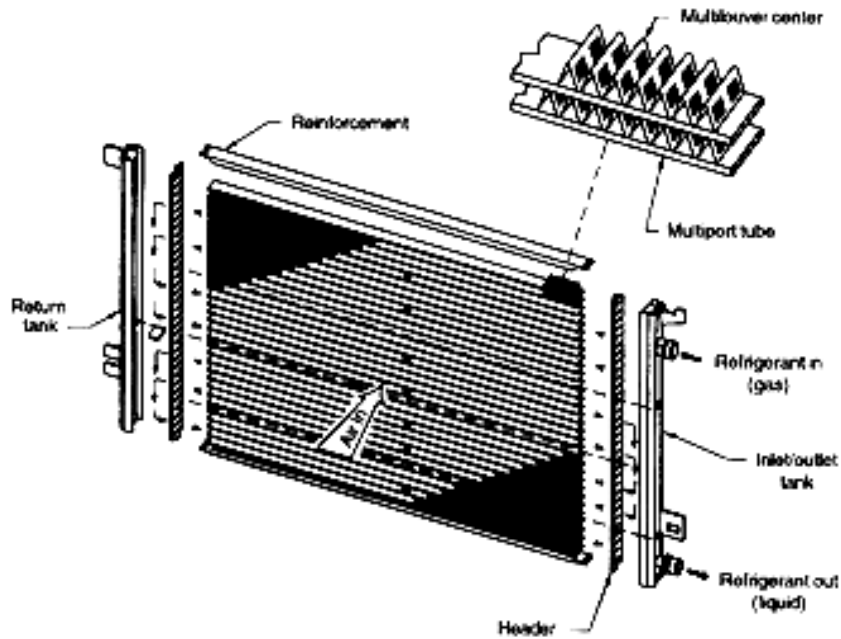


Figure 4-4 A Heat exchanger design. Compact heat exchanger – flat webbed tube and multilouver fin automotive condenser [57]

Chapter 5 SUSTAINABILITY METRICS AND IRREVERSIBILITY MODELS

5.1 Quality of energy utilization at different processing stages

After realizing the surprisingly low energy efficiency of the process used for generating the net shape, we proceed to evaluate the actual energy utilization of the brazing furnace at different processing stages. Two figures of merit of energy utilization along the segments of the considered open system are defined. The first is based on the First Law of Thermodynamics and the second one on both First and Second Law of Thermodynamics. These are *standard energy and exergy efficiencies*, as defined by energy/exergy analysis [15], and have been used to describe energy utilization in any open system exposed to a *thermal interaction*. These distributions are based on empirical (measured) values of energy demands for the brazing cycle of a system presented in Fig. 3-1, [12]. In Fig. 5-1, the results of calculations of both figures of merit for the system of Fig. 3-1 characterized by energy flows of Fig. 4-2 and exergy flows of Fig. 4-3 are summarized.

The First Law of Thermodynamics efficiency, ε , and the Second Law of Thermodynamics efficiency η may be defined as follows, [11][65]:

The First Law efficiency for a delivery of energy in form of heat from a temperature level i , Q_{hr} to a system that changes enthalpy for a magnitude $\Delta\dot{H}_{HEX}$ is as follows

$$\varepsilon_i = \left(\frac{\Delta\dot{H}_{HEX}}{\dot{Q}_{Hr}} \right)_i \quad (5.1)$$

The Second Law efficiency for the same process is equals First Law efficiency times the Carnot Factor (CF).

$$\eta_i = \varepsilon_i \left(\frac{1 - \frac{T_o}{T_{HEX}}}{1 - \frac{T_o}{T_{Htr}}} \right) \quad (5.2)$$

The First and Second law efficiencies as defined above are calculated for each of the heating stages of the process and are collected in Table 5.1. The change in enthalpy of heat exchanger for a given cell is $\Delta\dot{H}_{Hex}$. The reference temperature (T_o) is taken as 300K.

Cell	T_{HEX}	T_{Htr}	$\Delta\dot{H}_{Hex}$	Q_{htr}	ε_i	η_i	CF
2	538	743	16.51	36.0	0.46	0.34	0.74
3	612	798	17.70	41.4	0.43	0.35	0.82
4	685	838	17.28	30.0	0.58	0.50	0.87
5	744	843	11.75	30.7	0.38	0.35	0.93
6	793	883	13.33	39.4	0.34	0.32	0.94
7	834	886	7.60	23.5	0.32	0.31	0.97
8	857	889	4.51	20.1	0.22	0.22	0.98
9	873	896	4.28	12.7	0.34	0.33	0.99
10	882	896	0.27	16.9	0.02	0.02	0.99
	K	K	kW	kW	%	%	

Table 5.1 First and Second Law efficiency

In order to clearly interpret the energy utilization at different processing stages (See plot in Fig 5-1) it is very pertinent to have a clear understanding of how the figures of merit are defined and what they signify. The merit based on First Law of Thermodynamics, reveals to what extent the heating energy supplied is effectively utilized, i.e., is used to change the enthalpy of the heat exchanger core. In thermodynamics terms it is referred to as “conversion efficiency”. The figure of merit based on the Second Law of Thermodynamics is as indicated above, the FLT efficiency times the Carnot factor. This physically signifies how the temperature levels modify the quality value of an energy delivery vs. the level of energy utilization. It is evident from Table 5.1 that the influence of Carnot factor on the Second law efficiency is higher at the earlier stages of processing because the delivery of electrical energy in the form of heating energy is at higher temperatures than are the receiving temperature levels in a given zone when compared to all subsequent (higher) temperature stages of the process in the direction of the principal

material flow. Both efficiencies approach each other at higher temperature levels for the same reason i.e., gradual decrease of temperature differences between the heating sources and the processed material. Therefore, the presence of larger differences between the First and Second Law of Thermodynamics efficiencies at lower temperature zones vs. the values at higher temperature zones leads to realization that available energy utilization is less efficient at lower temperatures processing. The energy efficiency utilization is still lower at the higher temperature levels. This is due to the significant decrease of the First Law of Thermodynamics efficiency at the higher temperature levels. These temperature levels are adjusted so as to achieve required peak brazing temperature in required processing time within the imposed margin of temperature variations. In this process of achieving the brazing temperature especially at higher temperature levels, significant heat losses are present. This is why the first law efficiency at the latest heating zones at higher temperature levels is lower.

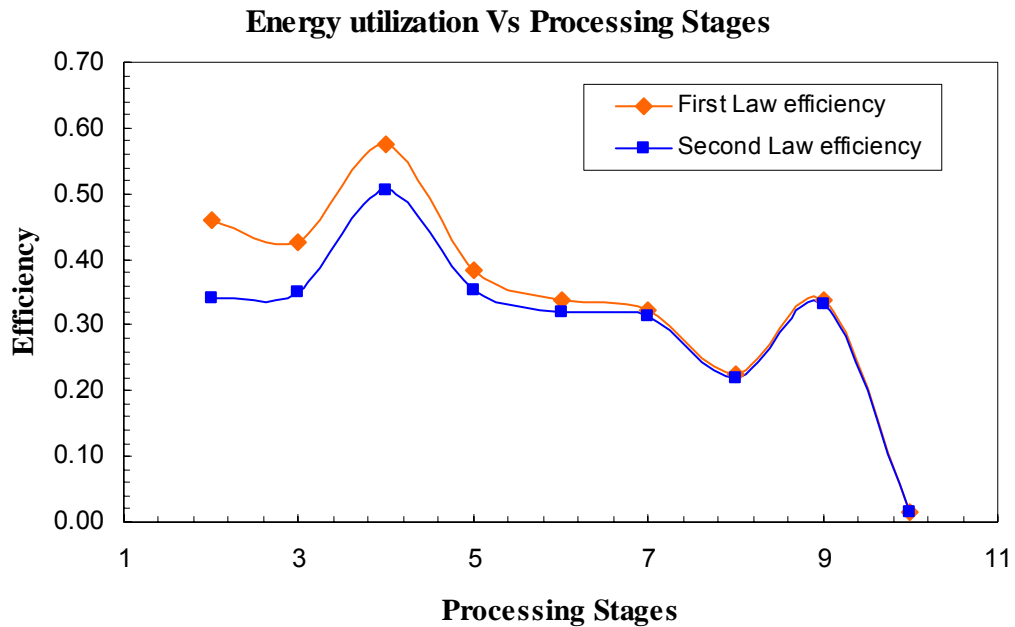


Figure 5-1 The First & Second Law of Thermodynamics efficiencies of energy utilization within the continuous CAB brazing furnace (Processing stages, 2 through 10, indicate the heating cells)

The key conclusion from this efficiency determination exercise is that both efficiencies may decrease dramatically at high temperature levels due to a significant decrease of the First Law of Thermodynamics efficiency anyway.

The system under consideration represents a state-of-the-art process. However, to achieve the desired task (a uniform peak brazing temperature throughout the heat exchanger core), a variable energy input is needed for a unit of enthalpy change of the processed object at different zones of the process, with less of it utilized for the net effect at the higher temperature level. The figures of merit considered here convey very clearly the differences in energy utilization levels at different processing stages.

5.2 Sources of irreversibility

From the discussion of the results presented in Fig. 5-1 several interesting observations may be formulated. The difference between the First Law of Thermodynamics efficiency and the Second Law of Thermodynamics efficiency dramatically decreases along the direction of materials processing. These trends can be attributed to the irreversibility levels of associated heat transfer processes due to the existence of finite temperature differences across which radiation heat transfer is delivered from electrical energy sources to the materials' streams. From Gouy-Stodolla theorem, we know that the entropy generation and exergy destruction (in energy terms) are directly related (see Eq.(1.4). Hence, by trying to identify the sources of irreversibility we try to correlate the process parameters that cause the inefficiency in the processing sequence with the energy utilization. Such an effort if pursued further may lead to a synthesis of a new approach for process optimization to the existing one by tracing the paths of irreversibility.

These irreversibilities are generated during the following processes [27]:

- (1) Thermal radiation across the finite temperature differences *between* the heating elements, heat exchanger cores, and other participants in that exchange

- (2) Thermal radiation convection and conduction *within* the heat exchanger cores, fixtures and conveyor and across the finite temperature differences during heating stages of the process.
- (3) Solid state diffusion of silicon across the clad-core interfaces.
- (4) Melting of the flux and Al-Si alloy.
- (5) Reactive flow of molten clad and friction phenomena at the peak brazing temperature.
- (6) Solidification and joint formation at the peak temperature and/or during the quench
- (7) Radiation cooling across finite temperature differences during the rapid quench (including conduction heat transfer mechanisms).
- (8) Convective cooling before and during the early stages of air blast.

Each of the listed processes contributes to the available exergy destruction through the corresponding irreversibility contributions caused by heat transfer across finite temperature differences, fluid friction, phase change and the series of irreversible mass diffusion processes.

5.3 Sustainability metrics and irreversibilities

To have a better understanding on how temperature uniformity affects the utilization of energy during the processing, its correlation with entropy generation is considered. As it is known, the Gouy-Stodolla Theorem [66] relates the loss of exergy to entropy generation through a relationship $\Delta\dot{E}x = T_{ref} \Delta\dot{S}_{gen}$, where $\Delta\dot{S}_{gen}$ represents entropy generation (a non-property, i.e., an additional production of entropy in excess to the entropy change $\Delta S = mc \ln\left(\frac{T_{final}}{T_{initial}}\right)$ due to a state change of the mass m in an idealized

reversible process). To be able to uncover these relationships an idealized lumped and realistic spatially distributed heating cases will be considered.

Let us analyze a simplified model, Fig. 5-2, for these two selected cases and two particular heating strategies. Let us assume that an object exposed to processing (a heat exchanger core in the considered manufacturing process) is being heated from the given temperature to a peak processing temperature. A graphical illustration of material processing models with two heating strategies is shown in Fig. 5-2.

“The first situation, Case A, represents an idealized limiting case: a uniform temperature is kept throughout the material (shown in the figure with a uniform color) at any instant of time. That is, the processed material is behaving as being exposed to a spatially lumped transient heating [67]. The second, Case B, represents processing accomplished under assumed finite thermal conductance to heat conduction within the material (shown in the figure with a color variation from the center to the periphery), i.e., an effective convection resistance (including a dominant radiation mechanism from the heaters) is not controlling mechanism of heat transfer. In that more realistic case, a transient heating of the object assumes a spatially distributed temperature within the material. This, in turn, inevitably leads to an irreversibility of the heat conduction within the material, and to an existence of entropy generation. This entropy generation can be calculated as follows” [28].

$$S_{gen} = \Delta S - \int \frac{dQ}{T} \quad (5.3)$$

Where ΔS is the entropy change and is calculated as follows:

$$\Delta S = mc \ln\left(\frac{T_{final}}{T_{initial}}\right) \quad (5.4)$$

And $\int \frac{dQ}{T_s}$ is the entropy flow, which is calculated using respective heat transfer relations of the model employed [68].

Case A. Eqs (5.5-5.9) [68]

The total heating energy required to heat the core from initial to final desired temperature is:

$$Q = \rho v C (T_1 - T_\infty) [1 - \exp(-\frac{t}{\tau_i})] \quad (5.5)$$

Differentiating this expression with respect to time t, we get:

$$dQ = mc (T_\infty - T_1) (-e^{-\frac{t}{\tau_i}}) (-\frac{1}{\tau_i}) \quad (5.6)$$

The temperature of the core exposed to a heating source Q at temperature T_∞ , for any instant of time t is given by:

$$T_f = T_\infty + (T_i - T_\infty) [1 - e^{-\frac{t}{\tau_i}}] \quad (5.7)$$

Dividing Eq (5.6) by (5.7), and integrate the resultant expression will be: (See *Appendix E* for detailed calculation routine)

$$\therefore \int \frac{dQ}{T} = -mc \left[\frac{t}{\tau_i} - \ln \left(\frac{T_\infty e^{\frac{t}{\tau_i}} - (T_\infty - T_1)}{T_1} \right) \right] \quad (5.8)$$

Substituting Eq (5.8) and (5.4) in (5.3) the eventual, entropy generation equation for this case is as follows:

$$S_{gen} = mc \ln \left(\frac{T_f}{T_1} \right) + mc \left[\frac{t}{\tau_i} - \ln \left(\frac{T_\infty e^{\frac{t}{\tau_i}} - (T_\infty - T_1)}{T_1} \right) \right] \quad (5.9)$$

Case B, Eqs (5.10-5.12) [68]

The total heating energy required to heat the core from initial to final desired temperature is:

$$Q = mc (T_1 - T_\infty) \left[1 - \frac{\sin \zeta_1}{\zeta_1} C_1 e^{\frac{\zeta_1^2 \alpha t}{L^2}} \right] \quad (5.10)$$

The temperature of the core exposed to a heating source Q at temperature T_∞ , for any instant of time t is given by:

$$T_f = T_\infty + (T_i - T_\infty) C_1 * e^{\frac{\zeta_1^2 * \alpha * t}{L^2}} * \cos(\zeta_1 * x^*) \quad (5.11)$$

From Eq's 5.10 -5.11, following Entropy generation equation is obtained (See *Appendix E*)

$$\therefore S_{gen} = mc \ln\left(\frac{T_f}{T_1}\right) + mc \frac{\tan \zeta_1}{\zeta_1} \left[\zeta_1^2 \frac{\alpha}{L^2} t - \ln \left(\frac{T_\infty e^{\frac{\zeta_1^2 \alpha t}{L^2}} - (T_\infty - T_1) \cos \zeta_1 C_1}{T_\infty - (T_\infty - T_1) \cos \zeta_1 C_1} \right) \right] \quad (5.12)$$

In either of the two cases, two heating strategies will be considered; Strategy 1 and Strategy 2 (see Fig 5-2). The first one assumes a constant heating source temperature level, i.e., during the entire heating (processing), the heat transfer rate is delivered to the processed material from a given high temperature level (Shown in Figure (5.2) with a uniform color in the outer ring). The second heating strategy is accomplished in a more sophisticated manner. A number of temperature levels from a number of heaters along the time line of processing deliver the required heat transfer rate (shown in the figure as intermittent heaters each with a temperature greater than the previous). In this second heating strategy, the temperature differences under which the heat transfer rate is delivered from a heater temperature level to the surface of the material are significantly reduced along the time line of heating. At the same time, the corresponding differences in the first strategy (a constant heating temperature) are at first significantly larger than for the second strategy, but subsequently may become smaller due to faster heating of the materials in a shorter period of time.

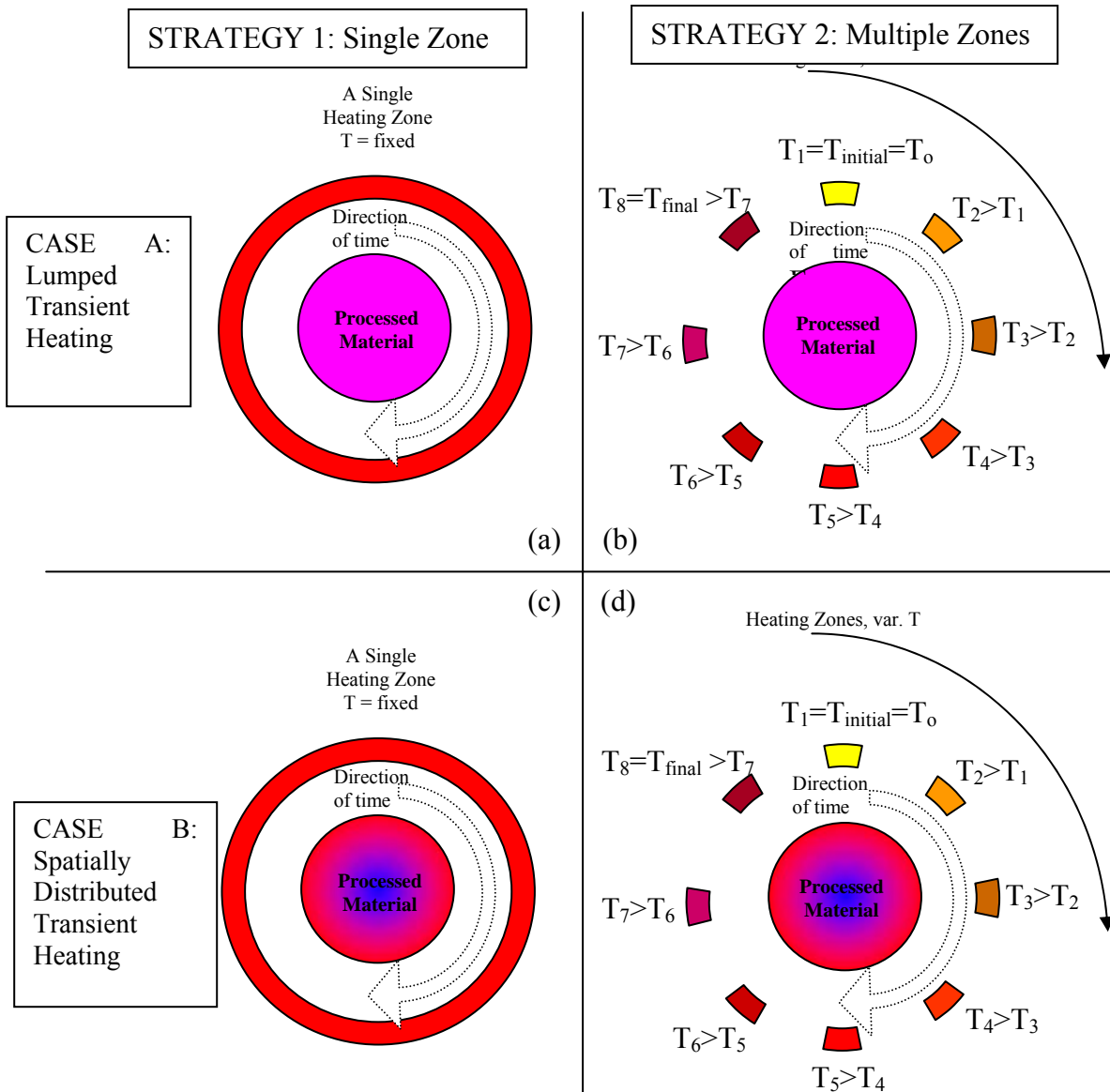


Figure 5-2 A symbolic representation of a simplified model of materials processing. Two particular cases correspond to lumped and to spatially distributed heating accomplished through two heating strategies, with either single or multiple heating stages (in time). (a) lumped transient heating with constant heating source temperature throughout (at any instant of time material has uniform but different temperature), (b) the same as (a) but the heating accomplished by using a series of heaters, each at a different, increasing temperature, (c) Spatially distributed heating with constant heat source, (d) the same as (c) but with a series of heaters, each at a different, increasing temperature [28].

Strategy	B1	B2
Tim-Seg	dT	dT
0-1.7	303	154
1.7-3.4	225	129
3.4-5.1	167	113
5.1-6.8	124	125
6.8-8.5	92	122
8.5-10.2	68	94
10.2-11.9	51	100
11.9-13.6	37	76
13.6-15.3	28	58
15.3-17	21	49
17-18.7		36
18.7-20.4		30
20.4-22.1		22
min	T(K)	T(K)

Table 5.2 Temperature differences between source and core effecting energy utilization quality.

Why such strategies are selected needs to be clear. In the second strategy, due to reduced temperature differences between the heater source and material sink, at each instant of time at the beginning of heating, the related entropy generation would be reduced vs. the strategy in which the heater temperature level is kept constant. These consequences of the selected strategies in turn will demonstrate how the quality of energy utilization during processing may be enhanced with a more sophisticated heating strategy. However, at higher temperature levels a reversal in the quality of energy utilization is possible, because of the delay in attaining the peak brazing temperature via strategy B2 and more predominantly because of greater entropy generation via Strategy B2. This can be easily attributed to the **increase** in temperature difference from level it is delivered (heater) to the level at which it is received (core). From Table 5.2, the increase in this difference in temperature is evident from the 5th time segment.

5.4 Temperature - entropy plots

Case A vs. Case B (lumped vs. spatially distributed temperature within the object) regardless of heating strategies applied demonstrate that, in the idealized Case A, entropy generation due to internal heat transfer evolution at infinite speed of thermal equalization

propagation leads to a zero entropy generation (i.e., no temperature difference exists within the material). In a realistic Case B, where spatial temperature distribution exists, thermal conduction within the material evolves with a finite resistance and thus entropy generation becomes different than zero. In that sense, the non-uniformity of a property (in this case the temperature) indicates a departure from an ideal case, i.e., from the energy utilization point of view, the quality of the processing becomes lower. At the same time, this non-uniformity is directly related to less than the optimal conditions needed for making a good quality compact heat exchanger [59], [57].

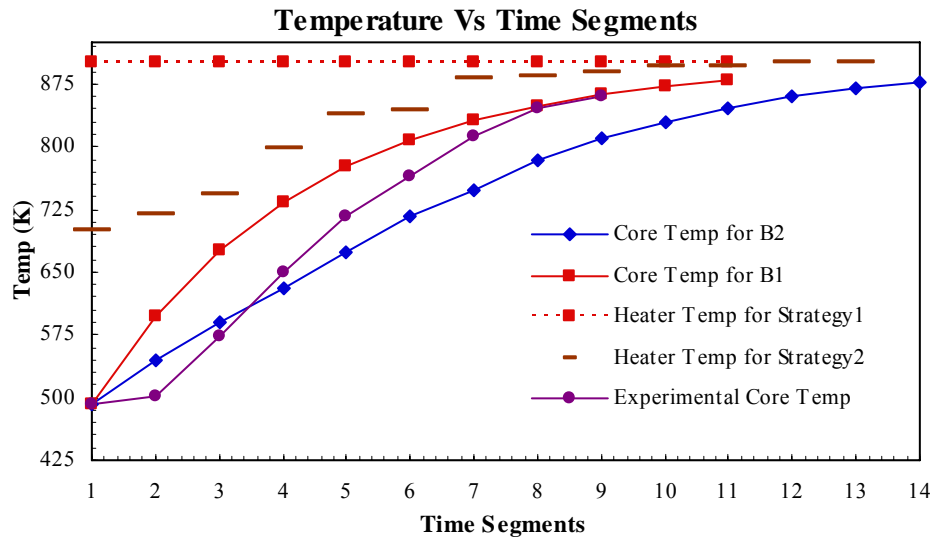


Figure 5-3 Various temperature distributions. Case (a) corresponds to the pair: Constant $T_m = T_s$ and Constant T_{hr} ; Case (c) Variable T_m and Constant T_{hr} ; (d) Variable T_m and variable T_{hr} . For the sake of comparison, the actual material temperature distribution, if the material were exposed to the same variable heater distribution as for (d), is included as well. [28]

Temperature behavior of a heat exchanger equivalent in three characteristic situations is presented in Fig. 5-3. For case A, the calculation leads to zero entropy generation, see Fig. 5-4! This is an expected result. Case A (Fig. 5-2a), a lumped heat transfer process (i.e., a uniform temperature distribution within a material at any instant of time) is, by definition, an ideal process that ensures the quality of the final product - if the

other brazing process parameters are achieved [58]. Case B (Fig. 5-2c) corresponds to a realistic situation; the entropy generation is finite, and its level indicates how far from the ideal processing the actual manufacturing outcome will be if heater temperature is constant. If the second strategy is selected (Fig. 5-3d) the temperature differences between the material and the heaters become significantly smaller in the initial stages of heating where the temperature differences between the source and material are inherently larger.

For each case, strategy and segment of heating, the corresponding entropy generation is calculated using Eq's 5.9 and 5.12 and presented in Fig. 5-4 as a function of time segments. (See *Appendix F Entropy generation calculation* spreadsheet for the calculation routine for each cell). An expected result is obtained. The constant temperature heating source (i.e., a single temperature level for the entire processing) leads to a distribution of entropy generation in time that features significantly larger irreversibilities at the beginning of the processing due to significant local (in time) temperature differences (larger than in the case of variable temperature sources). That is a clear indicator that an optimal distribution of sources may exist between the two limiting situations, Case A (idealized) and Case B. This result and the underlying logic must be explored in further studies. The area under each curve indicates the respective total entropy generated $\int \dot{S}_{gen} dt$ by process irreversibilities. This area is computed by summing up all the entropies generated for each processing cell as shown in Table 5.3. From this, it is evident that, though there is no significant difference, the total entropy generated for strategy B1 is more than that for strategy B2. This interpretation warrants a further, exploration of different materials processing models that may yield a good quality energy utilization. This aspect is not considered here.

In Fig. 5-4, the starting temperature of the processed material is 498 K, the temperature at the onset of brazing process after thermal degreasing. The experimental data for entropy generation for each heating segment are also presented in Fig. 5-4. The theoretical calculations (for Cases A and B) assume the size and mass of the processed structure to be the same as for the actual brazed heat exchanger, but with the equivalent properties defined by considering the processed unit as a porous-like structure (i.e., a

fin/tube core), with an equivalent thermal conductivity and specific heat that take into account the actual object porosity. (See *Appendix F* for detailed calculations)

	B1	B2
Tim-Seg	Sgen	Sgen(J/K)
0-1.7	76.01	38.35
1.7-3.4	46.08	28.90
3.4-5.1	30.09	23.29
5.1-6.8	20.50	24.09
6.8-8.5	14.34	22.07
8.5-10.2	10.20	16.00
10.2-11.9	7.35	16.17
11.9-13.6	5.33	11.73
13.6-15.3	3.90	8.75
15.3-17	2.86	7.08
17-18.7		5.15
18.7-20.4		4.23
20.4-22.1		3.10
min	216 (J/K)	208 (J/K)

Table 5.3 Total entropy generated for material processing models B1 and B2.

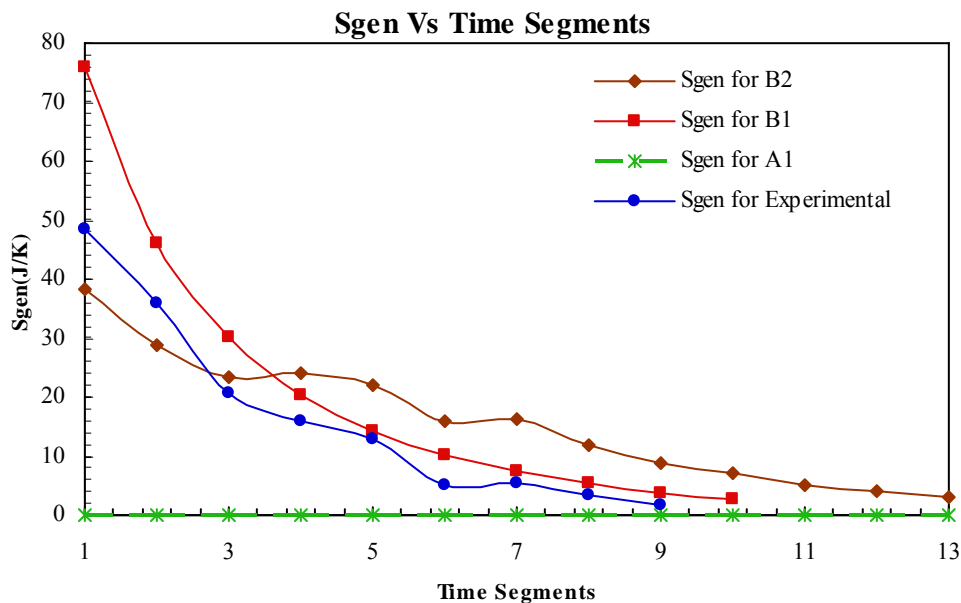


Figure 5-4 Entropy generation for theoretical model [ideal (lumped) case, and spatially distributed cases (constant and variable heating sources)], and experimental data [28]

Various scenarios may exist for performing a given task and these are not equivalent as far as the energy utilization is concerned. The worst scenario for energy utilization in the analyzed materials processing would be to keep constant temperature of the heating sources, in particular at initial time segments of processing. Variability of the temperature levels can reduce entropy generation locally (see the initial time segments in Fig. 7), but optimization of this distribution is a complex matter and an overall reduction of energy utilization may be achieved with different scenarios. It is interesting to note that the data taken from an actual system indicate poorer entropy generation status at the initial stages than obtained using a simplified model and a distribution of sources. At the later time segments of processing, the considered system seems to be well tuned.

5.5 Non-uniform temperature, product quality and sustainability metric

As it is stated earlier, the objective of the net shape manufacturing system under study is to deliver a good quality product, which in this case is a brazed heat exchanger core for automotive applications. There may be different criteria to decide the quality of the heat exchanger core. The good quality in this case is existence of joint formations at all the mating surfaces meeting points. For a given selection of material and optimal selection of brazing parameters, this goal may be achieved only with a as uniform temperature distribution within the core as possible. So, uniform core temperature is the criterion which must be satisfied to get needed mechanical joint integrity and thereby the quality of product. In this section, an attempt to quantitatively establish a sustainability metric that may link the non-uniformity in the product temperature to energy utilization is made. So, an assumption is that both the good quality and good energy efficiency are compatible objectives and it can be achieved with appropriate irreversibility of processing control [69]

5.5.1 Temperature non-uniformity across the heat exchanger core

We start an analysis of quality vs. energy efficiency with establishing the point of existence of non-uniformity in temperature across the core. The heat exchanger core is exposed to an influence of a series of electrical heaters located at the top and bottom of the

braze furnace muffle. The cross sectional view of the braze furnace muffle and the illustrated positions of core with respective heating inputs are shown in Fig.(5.5).

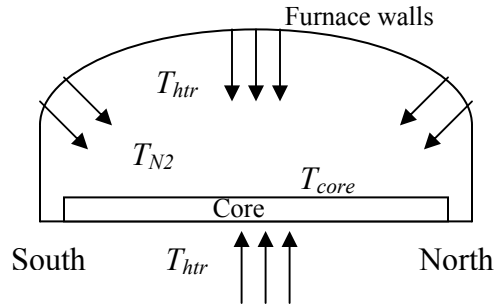


Figure 5-5 Cross sectional view of brazing furnace muffle

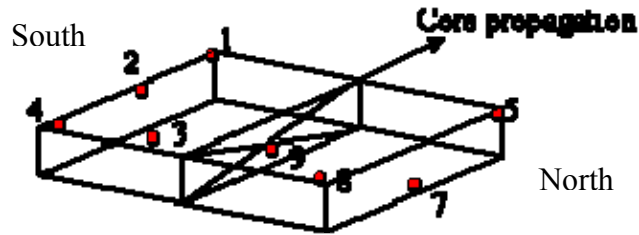


Figure 5-6 Thermocouple locations on traversing Heat exchanger core

Temperature distributions of the heat exchanger core that are monitored in real time continuously throughout the processing sequence at eight different locations on the core is known. The locations of the thermocouples monitoring temperature at each instant of time are shown in Fig 5-6 below. (See *Appendix B (a) Temperatures of each cell*, for the measured values of temperature at the entry and exit ports of each cell)

In the following plots Fig 5-7 and Fig 5-8 the temperature profiles of selected points of the core are plotted. These plots further reveal the existence of the non-uniform temperature, especially at peak brazing temperature.

1) Thermocouples: (1st T/H South; 22 T/H south; 44 T/H North, Mid-core)

Thermocouple locations:

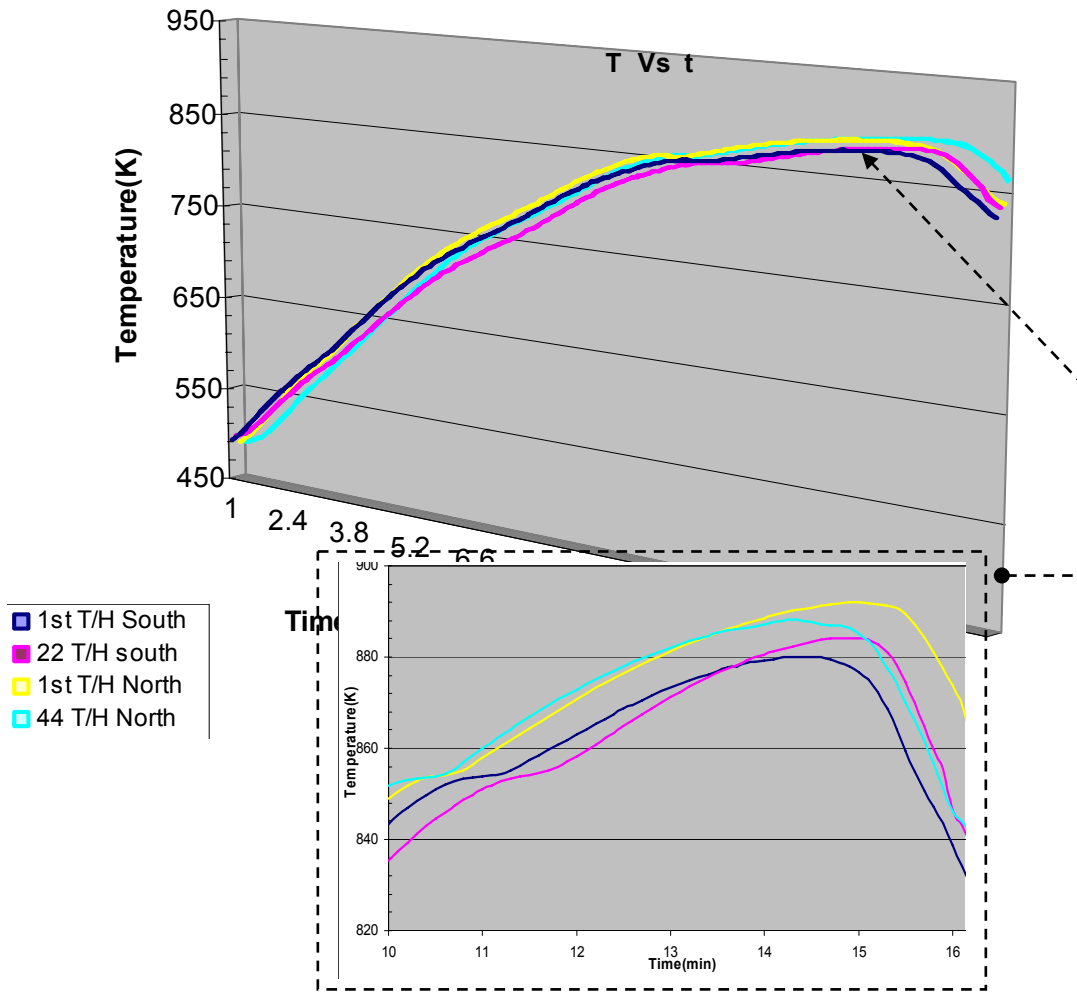
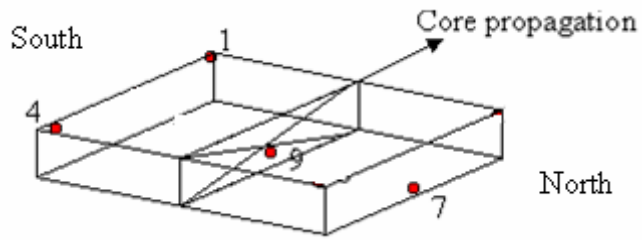


Figure 5-7 Temperature Non-Uniformity measured by thermocouples at points across the 2nd diagonal @ peak brazing temperature 875K

2) Thermocouples: (1st T/H South; 44 T/H North; 22 T/H south; 1st T/H North)

Thermocouple locations:

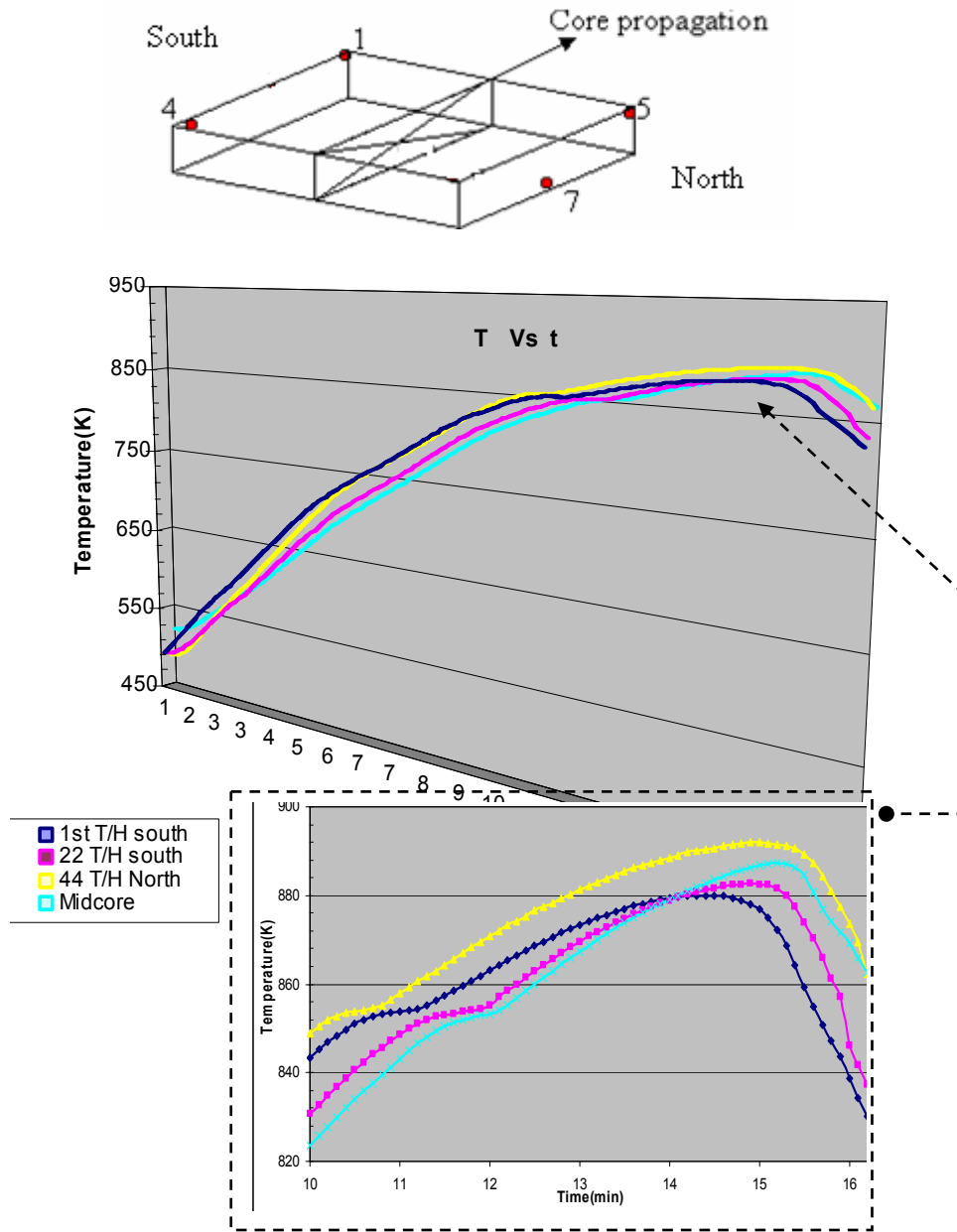


Figure 5-8 Temperature Non-Uniformity measured by thermocouples at points across the 2nd diagonal @ peak brazing temperature 875K

“An important additional aspect of the insight gained is worth emphasizing. An apparent indicator of the expected energy resources utilization deterioration in terms of entropy production is the processed material temperature non-uniformity. In real processing, as long as conventional radiation or convective heating is used, temperature non-uniformity is inevitable. In Figures 5-7 and 5-8, experimental data for the temperature difference across a core unit (between the diagonal corners of a rectangular core located at top surface of the unit) during processing is indicated. The largest temperature differences before the onset of a quench (i.e., for time less than 13 minutes) are within the first four stages of the process, the same ones that feature the largest differences between the First and Second Law of Thermodynamics efficiencies and the largest entropy generation. The maximum allowed margin of +/- 10 K at peak brazing temperature leads to an acceptable product quality, but requires a prolonged heating cycle. In any case, optimization of temperature regimes through selection of heat sources and temperature levels clearly may be performed and should be utilized” [28].

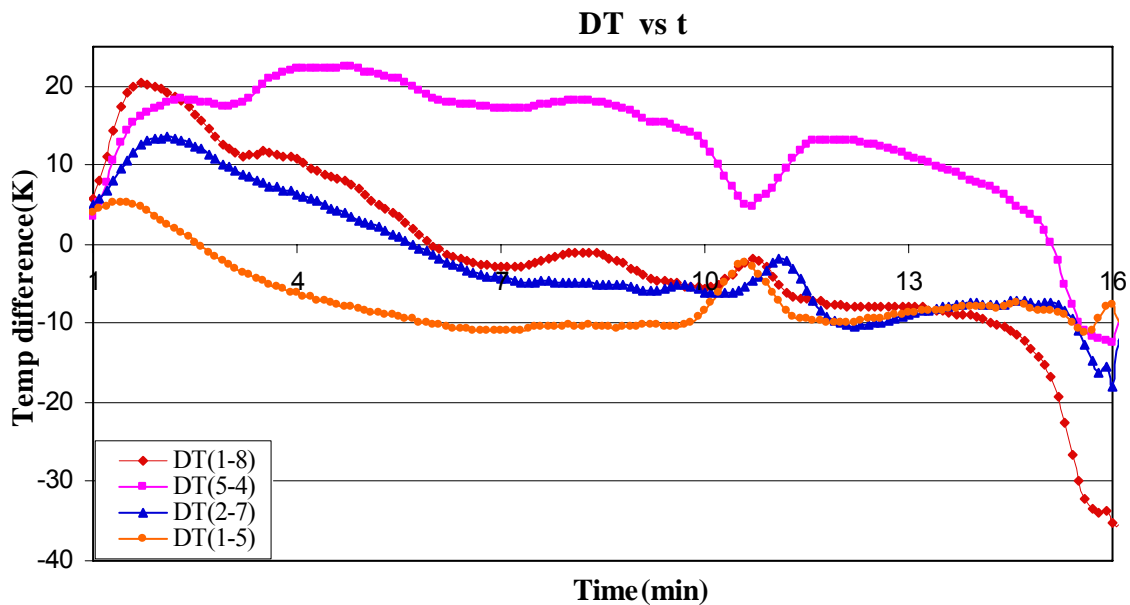


Figure 5-9 Temperature differences history across different locations on the processed material.

5.5.2 Prolegomena for a sustainability metric, uniform core temperature and product quality

At several instances earlier in Chapters 3 and 4, the fundamental role of the ‘difference in temperature’ between the level at which the heating energy is delivered (heater) and the level at which it is received (core) is indicated. We have seen its influence on First and Second Law figures of merit for energy utilization and also on entropy generated in simplified materials processing models with two heating strategies, discussed earlier in this chapter. Hence, a closer look at this parameter is warranted. The difference in the heater temperature (an average value determined by considering the heater draw measured for 30 min) and equivalent core temperature (average value of all the eight local temperatures within the core), is calculated and its variation with respect to different processing stages of the brazing furnace is plotted in Fig 5-10. It is interesting to note that from the Figure 5-10 below, that the temperature difference between core and heater decreases continuously towards the last heating zone.

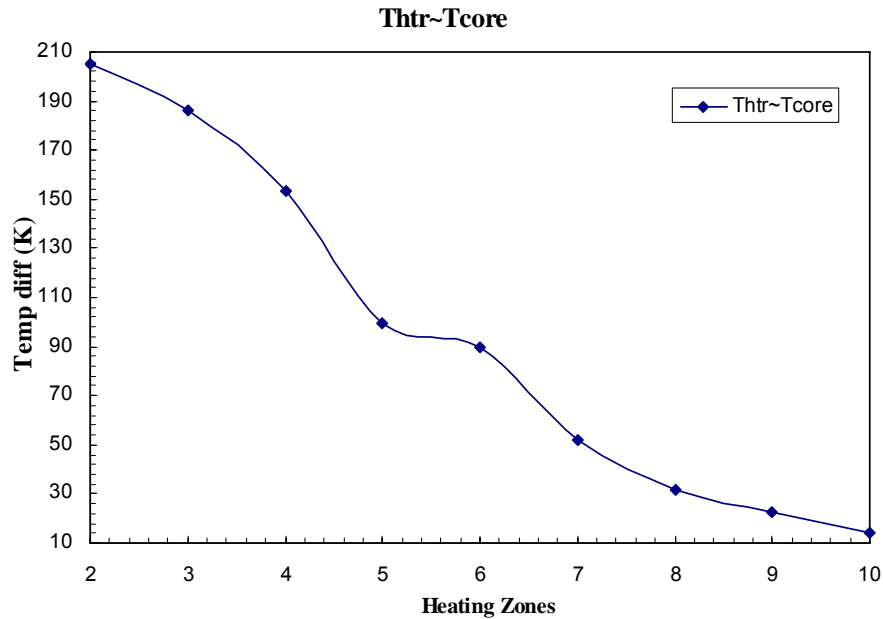


Figure 5-10 Temperature difference between Heater (T_s) and processed material (T_{core}). Zones 2-8, indicate the heating stages of the process of the furnace.

The First and Second Law figures merit discussed in Sec § 5.1, elucidate about the quality of energy utilization at different energy delivery levels, which is a valuable tool to identify and trace the locations of inefficiency at different processing stages of the CAB furnace, and thereby interpret the associated irreversibilities. Now, to establish a link between the quality of the product and sustainable energy utilization a metric ‘exergy inefficiency’ that deals with exergy destruction is more apt. Such a sustainability metric that may quantitatively indicate the product quality based on the temperature uniformity across the heat exchanger core will be an indispensable tool in identifying a given manufacturing system as a ‘sustainable’ system.

The exergy inefficiency of a processing zone i , for delivery of electrical exergy in from of Joule heating inputs from a temperature level i , to a system that changes exergy of the core is as follows:

$$v_{Ex,i} = 1 - \frac{\dot{Ex}_{core,i}^{out}}{\dot{Ex}_{supplied,i}} \quad (5.12)$$

The values of total exergy supplied and exergy of the core at the outlet of each cell are calculated and are illustrated in the following table.

Cell	$\dot{Ex}_{supplied}$	$\dot{Ex}_{core,i}^{out}$	$v_{Ex,i}$
1	15.0	7.4	0.50
2	53.4	26.9	0.50
3	70.9	45.8	0.35
4	77.5	61.5	0.21
5	93.6	78.3	0.16
6	119.3	100.7	0.16
7	125.4	115.4	0.08
8	135.5	126.7	0.06
9	139.0	131.6	0.05
10	146.3	138.1	0.06
11	131.8	127.6	0.03
12	95.0	89.1	0.06
13	69.0	65.1	0.06
Exit	50.8	43.7	0.14
AB	31.3	0.6	0.98
	kW	kW	%

Table 5.4 Exergy inefficiency of the different processing stages.

In Fig 5-11, the exergy inefficiency with respect to each processing stage of brazing furnace is plotted. It is very interesting to note from this plot that the exergy destruction is relatively larger at the initial and later stages, but not at the peak heating stages of the process. This can be easily attributed to the larger differences between heater and core temperatures at the initial stages and to the large dumping of quality energy in the water and air cooling zones at later stages.

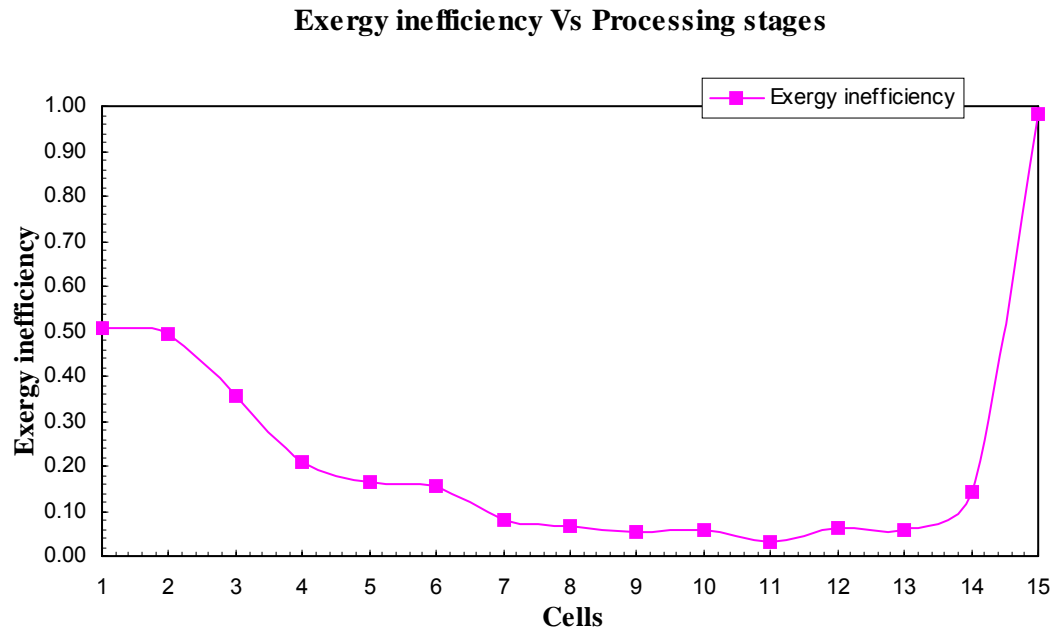


Figure 5-11 Exergy inefficiency of the different processing stages.

While the finite temperature difference were established between heater and a heat exchanger unit, the finite temperature differences were formed *within* the unit itself, see Figure 5-12. If we take a closer look at the Figure 5-11 and Figure 5-12 (temperature differences history across the process material), an intuitive relation between the product quality and sustainable energy usage may be revealed. The trend in these two plots appears to be the same, having higher exergy destruction for higher temperature difference across the core and vice-versa.

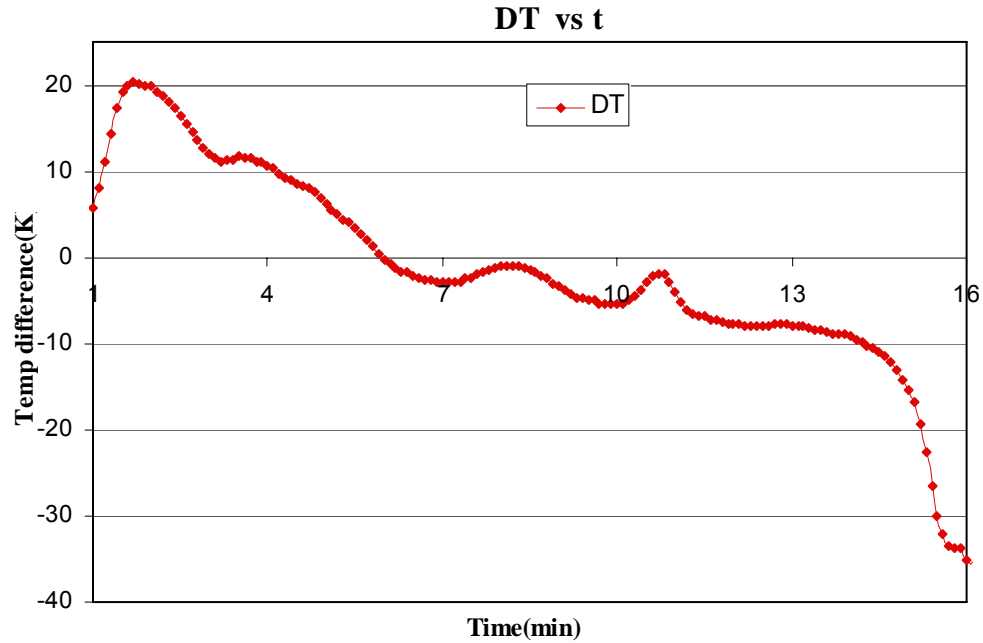


Figure 5-12 Temperature differences history across the processed material. The difference measured across the top surface diagonal of a heat exchanger unit during processing in a continuous controlled atmosphere-brazing furnace [28].

Although these inferences may be the interpretation of the results in the defined way, a more thorough and rigorous approach considering the other important factors of product quality needs to be developed. Such an analysis, based on exergy based figure of merit, would identify the sustainable ‘energy utilization’ of a given manufacturing system.

Chapter 6 CONCLUSIONS AND FUTURE WORK

6.1 Conclusions

The analysis reveals that, there is a good potential for an improvement of energy efficiency in even a most widespread, state-of-the-art manufacturing process, such as CAB brazing. This process is characterized with the extremely low efficiency. An approach based on an identification of inherent irreversibilities in materials processing is developed. It is shown that an energy balancing and exergy based analysis can provide an insight into both First Law and Second Law of Thermodynamics efficiencies of materials processing segments. It is demonstrated that the analysis tools developed for energy systems sustainability studies can be applied to sustainability analysis of manufacturing systems and processes.

A study of energy and exergy flows through a continuous net shape manufacturing process associated with CAB of compact heat exchangers in mass production indicates in particular that

1. Temperature differences at lower temperature levels should be reduced (what may be accomplished, for example, by adjusting the number of temperature zones with the lower set-point temperatures)
2. The energy dissipation at higher temperature levels should be reduced, say, by pre-heating of the nitrogen flows (not likely), by a better insulation and/or by making modifications of the furnace geometry (more likely).
3. Water cooling and air blast processes are the sources of major energy inefficiencies in the system.
4. The use of non-localized energy flux to perform the task (i.e., realization of joint formation) seems to be the inherent source of problems leading to lower energy utilization and larger entropy generation. These effects are quantitatively identified.

The following insights on the considered process in general, have been gained from the analysis conducted:

- ❖ The measure of irreversibility based effectiveness may be used as a figure of merit of the energy utilization of the analyzed process.
- ❖ Entropy generation approach provides an insight into non-energy related aspects of materials processing important for process development/optimization of a manufacturing system.
- ❖ The low efficiency may not be a consequence of system imperfection - it may be inherent to the manufacturing process!
- ❖ Lower energy utilization efficiency of a state-of-art system clearly indicates a need for further development of the process, or development of a new and more efficient one.
- ❖ The main goal in selecting an energy efficient process may not be to achieve maximum efficiency; rather to achieve an optimal trade-off between efficiency and factors such as economics, sustainability, environmental impact, safety, and societal and political acceptability, while, at the same time to generate the high quality product.

6.2 Future work

The following aspects of the CAB process which are not considered in detail in this thesis, and which are beyond the current scope, should be investigated further.

- ❖ A detailed study of individual irreversibility contributions during material's processing (uncovering relationships between process parameters and irreversibility levels).
- ❖ Optimization of temperature levels for delivery of needed heat transfer rates in the most efficient manner.
- ❖ Optimization of materials and energy flows and identification of their practical implications on a departure from optimum.
- ❖ Study of possible heating options, mainly the use of localized energy flux, like heating induced by an electromagnetic field, to perform the joint formation and its economic feasibility for a large scale operation.
- ❖ Uncovering the relationship between product quality and efficient utilization of energy resources through irreversibility analysis.

As this research clearly identifies the potential of an exergy based approach for doing a sustainable 'energy utilization' analysis for a continuous manufacturing system, there are various aspects of the approach that should be further investigated. To accomplish this, the following key directions are identified:

- ❖ Inclusion of environmental influences through an identification of the effluent flows, in terms of exergy.

- ❖ An exergy flow deterioration (identified either through the exergy balance or entropy generation calculation), may be related, at least in principle, to a monetary value of its rate. The relation between technical features of the processing and monetary values of losses may allow building of an objective function that may be optimized in the same manner as has been done for energy systems using the tools of thermo-economics.

- ❖ To assess the potential of increased energy efficiency as a measure for promoting sustainable development by considering practical limitations on increased energy efficiency.

Eventually, the idea is to extend this approach of exergy based study of sustainability analysis to other manufacturing (materials processing) processes. The approach developed in this study is of relevance for any other manufacturing process if a rigorous identification of its interaction with the surroundings (energy, materials, economic) can be defined. It will represent the coherent framework for developing an energy efficient, economically affordable and environmentally friendly manufacturing technology.

References

- 1 Visionary Manufacturing Challenges for 2020, (NRC Report, National Academy of Sciences), National Academy Press, 1998.
- 2 I.S. Jawahir, *Research Collaborative Grant (RCG) Proposal: Planning Grant for Establishing a NSF-Funded Engineering Research Center (ERC) for Sustainable Products, Processes and Systems at the University of Kentucky*, 2003.
- 3 Marechal, F., Favrat, D., and Jochem, E., Energy in the perspective of the sustainable development: The 2000 W society challenge, Resources, Conservation and Recycling, *Resources, Conservation and Recycling*, Vol. 44, No. 3, June, 2005, pp. 245-262
- 4 DOE-EIA, 2004 *Annual Energy Review 2003*, <http://www.eia.doe.gov/emeu/aer/contents.html> (April 3, 2005).
- 5 Christopher Russell, *Efficiency and Innovation In US Manufacturing Energy Use* - U.S. National Association of Manufacturers (NAM), Energy Efficiency Forum - Washington, D.C., 2004, pp. 1-37.
- 6 SECO/Warwick, *Controlled Atmospheric Aluminum Brazing System*, BZ134, p.6
- 7 Swidersky, H.-W., *Aluminium brazing with non-corrosive fluxes - state of the art and trends in NOCOLOK® flux technology*, Tagungsband Hartund Hochtemperaturlöten und Diffusionsschweißen, DVS-Berichte Bd. 212, Düsseldorf: DVS-Verlag, 2001, pp. 164-169.
- 8 Sekulic, D. P., University of Kentucky, Lexington, Personal Communication, 2004.
- 9 Sekulic, D. P., University of Kentucky, Lexington, Personal Communication, 2003.
- 10 Pelster, S., Favrat, D., and von Spakovsky, M.R. The Thermo-economic and environmental modeling and optimization of the synthesis, design, and operation of combined cycles with advanced options, *J. of Engineering of Gas Turbines and Power*, Vol. 123, 2001, pp. 717-726.

- 11 Bejan A., Tsatsaronis, G., and Moran, M., *Thermal Design & Optimization*, John Wiley, New York, 1996.
- 12 Bosanjakovic, F., *Technical Thermodynamics*, Holt Reinhart and Winston. New York, 1965 (6th German ed., *Technische Thermodynamik*, Steinkopf, Dresden, 1972)
- 13 Keenan, J.H., Availability and irreversibility in thermodynamics, *British J. of Applied Physics*, Vol 2, July 1951, pp. 183-192.
- 14 Gaggioli R.A., Principles for Thermodynamic Modeling and Analysis of Processes, *AES-Vol.36, Proc. of the ASME Advanced Energy Systems Division*, ASME 1996, pp. 265-270.
- 15 Bejan, A., *Advanced Engineering Thermodynamics*, 1988, John Willey and Sons, New York, 1988.
- 16 Valero, A, Tsatsaronis, G., eds., *Proc. of the Int. Symp. On Efficiency, Costs, Optimization and Simulation of Energy Systems, ECOS 92*, ASME, New York, 1992.
- 17 Rant, Z., Exergy, ein neues Wort fur "technische Arbeitsfahigkeit" *Forsch. Ing. Wes.*, Vol. 22, No. 1, 1956, pp. 36-37.
- 18 Kotas, T.J., *The Exergy Method of Thermal Plant Analysis*, Butterworth, London, 1985.
- 19 Bejan, A., *Entropy Generation through Heat and Fluid Flow*, Wiley, New York, 1982.
- 20 Aceves-Saborio, S., Ranashinge, J., and Reistad, G.M. (1989) An extension to the Irreversibility Minimization Analysis Applied to Heat Exchangers, *J. Heat Transfer, Trans ASME*, Vol. 111., pp. 29-36.
- 21 Proc. Of the ASME Advanced Energy Systems Division, AES-Vol.36, 1996.
- 22 Proc. Of the ASME Advanced Energy Systems Division, AES-Vol.33, 1994.
- 23 Bejan A., Mamut, E. (1999) Thermodynamic optimization of complex energy systems, NATO Science Series, 3. High Technology, Vol. 69, Kluwer, Dordrecht.

- 24 Szargut, J., Morris, D.R., and Steward, F.R., *Exergy Analysis of Thermal, Chemical and Metallurgical Processes*, John Benjamins Publ., 1988.
- 25 Mihelcic, J.R., Crittenden, J.C., Small, M.J., Shonnard, D.R., Hokanson, D.R., Zhang, Q., Chen, H., Sorby, A., James, V.U., Sutherland, J.W., and Schnoor, J.L., Sustainability Science and Engineering: The Emergence of a New Metadiscipline, *Environ. Sci. Technol.*, Vol. 37, 2003, pp. 5314-5324.
- 26 Anastas, P.T., Heine, L.G., Williamson, T.C., *Green Engineering*, ACS Symposium Series 766, American Chemical Society, Washington, DC, 2001.
- 27 Sankara, J., and Sekulic, D.P., Irreversibility Approach for Sustainability Analysis of a Netshape Manufacturing System, *IMECE2004-61592*, Vol. 3, ASME, New York, 2004.
- 28 Sekulic, D.P., and Sankara, J., Advanced Thermodynamics Metrics for Sustainability Assessments of Open Engineering Systems, *Thermal Science Journal*, *to be published*
- 29 Bakshi, B.R., A Thermodynamic Framework for Ecologically Conscious Process Systems Engineering *Computers and Chemical Engineering*, Vol. 26, 2002, No. 2, pp. 269-282.
- 30 Brundtland commission, Our Common Future, World Commission on Environment and Development, Oxford University Press, Oxford. 1987.
- 31 Norton, R., An overview of a sustainable city strategy, Report Prepared for the Global Energy Assessment Planning for Cities and Municipalities, Montreal, Quebec, 1991.
- 32 MacRae, K. M., *Realizing the Benefits of Community Integrated Energy Systems*, Canadian Energy Research Institute, Alberta, 1992.
- 33 Rosen, M. A., The role of energy efficiency in sustainable development, *Technol. Soc.*, Vol.15, No. 4, pp. 21-26, 1996.
- 34 Dincer, I., and Rosena, M., Worldwide Perspective On Energy, Environment & Sustainable Development *Int. J. Energy Res.*, Vol 22, pp. 1305- 1321, 1998.

- 35 Tassios, D., Management of Resources for sustainable development: Entropy “shows” the way; *Global Nest: the Int. J.*, Vol. 2, No. 3, pp. 293-299, 2000.
- 36 Bejan, A., Fundamentals of exergy analysis, entropy generation minimization, and the generation of flow architecture, *Int.J. Energy Research*. 2002; Vol. 26, pp. 545-565.
- 37 Dincer, I. and Cengel, Y.A. Energy, Entropy and Exergy Concepts and Their Roles in Thermal Engineering, *Entropy*, 2001, Vol. 3, pp. 116-149.
- 38 Dincer, I. and Cengel, Y.A. ‘Thermodynamic aspects of renewables and sustainable development’ Renewable and Sustainable Energy reviews, Vol. 9, 2005, pp 169-189.
- 39 Baehr, H. D., Definition und Berechnung von Exergie und Anergie, *BWK*, Vol. 17, No.1, 1965., p. 1-7.
- 40 Evans, A proof that exergy is the only consistent measure of potential work (for chemical systems). Ph.D. Thesis. Dartmouth College: Hanover, New Hampshire, 1969.
- 41 Reistad GM., Availability: Concepts and Applications. Ph.D. Thesis, University of Wisconsin, Madison, 1970.
- 42 Nerescu I, and Radcenco V. Exergy Analysis of Thermal Processes. Editura Technica: Bucharest, 1970.
- 43 Brodyanskii, VM. Exergy Method of Thermodynamic Analysis. Energiia: Moskow, 1973.
- 44 Haywood RW, Equilibrium Thermodynamics. Wiley: New York, 1980.
- 45 Ahern, JE., The Exergy Method of Energy Systems Analysis. Wiley: New York, 1980.
- 46 Feidt, *Thermodynamique et optimisation Energetique des Systems et Procedes*, Technique et Documentation, Lavoisier, 1987.
- 47 Kotas, TJ., The Exergy method of thermal plant analysis. Krieger: Melbourne, FL, 1995.

- 48 Moran, MJ, Shapiro HN, *Fundamentals of Engineering Thermodynamics* (3rd edn). Wiley: New York, 1995.
- 49 Radcenco, V. *Generalized Thermodynamics*. Editura Technica, Bucharest, 1994.
- 50 Shiner, JS ed *Entropy and Entropy Generation*. Kluwer Academic Publishers: Dordrecht, 1996.
- 51 Stecco, SS; Moran, MJ. (eds). *A Future for Energy*. Pergamon; Oxford, UK, 1990.
- 52 Stecco, SS; Moran, MJ. (eds). *Energy for the Transition Age*. Nova Science, New York, 1992.
- 53 Valero and Tsatsaronis, (eds). ECOS'92, Proceedings of the International Symposium on Efficiency, Costs, Optimization and Simulation of Energy systems, Zaragoza, Spain. ASME Press, New York, 1992.
- 54 Bejan, A. Vadasz P, Kroger DG. (eds). *Energy and Environment*. Kluwer Academic Publishers: Dordrecht, The Netherlands, 1999.
- 55 Wang, Y., Xiao, F., Exergy analysis involving resource utilization and environmental influence, *Computers and Chemical Engineering*, Vol. 24, 2000, pp 1243-1246.
- 56 Rivero, The Exergoecologic improvement potential of industrial processes, Proceedings of TAIES'97, Beijing, June 10-13, 1997.
- 57 Shah, R.K., and Sekulic, D.P. *Fundamentals of Heat Exchanger Design*, John Wiley, Hoboken, NJ, 2003.
- 58 Sekulic, D.P., Gao, F., Zhao, H., Zellmer, B., and Qian, Y.Y. Prediction of the Fillet Mass and Topology of Aluminum Brazed Joints, *Welding Journal*, Vol. 83, No. 3, 2004, pp. 102-110.
- 59 Sekulic, D.P., Salazar, J.A., Gao, F., Rosen, S.J., and Hutchins, F.H. Local Transient behavior of compact heat exchanger core during brazing. Equivalent zonal (EZ) approach, *Int. J. of Heat Exchangers*, Vol. 4, No. 1, , 2003, pp. 91 - 108.
- 60 Sekulic, D.P., KSEF Final Technical Report, June 30, 2004.

- 61 M.,Gong and G., Wall., On Exergetics, Economics And Optimization Of Technical Processes To Meet Environmental Conditions, Proceedings of TAIES'97, June 10-13, Beijing, 1997.
- 62 Utgikar, P.S., Dubey, S.P.; Prasada Rao, P.J., Thermoeconomic analysis of gas turbine cogeneration plant -a case study, *Proceedings of the Institution of Mechanical Engineers, Part A: Journal of Power and Energy*, Vol. 209, No.1, 1995, pp 45-54.
- 63 NIST Chemistry WebBook, <http://webbook.nist.gov/chemistry/form-ser.html>, June 2005.
- 64 Cengel, Y.A and Boles, M.A. Thermodynamics: An Engineering approach, 4th edition, McGraw Hill, New York, 2001.
- 65 Moran, M. Availability Analysis: *A Guide to Efficient Energy Use*, ASME Press, New York, 1989.
- 66 Kotas, T.J., Mayhew, Y.R., and Raichura, R.C., Nomenclature for exergy analysis, *Proc. Inst. Mech. Engrs.*, Vol. 209, 1995, pp. 275-280.
- 67 Mills, A., *Heat and Mass Transfer*, Irwin, Chicago, 1995.
- 68 Incropera, F. P., and De Witt, D. P., *Fundamentals of Heat and Mass Transfer*, John Wiley, New York, 1990.
- 69 Sekulic, D. P., University of Kentucky, Lexington, Personal Communication, 2005.

Appendix A System integration

Variable	Cell															Units
	1	2	3	4	5	6	7	8	9	10	11	12	13	14	15	
u	1.4														1.4	m/min
L	0.525															m
D	0.304															m
$m_{HEX,i}^{in}$	8.07															kg
$m_{HEX,i}^{out}$	8.07															kg
$T_{core/flux/fix}^{in}$	491	502	574	649	720	767	819	848	865	881	882	808	742	690	650	K
$T_{core/flux/fix}^{out}$	502	574	649	720	767	819	848	865	881	882	808	742	690	650	283	K
T_{CON}^{out}	302	330	420	520	555	630	725	780	830	840	880	745	640	558	296	K
T_{CON}^{out}	330	420	520	555	630	725	780	830	840	880	745	640	558	550	301	K
w	1.2															m
$\rho_{L,CON}^{in}$	12.695														11.10	kg/m ²
$\rho_{L,CON}^{out}$	12.695														11.10	kg/m ²
$m_{FLUX,i}^{in/out}$	0.120															kg
$\dot{m}_{core,i}^{in/out}$	13.63															kg/min
$\dot{m}_{flux,i}^{in/out}$	0.203															kg/min
$\dot{m}_{fix,i}^{in/out}$	6.498															kg/min
$\dot{m}_{con,i}^{in/out}$	21.33														18.66	kg/min
$\dot{m}_{air,i}^{in/out}$	-														835.92	kg/hr
T_{air}^{in}	-														282	K
T_{air}^{out}	-														306	K
T_{N2}^{in}	669	743	784	816	846	888	895	888	876	794	623	520	499	344	-	K
T_{N2}^{out}	300	669	743	784	816	846	888	895	888	876	794	623	520	499	-	K
$\rho_{N2,i}^{in/out}$	1.15	1.15	1.15	1.15	1.15	1.15	1.15	1.15	1.15	1.15	1.15	1.15	1.15	1.15	0	kg/m ³
$\dot{V}_{N2,i}^{in/out}$	70.4	63.1	63.1	63.1	63.1	63.1	63.1	63.1	63.1	63.1	71	10.6	15.9	18	0	Nm ³ /hr
$\dot{m}_{N2,i}^{in/out}$	80.96	72.56	72.56	72.56	72.56	72.56	72.56	72.56	72.56	72.56	81.65	12.19	18.28	20.7	0	kg/hr
$\dot{m}_{H2O,i}^{in}$	0	0	0	0	0	0	0	0	0	0	3.8	2.28	2.28	0	0	kg/s
T_{H2O}^{in}	-	-	-	-	-	-	-	-	-	-	298			-	-	K
T_{H2O}^{out}	-	-	-	-	-	-	-	-	-	-	309	311	307	-	-	K
$\rho_{Air,i}^{in}$	-	-	-	-	-	-	-	-	-	-	-	-	-	-	1.11	kg/m ³
$d_{Air,i}^{in/out}$	-	-	-	-	-	-	-	-	-	-	-	-	-	-	0.8/0.9	m
$v_{Air,i}^{in/out}$	0	0	0	0	0	0	0	0	0	0	0	0	0	0	4/6.5	Nm ³ /hr
$m_{FIX,i}^{in/out}$	3.848															kg
ξ	0	60	69	50	32/64	71/62	32/44	1.4/55	9.5/36	2.2/36	0	0	0	0	0	%
$\dot{E}_{RH,i}^{in}$	0	60	60	60	24/36	24/36	24/36	24/36	24/29	30/45	0	0	0	0	0	kW

Appendix B Reduced temperature, temperature and mass flow rate calculations

a) Temperatures of Each cell

Conveyor		Core/flux/fixture		Nitrogen				
Cell	t_{in}	t_{out}	t_{in}	t_{out}	t_{in}	t_{out}		
1	0.302	0.368	0.491	0.502	0.669	0.3		
2	0.368	0.655	0.502	0.574	0.745	0.669		
3	0.655	0.780	0.574	0.649	0.784	0.745		
4	0.780	0.822	0.649	0.716	0.814	0.784		
5	0.822	0.840	0.716	0.764	0.845	0.814		
6	0.840	0.893	0.764	0.813	0.883	0.845		
7	0.893	0.908	0.813	0.845	0.896	0.883		
8	0.908	0.906	0.845	0.860	0.891	0.896		
9	0.906	0.908	0.860	0.877	0.883	0.891		
10	0.908	0.902	0.877	0.885	0.848	0.883		
11	0.902	0.724	0.885	0.842	0.664	0.848		
12	0.724	0.61	0.842	0.780	0.604	0.664		
13	0.61	0.524	0.780	0.72	0.508	0.604		
Exit	0.524	0.401	0.72	0.285	0.30	0.508		
Air	0.302	0.380	0.285	0.282	0	0		
t=T(K)/1000		t=T(K)/1000		t=T(K)/1000				

Water		
Cell #.	t_{in}	t_{out}
11	0.303	0.323
12	0.303	0.323
13	0.303	0.323
t=T(K)/1000		
Air	291.00	295.00
Air		

b) Mass flow rate calculation:

1 Mass flow rate of Core				
<i>u</i>	<i>L</i>	<i>D</i>	<i>m</i>	M_hex in/out
1.4	0.525	0.304	8.07	13.63 <i>Cells 1-15</i>
m/min	m	m	Kg	Kg/min
M_hex	(In/out)= $u*m/(L+D)$			

2 Mass flow rate of Fix				
<i>u</i>	<i>L</i>	<i>D</i>	<i>m</i>	M_fix in/out
1.4	0.525	0.304	3.848	6.498 <i>Cells 1-15</i>
m/min	m	m	Kg	Kg/min
M_fix	(In/out)= $u*m/(L+D)$			

3 Mass flow rate of Conveyor				
<i>u</i>	<i>w</i>	<i>p</i>	M_con in/out	
1.4	1.2	12.695		21.33 <i>Cells 1-14</i>
1.4	1.2	11.108		18.66 <i>Cell 15</i>
m/min	m	Kg/m ²		Kg/min
M_con	(In/out)= $u*w*p$			

4 Mass flow rate of Flux				
<i>u</i>	<i>L</i>	<i>D</i>	<i>m</i>	M_Flux in/OUT
1.4	0.525	0.304	0.12	0.203 <i>Cells 1-15</i>
m/min	m	m	Kg	Kg/min
M_Flux	(In/out)= $u*m/(L+D)$			

7. Mass flow rate of Water		
CELL	M_h2o_in	M_h2o_out
13	3.8	3.8
14	2.275	2.275
15	2.275	2.275
	Nm ³ /hr	Nm ³ /hr

5 Mass flow rate of Nitrogen			At Normal conditions		
CELL	M_n2_in	M_n2_out	<i>p_in</i>	<i>v_in</i>	MFR N2
1	80.96	80.96	1.15	70.4	0.022
2	72.57	72.57	Kg/m ³	63.1	0.020
3	72.57	72.57		63.1	0.020
4	72.57	72.57		63.1	0.020
5	72.57	72.57		63.1	0.020
6	72.57	72.57		63.1	0.020
7	72.57	72.57		63.1	0.020
8	72.57	72.57		63.1	0.020
9	72.57	72.57		63.1	0.020
10	72.57	72.57		63.1	0.020
11	81.65	81.65		71	0.023
12	12.19	12.19		10.6	0.003
13	18.29	18.29		15.9	0.005
14	20.70	20.70		18	0.006
15	0.00	0.00		0	0.000
	Kg/hr	Kg/hr		Nm ³ /hr	Kg/sec
M_n2_in = $(p_in*v_in)/3600$			M_n2_out = $(p_out*v_out)/3600$		

6. Mass flow rate of Air					temp-8C	Area= $\pi*d*d/4$				
Exit	temp-343K									
<i>d</i>	<i>p_out</i>	<i>v_out</i>	Area	M_air out		Avg MFR				
0.25	1.02	16.00	0.05	0.82	<i>Cell 15</i>	6.82				
m	Kg/m ³	m/s	m ²	Kg/sec		Kg/sec				
					M_air_in/out = $p*v*Area$					
Air Exhaust		temp-313K			Air Intake	temp-281K				
<i>d</i>	<i>p_out</i>	<i>v_out</i>	Area	M_air out	Dia	<i>p_in</i>	<i>v_in</i>	Area	M_air_in	
<i>Cell 15</i>	0.91	1.11	6.50	0.66	9.50	0.81	1.00	4.00	0.52	4.15
	m	Kg/m ³	m ²	Kg/sec	m	Kg/m ³	m/s	m ²	Kg/sec	

Appendix C Enthalpy and energy balance calculation

a) Enthalpy calculation

		Enthalpy of Conveyor						Iron		M_con in		Enthalpy of Flux							
A	B	C	D	E	F	H	M	21.33	A	B	C	D	E	F	H	M	flux in		
18	24.64	-8.91	9.66	-0.01	-6.57	0.00	18.66	162.93	238.52	-115.99	19.87	-0.11	-3384.82	-3326.28	0.20				
Cell	t_in	t_out	h_con_in	h_con_out	H_con_in	H_con_out	kg/min	Cell	t_in	t_out	h_flux_in	h_flux_out	H_flux_in	H_flux_out	kg/min				
1	0.302	0.330	0.10	0.81	0.61	5.16		1	0.491	0.502	46.14	48.95	0.60	0.64					
2	0.330	0.420	0.81	3.23	5.16	20.53		2	0.502	0.574	48.95	67.69	0.64	0.89					
3	0.420	0.520	3.23	6.12	20.53	38.98		3	0.574	0.649	67.69	87.91	0.89	1.15					
4	0.520	0.555	6.12	7.19	38.98	45.79		4	0.649	0.720	87.91	107.65	1.15	1.41					
5	0.555	0.630	7.19	9.59	45.79	61.01		5	0.720	0.767	107.65	121.00	1.41	1.58					
6	0.630	0.725	9.59	12.82	61.01	81.57		6	0.767	0.819	121.00	136.02	1.58	1.78					
7	0.725	0.780	12.82	14.80	81.57	94.18		7	0.819	0.848	136.02	144.50	1.78	1.89					
8	0.780	0.830	14.80	16.67	94.18	106.12		8	0.848	0.865	144.50	149.51	1.89	1.96					
9	0.830	0.840	16.67	17.06	106.12	108.57		9	0.865	0.881	149.51	154.24	1.96	2.02					
10	0.840	0.880	17.06	18.62	108.57	118.54		10	0.881	0.882	154.24	154.54	2.02	2.02					
11	0.880	0.745	18.62	13.53	118.54	86.10		11	0.882	0.808	154.54	132.82	2.02	1.74					
12	0.745	0.64	13.53	10.05	86.10	63.94		12	0.808	0.742	132.82	113.87	1.74	1.49					
13	0.64	0.558	10.05	7.29	63.94	46.38		13	0.742	0.69	113.87	100.36	1.49	1.31					
Exit	0.558	0.550	7.29	7.04	46.38	44.80		Exit	0.69	0.650	100.36	88.19	1.31	1.15					
AB	0.296	0.301	-0.05	0.07	-0.30	0.40		AB	0.650	0.283		-3.38	1.15	-0.04					
	t=T(K)/1000		kJ/mol	kJ/mol	kJ/sec	kJ/sec			t=T(K)/1000		kJ/mol	kJ/mol	kJ/sec	kJ/sec					
		Enthalpy of Hex				Al				Enthalpy of N2									
A	B	C	D	E	F	H	M_hex in	A	B	C	D	E	F	H					
28	-5.41	8.56	3.43	-0.28	-9.15	0.00	13.63	26.09	8.2188	-1.9761	0.159274	0.044434	-7.98923	0					
Cell	t_in	t_out	h_hex_in	h_hex_out	H_hex_in	H_hex_out	kg/min	Cell	t_in	t_out	h_N2_in	h_N2_out	M_n2_in	M_n2_out	H_N2_in	H_N2_out			
1	0.491	0.502	4.94	5.24	41.63	44.11		1	0.669	0.3	11.05	0.04	80.96	80.96	8.87	0.03			
2	0.502	0.574	5.24	7.20	44.11	60.61		2	0.743	0.669	13.35	11.05	72.57	72.57	9.60	7.95			
3	0.574	0.649	7.20	9.30	60.61	78.31		3	0.784	0.743	14.63	13.35	72.57	72.57	10.53	9.60			
4	0.649	0.720	9.30	11.35	78.31	95.59		4	0.816	0.784	15.64	14.63	72.57	72.57	11.26	10.53			
5	0.720	0.767	11.35	12.75	95.59	107.34		5	0.846	0.816	16.59	15.64	72.57	72.57	11.94	11.26			
6	0.767	0.819	12.75	14.33	107.34	120.67		6	0.888	0.846	17.93	16.59	72.57	72.57	12.90	11.94			
7	0.819	0.848	14.33	15.24	120.67	128.27		7	0.895	0.888	18.16	17.93	72.57	72.57	13.07	12.90			
8	0.848	0.865	15.24	15.77	128.27	132.78		8	0.888	0.895	17.93	18.16	72.57	72.57	12.90	13.07			
9	0.865	0.881	15.77	16.28	132.78	137.06		9	0.876	0.888	17.55	17.93	72.57	72.57	12.63	12.90			
10	0.881	0.882	16.28	16.31	137.06	137.33		10	0.794	0.876	14.95	17.55	72.57	72.57	10.76	12.63			
11	0.882	0.808	16.31	14.00	137.33	117.82		11	0.623	0.794	9.64	14.95	81.65	81.65	7.80	12.10			
12	0.808	0.742	14.00	12.00	117.82	101.06		12	0.52	0.623	6.51	9.64	12.19	12.19	0.79	1.16			
13	0.742	0.69	12.00	10.59	101.06	89.20		13	0.499	0.52	5.89	6.51	18.29	18.29	1.07	1.18			
Exit	0.69	0.650	10.59	9.33	89.20	78.55		Exit	0.344	0.499	1.32	5.89	20.70	20.70	0.27	1.21			
AB	0.650	0.283	9.33	-0.37	78.55	-3.11		AB	0	0.00	0	0	0.00	0.00	0.00	0.00			
	t=T(K)/1000		kJ/mol	kJ/mol	kJ/sec	kJ/sec			t=T(K)/1000		kJ/mol	kJ/mol			kJ/sec	kJ/sec			

Enthalpy of water								Enthalpy of Air							
A	B	C	D	E	F	H	M_h20_in	A	B	C	D	M_air_in	M_air_out		
-204	1523.29	-3196	2474	3.86	-256.55	-285.83	3.80	28.11	0.002	5E-06	-2E-09	4.15	4.15		
Cell #.	t_in	t_out	h_H2O	h_H2O	H_H20_in	H_H20_ou	2.28	Cell #.	t_in	t_out	h_air_in	h_air_ou	H_air_in	H_air_out	
11	0.298	0.309	-0.01	0.82	-0.580643	47.96	2.28	Exit	281	343	8009	9815.23	1146.99	1405.66	
12	0.298	0.311	-0.01	0.97	-0.347622	34.00		Airblast	282	306	8043.8	8735.30	1151.97	1251.00	
13	0.298	0.307	-0.01	0.67	-0.347622	23.43		t=T(K)			kJ/kmol	kJ/kmol	kJ/sec	kJ/sec	
	t=T(K)/1000		kJ/mol	kJ/mol	kJ/sec	kJ/sec		298.00			8502.6		1217.67		
Enthalpy of fixture															
A	B	C	D	E	F	H	M_fix_in								
18	24.64	-8.91	9.66	-0.01	-6.57	0.00	6.50								
Cell	t_in	t_out	h_fxt_i	h_fxt_o	H_fxt_in	H_fxt_out	Kg/min								
1	0.491	0.502	5.26	5.59	10.20	10.83									
2	0.502	0.574	5.59	7.79	10.83	15.10									
3	0.574	0.649	7.79	10.21	15.10	19.81		Formula for conveyor(Cell 1)							
4	0.649	0.720	10.21	12.64	19.81	24.51		h_con_in = $((A^3*B5)+((B^3*B5^2)/2)+((C^3*B5^3)/3)+((D^3*B5^4)/4)-(E^3/B5)+F^3-G^3)$							
5	0.720	0.767	12.64	14.32	24.51	27.77		h_con_out = $((A^3*C5)+((B^3*C5^2)/2)+((C^3*C5^3)/3)+((D^3*C5^4)/4)-(E^3/C5)+F^3-G^3)$							
6	0.767	0.819	14.32	16.26	27.77	31.52		H_con_in = $((D5*H^2*10^2)/(55.85*6))$							
7	0.819	0.848	16.26	17.37	31.52	33.68		H_con_out = $((E5*H^2*10^2)/(55.85*6))$							
8	0.848	0.865	17.37	18.03	33.68	34.97									
9	0.865	0.881	18.03	18.66	34.97	36.19									
10	0.881	0.882	18.66	18.70	36.19	36.27									
11	0.882	0.808	18.70	15.84	36.27	30.72		A,B,C,D,E,F,G,H values taken from the NIST (refer to the sheets attached)							
12	0.808	0.742	15.84	13.42	30.72	26.03									
13	0.742	0.69	13.42	11.74	26.03	22.76									
Exit	0.69	0.650	11.74	10.25	22.76	19.87									
AB	0.650	0.283	10.25	-0.38	19.87	-0.74									
	t=T(K)/1000		kJ/mol	kJ/mol	kJ/sec	kJ/sec									

Note: A generic formula for Cell 1, for calculating the enthalpies of conveyor is given above. The respective formulae for rest of the cells and for the other materials follow the same notation.

b) Energy balance calculation

Cell	hex_in	hex_out	con_in	con_out	fxt_in	fxt_out	flx_in	flx_out	N2_in	N2_out	h2O_in	h2O_out	air_in	air_out	W_Rh	W_aux	Q_diffr			
1	41.6	44.1	0.6	5.2	10.2	10.8	0.6	0.6	8.87	0.03	0.0	0.0	0.0	0.0	0.0	0.0	1.1			
2	44.1	60.6	5.2	20.5	10.8	15.1	0.6	0.9	9.60	7.95	0.0	0.0	0.0	0.0	36.0	0.0	1.3			
3	60.6	78.3	20.5	39.0	15.1	19.8	0.9	1.1	10.53	9.60	0.0	0.0	0.0	0.0	41.4	0.0	1.2			
4	78.3	95.6	39.0	45.8	19.8	24.5	1.1	1.4	11.26	10.53	0.0	0.0	0.0	0.0	30.0	0.0	1.7	Heating		
5	95.6	107.3	45.8	61.0	24.5	27.8	1.4	1.6	11.94	11.26	0.0	0.0	0.0	0.0	30.7	0.0	1.0			
6	107.3	120.7	61.0	81.6	27.8	31.5	1.6	1.8	12.90	11.94	0.0	0.0	0.0	0.0	39.4	0.0	2.5			
7	120.7	128.3	81.6	94.2	31.5	33.7	1.8	1.9	13.07	12.90	0.0	0.0	0.0	0.0	23.5	0.0	1.2			
8	128.3	132.8	94.2	106.1	33.7	35.0	1.9	2.0	12.90	13.07	0.0	0.0	0.0	0.0	20.1	0.0	2.2			
9	132.8	137.1	106.1	108.6	35.0	36.2	2.0	2.0	12.63	12.90	0.0	0.0	0.0	0.0	12.7	0.0	4.4			
10	137.1	137.3	108.6	118.5	36.2	36.3	2.0	2.0	10.76	12.63	0.0	0.0	0.0	0.0	16.9	0.0	4.7			
11	137.3	117.8	118.5	86.1	36.3	30.7	2.0	1.7	7.80	12.10	-0.6	48.0	0.0	0.0	0.0	0.0	4.9			
12	117.8	101.1	86.1	63.9	30.7	26.0	1.7	1.5	0.79	1.16	-0.3	34.0	0.0	0.0	0.0	0.0	9.1	Wtr cool		
13	101.1	89.2	63.9	46.4	26.0	22.8	1.5	1.3	1.07	1.18	-0.3	23.4	0.0	0.0	0.0	0.0	9.0			
Exit	89.2	78.5	46.4	44.8	22.8	19.9	1.3	1.2	0.27	1.21	0.0	0.0	0.0	0.0	0.0	0.0	14.3			
AB	78.5	-3.1	-0.3	0.4	19.9	-0.7	1.2	0.0	0.00	0.00	0.0	0.0	1152	1251.0	0.0	0.0	3.7	Air blast		
	KW	KW	KW	KW	KW	KW	KW	KW	KW	KW	KW	KW	KW	KW	KW	KW	62.4	KW		
										124.4	118.48									
	Q_diff-i = (Bi+Di+Fi+Hi+Ji+Li+Ni+Pi+Qi-Ci-Ei-Gi-Ii-Ki-Mi-Oi)										Total Q_diffr = SumQ_diff-I for Control Volumes (W)						62365	W		
Cell #	Tot H in	Tot Ergy in	Tot H out	Q_diffr			e		E	W_Rh										
1	61.9	0.0	60.8	1.1			0.00		0	0										
2	70.3	36.0	105.1	1.3			0.60		60	36									Tot Enthpy in = (B2+D2+F2+H2+J2+L2+N2)	
3	107.7	41.4	147.9	1.2			0.69		60	41.4									Tot Enthpy out (C2+E2+G2+I2+K2+M2+O2)	
4	149.5	30.0	177.8	1.7			0.50		60	30									W_Rh = ((I25*K25)+(J25*L25))*1000	
5	179.2	30.7	209.0	1.0			0.32	0.64	24.00	36	30.72									
6	210.6	39.4	247.5	2.5			0.71	0.62	24.00	36	39.36									
7	248.6	23.5	270.9	1.2			0.32	0.44	24.00	36	23.52									
8	270.9	20.1	288.9	2.2			0.014	0.55	24.00	36	20.136									
9	288.5	12.7	296.7	4.4			0.095	0.36	24.00	29	12.72									
10	294.6	16.9	306.8	4.7			0.022	0.36	30.00	45	16.86									
11	301.4	0.0	296.4	4.9			0.00		0	0										
12	236.8	0.0	227.7	9.1			0.00		0	0										
13	193.2	0.0	184.3	9.0			0.00		0	0										
Exit	159.9	0.0	145.6	14.3			0.00		0	0										
AB	1251.2	0.0	1247	3.7			0.00		0	0										
	4024	250.7	4213	62.4			B	%	kW	W										
	KW	KW	KW	KW																
	Tot Egr in= W_Rh																			
1	Tot H_in to the system 4024.45 KW																			
2	Tot Ergy into the system 250.7 KW																			
3	Tot H_out of the system 4212.8 KW																			
4	Tot Q_diffr of the system 62.4 KW (4 = 1 + 2 - 3)																			
	Tot H in =H_hex_in + H_con_in + H_fxt_in + H_flx_in + H_N2_in + H_h2O_in + H_air_in																			
	Tot H out =H_hex_out+H_con_out+ H_fxt_out+H_flx_out+H_N2_out+H_h2O_out+H_air_out																			

Appendix D Entropy and exergy balance calculation

a) Entropy calculation

66

		Entropy of Conveyor							M _{con_in}	Entropy of Flux							
A	B	C	D	E	F	H	G		A	B	C	D	E	F	H	G	M _{flux_in}
18.43	24.64	-8.91	9.66	-0.01	-6.57	0.00	42.51	0.36	162.93	238.52	-115.99	19.87	-0.11	-3384.82	-3326.28	415.01	0.0034
Cell	h _{con_in}	h _{con_out}	s _{con_in}	s _{con_out}	s _o	E _{con_in}	E _{con_out}	kg/sec	Cell	h _{flux_in}	h _{flux_out}	s _{fix_in}	s _{fix_out}	s _o	E _{flux_in}	E _{flux_out}	kg/sec
1	1.72	14.51	0.49	0.53	0.49	-0.03	0.21		1	178.66	189.51	1.56	1.58	1.10	0.14	0.15	
2	14.51	57.76	0.53	0.65	0.49	0.21	3.28		2	189.51	262.09	1.58	1.72	1.10	0.15	0.26	
3	57.76	109.67	0.65	0.76	0.49	3.28	9.98		3	262.09	340.39	1.72	1.85	1.10	0.26	0.40	
4	109.67	128.81	0.76	0.80	0.49	9.98	13.01		4	340.39	416.80	1.85	1.96	1.10	0.40	0.54	
5	128.81	171.62	0.80	0.87	0.49	13.01	20.56		5	416.80	468.51	1.96	2.03	1.10	0.54	0.65	
6	171.62	229.49	0.87	0.96	0.49	20.56	32.06		6	468.51	526.66	2.03	2.10	1.10	0.65	0.77	
7	229.49	264.97	0.96	1.00	0.49	32.06	39.67		7	526.66	559.51	2.10	2.14	1.10	0.77	0.84	
8	264.97	298.55	1.00	1.04	0.49	39.67	47.19		8	559.51	578.89	2.14	2.16	1.10	0.84	0.88	
9	298.55	305.43	1.04	1.05	0.49	47.19	48.76		9	578.89	597.22	2.16	2.18	1.10	0.88	0.93	
10	305.43	333.47	1.05	1.08	0.49	48.76	55.27		10	597.22	598.37	2.18	2.19	1.10	0.93	0.93	
11	333.47	242.22	1.08	0.97	0.49	55.27	34.75		11	598.37	514.28	2.19	2.09	1.10	0.93	0.74	
12	242.22	179.89	0.97	0.88	0.49	34.75	22.12		12	514.28	440.90	2.09	1.99	1.10	0.74	0.59	
13	179.89	130.48	0.88	0.80	0.49	22.12	13.28		13	440.90	388.58	1.99	1.92	1.10	0.59	0.49	
Exit	130.48	126.05	0.80	0.79	0.49	13.28	12.56		Exit	388.58	341.45	1.92	1.85	1.10	0.49	0.40	
AB	-0.97	1.27	0.48	0.49	0.49	-0.02	-0.02		AB	341.45	-13.10	1.85	1.05	1.10	0.40	0.00	
	kJ/kg	kJ/kg	kJ/kg*k	kJ/kg*k	kJ/kg*k	kJ/kg*k	kJ/kg*k			kJ/kg	kJ/kg	kJ/kg*k	kJ/kg*k	kJ/kg*k	kJ/kg*k	kJ/kg*k	
Entropy of Hex										Entropy of fixture							
A	B	C	D	E	F	H	G	M _{hex_in}	A	B	C	D	E	F	H	G	M _{fix_in}
28.09	-5.41	8.56	3.43	-0.28	-9.15	0.00	61.90	0.23	18.43	24.64	-8.91	9.66	-0.01	-6.57	0.00	42.51	0.11
Cell	h _{hex_in}	h _{hex_out}	s _{hex_in}	s _{hex_out}	s _o	E _{hex_in}	E _{hex_out}	kg/sec	Cell	h _{fix_in}	h _{fix_out}	s _{fix_in}	s _{fix_out}	s _o	E _{fix_in}	E _{fix_out}	kg/sec
1	183.26	194.19	1.50	1.52	0.99	7.11	8.03		1	94.19	100.02	0.73	0.74	0.49	2.36	2.61	
2	194.19	266.86	1.52	1.66	0.99	8.03	15.03		2	100.02	139.43	0.74	0.82	0.49	2.61	4.51	
3	266.86	344.76	1.66	1.79	0.99	15.03	23.84		3	139.43	182.86	0.82	0.89	0.49	4.51	6.91	
4	344.76	420.83	1.79	1.91	0.99	23.84	33.40		4	182.86	226.34	0.89	0.95	0.49	6.91	9.57	
5	420.83	472.58	1.91	1.98	0.99	33.40	40.34		5	226.34	256.44	0.95	0.99	0.49	9.57	11.52	
6	472.58	531.27	1.98	2.06	0.99	40.34	48.55		6	256.44	291.05	0.99	1.03	0.49	11.52	13.86	
7	531.27	564.71	2.06	2.10	0.99	48.55	53.38		7	291.05	310.97	1.03	1.06	0.49	13.86	15.24	
8	564.71	584.56	2.10	2.12	0.99	53.38	56.29		8	310.97	322.85	1.06	1.07	0.49	15.24	16.08	
9	584.56	603.42	2.12	2.14	0.99	56.29	59.09		9	322.85	334.19	1.07	1.09	0.49	16.08	16.89	
10	603.42	604.60	2.14	2.14	0.99	59.09	59.27		10	334.19	334.90	1.09	1.09	0.49	16.89	16.94	
11	604.60	518.72	2.14	2.04	0.99	59.27	46.77		11	334.90	283.61	1.09	1.03	0.49	16.94	13.35	
12	518.72	444.91	2.04	1.94	0.99	46.77	36.59		12	283.61	240.29	1.03	0.97	0.49	13.35	10.46	
13	444.91	392.70	1.94	1.87	0.99	36.59	29.77		13	240.29	210.14	0.97	0.93	0.49	10.46	8.55	
Exit	392.70	345.82	1.87	1.80	0.99	29.77	23.96		Exit	210.14	183.46	0.93	0.89	0.49	8.55	6.95	
AB	345.82	-13.69	1.80	0.94	0.99	23.96	0.48		AB	183.46	-6.86	0.89	0.46	0.49	6.95	0.02	
	kJ/kg	kJ/kg	kJ/kg*k	kJ/kg*k	kJ/kg*k	kJ/kg*k	kJ/kg*k			kJ/kg	kJ/kg	kJ/kg*k	kJ/kg*k	kJ/kg*k	kJ/kg*k	kJ/kg*k	

Entropy of water									Entropy of Air								
A	B	C	D	E	F	H	G	M_h20_in	A	B	C	D	M_air_in	M_air_out			
-203.61	1523.29	-3196.41	2474.46	3.86	-256.55	-285.83	-488.71	1.06	28.11	0.00	0.00	0.00	0.2322	0.2322			kg/sec
Cell #.	h_H20_in	h_H20_out	s_h20_in	s_h20_out	s_o	E_h20_in	E_h20_out	0.63	Cell #.	h_air_in	h_air_out	s_air_in	s_air_out	s_o	E_air_in	E_air_out	
11.00	-0.55	45.44	5.08	5.14	5.08	-0.58	27.02	0.63	Air	278.33	302.26	5.49	5.57	5.54	0.01	0.12	
12.00	-0.55	53.80	5.08	5.16	5.08	-0.35	19.16	kg/sec		kJ/kg	kJ/kg	kJ/kg*k	kJ/kg*k	kJ/kg*k	kJ/sec	kJ/sec	
13.00	-0.55	37.08	5.08	5.13	5.08	-0.35	13.22	3.52									
	kJ/kg	kJ/kg	kJ/kg*k	kJ/kg*k	kJ/kg*k	kJ/kg*k	kJ/sec	kJ/sec									
Ht.Exchg	-13.11		5.06		5.08	-24.36											
Entropy of Nitrogen																	
A	B	C	D	E	F	H	G	M_N2_in									
26.092	8.218801	-1.976141	0.159274	0.044434	-7.98923	0	221.02	0.061394									
Cell	h_N2_in	h_N2_out	s_N2_in	s_N2_out	s_o	E_N2_in	E_N2_out	Kg/sec									
1	394.45	1.52	7.70	6.85	6.85	3.18	-0.01										
2	476.49	394.45	7.81	7.70	6.85	3.80	2.85										
3	522.39	476.49	7.87	7.81	6.85	4.37	3.80										
4	558.43	522.39	7.92	7.87	6.85	4.83	4.37										
5	592.40	558.43	7.96	7.92	6.85	5.27	4.83										
6	640.22	592.40	8.01	7.96	6.85	5.90	5.27										
7	648.22	640.22	8.02	8.01	6.85	6.01	5.90										
8	640.22	648.22	8.01	8.02	6.85	5.90	6.01										
9	626.52	640.22	8.00	8.01	6.85	5.72	5.90										
10	533.63	626.52	7.89	8.00	6.85	4.51	5.72										
11	344.00	533.63	7.62	7.89	6.85	2.59	5.08										
12	232.56	344.00	7.42	7.62	6.85	0.20	0.39										
13	210.10	232.56	7.38	7.42	6.85	0.26	0.31										
Exit	47.02	210.10	6.99	7.38	6.85	0.02	0.29										
AB	0.00	0.00	0.00	0.00	0.00	0.00	0.00										
	kJ/kg	kJ/kg	kJ/kg*k	kJ/kg*k	kJ/kg*k	kJ/sec	kJ/sec										
Formula for conveyor(Cell 1) $s_{con_in} = ((A\$3*LN(Enthalpy!B5))+(B\$3*Enthalpy!B5)+((C\$3*Enthalpy!B5^2)/2)+((D\$3*Enthalpy!B5^3)/3)-(E\$3/2*(Enthalpy!B5^2))+H\$3)/55.85$ $s_{con_ot} = ((A\$3*LN(Enthalpy!C5))+(B\$3*Enthalpy!C5)+((C\$3*Enthalpy!C5^2)/2)+((D\$3*Enthalpy!C5^3)/3)-(E\$3/2*(Enthalpy!C5^2))+H\$3)/55.85$ $E_{con_in} = (B5-298*(D5-F5))*I\2 $E_{con_ot} = (C5-298*(E5-F5))*I\2 Sp.Enthalpy h(kJ/kg)= {1000* Sp.Enthalpy h(kJ/mol)}/ Mol.Wt																	

Note: A generic formula for Cell 1, for calculating the entropies of conveyor is given above. The respective formulae for rest of the cells and for the other materials follow the same notation.

b) Exergy destruction calculation

Cell	T_hex	T_htr	Q_hex	Q_htr	e	n	Xrgy-Ht Tfr			
2	538	743	16.51	36	0.46	0.34	21.46			
3	611.5	798	17.70	41.4	0.43	0.35	25.84			
4	684.5	838	17.28	30	0.58	0.50	19.26			
5	743.5	843	11.75	30.72	0.38	0.35	19.79			
6	793	883	13.33	39.36	0.34	0.32	25.99			
7	833.5	885.5	7.60	23.52	0.32	0.31	15.55			
8	856.5	888.5	4.51	20.136	0.22	0.22	13.34			
9	873	895.5	4.28	12.72	0.34	0.33	8.46			
10	881.5	895.5	0.27	16.86	0.02	0.02	11.21			
	K	K	KW	KW	%	%				
		T_o =	300	e= Q_hex/Q_htr		n=F2*((1-(300/B2))/(1-(300/C2)))				
				Exergy destroyed						
Cell	H_hex_in	Temp	Q_Rcvd	H_fxt_in	Q_Rcvd	H_fx_in	Q_Rcvd	H_con_in	Temp	Q_Rcvd
1	2.48	496.50	0.98	0.63	0.25	0.04	0.01	4.54	316.00	0.23
2	16.51	538.00	7.30	4.27	1.89	0.25	0.11	15.37	375.00	3.07
3	17.70	611.50	9.01	4.70	2.40	0.26	0.13	18.45	470.00	6.67
4	17.28	684.50	9.71	4.71	2.64	0.26	0.14	6.81	537.50	3.01
5	11.75	743.50	7.01	3.26	1.95	0.17	0.10	15.22	592.50	7.51
6	13.33	793.00	8.29	3.75	2.33	0.20	0.12	20.57	677.50	11.46
7	7.60	833.50	4.86	2.16	1.38	0.11	0.07	12.61	752.50	7.58
8	4.51	856.50	2.93	1.29	0.84	0.07	0.04	11.94	805.00	7.49
9	4.28	873.00	2.81	1.23	0.81	0.06	0.04	2.44	835.00	1.57
10	0.27	881.50	0.18	0.08	0.05	0.00	0.00	9.97	860.00	6.49
11	-19.51	845.00	-12.58	-5.55	-3.58	-0.28	-0.18	-32.44	812.50	-20.46
12	-16.77	775.00	-10.28	-4.69	-2.88	-0.25	-0.15	-22.15	694.50	-12.58
13	-11.86	718.00	-6.90	-3.27	-1.90	-0.18	-0.10	-17.56	601.00	-8.80
Exit	-10.65	672.00	-5.89	-2.89	-1.60	-0.16	-0.09	-1.58	554.00	-0.72
AB	-81.66	466.40	-29.13	-20.61	-7.35	-1.20	-0.43	0.70	298.50	0.00
	kW	T	kW	kW	kW	kW	kW	kW	T	kW
			Q_Rcvd =B17*(1-D\$13/C17)							

C) Exergy Balance

Cell	E_hex_in	E_hex_out	E_con_in	E_con_out	E_fxt_in	E_fxt_out	E_fx_in	E_fx_out	E_N2_in	E_N2_out	E_h2O_in	E_h2O_out	E_air_in	E_air_out	W_Rh	
1	7.1	8.0	0.0	0.2	2.4	2.6	0.1	0.2	3.18	-0.01	0.0	0.0	0.0	0.0	0.0	
2	8.0	15.0	0.2	3.3	2.6	4.5	0.2	0.3	3.80	2.85	0.0	0.0	0.0	0.0	36.0	
3	15.0	23.8	3.3	10.0	4.5	6.9	0.3	0.4	4.37	3.80	0.0	0.0	0.0	0.0	41.4	
4	23.8	33.4	10.0	13.0	6.9	9.6	0.4	0.5	4.83	4.37	0.0	0.0	0.0	0.0	30.0	
5	33.4	40.3	13.0	20.6	9.6	11.5	0.5	0.6	5.27	4.83	0.0	0.0	0.0	0.0	30.7	
6	40.3	48.6	20.6	32.1	11.5	13.9	0.6	0.8	5.90	5.27	0.0	0.0	0.0	0.0	39.4	
7	48.6	53.4	32.1	39.7	13.9	15.2	0.8	0.8	6.01	5.90	0.0	0.0	0.0	0.0	23.5	
8	53.4	56.3	39.7	47.2	15.2	16.1	0.8	0.9	5.90	6.01	0.0	0.0	0.0	0.0	20.1	
9	56.3	59.1	47.2	48.8	16.1	16.9	0.9	0.9	5.72	5.90	0.0	0.0	0.0	0.0	12.7	
10	59.1	59.3	48.8	55.3	16.9	16.9	0.9	0.9	4.51	5.72	0.0	0.0	0.0	0.0	16.9	
11	59.3	46.8	55.3	34.7	16.9	13.3	0.9	0.7	2.59	5.08	-0.6	27.0	0.0	0.0	0.0	
12	46.8	36.6	34.7	22.1	13.3	10.5	0.7	0.6	0.20	0.39	-0.3	19.2	0.0	0.0	0.0	
13	36.6	29.8	22.1	13.3	10.5	8.6	0.6	0.5	0.26	0.31	-0.3	13.2	0.0	0.0	0.0	
Exit	29.8	24.0	13.3	12.6	8.6	6.9	0.5	0.4	0.02	0.29	0.0	0.0	0.0	0.0	0.0	
AB	24.0	0.5	0.0	0.0	6.9	0.0	0.4	0.0	0.00	0.00	0.0	0.0	0.0	0.1	0.0	
	kJ/sec	kJ/sec	kJ/sec	kJ/sec	kJ/sec	kJ/sec	kJ/sec	kJ/sec	kJ/sec	kJ/sec	kJ/sec	kJ/sec	kJ/sec	kJ/sec	kJ/sec	
				E_in - E_out - E_des = E_change												
												59.4				
Cell	Tot Ex IN	Tot Ex OUT	W	Q	Q_delivd	IN	OUT	E_N2_in	E_N2_out							
1	9.57	11.0	0	0		9.6	11.0	3.18	-0.01							
2	11.00	23.1	36	21.46	12.4	32.5	23.1	3.80	2.85							
3	23.08	41.1	41.4	25.84	18.2	48.9	41.1	4.37	3.80							
4	41.13	56.5	30	19.26	15.5	60.4	56.5	4.83	4.37							
5	56.52	73.1	30.72	19.79	16.6	76.3	73.1	5.27	4.83							
6	73.06	95.2	39.36	25.99	22.2	99.0	95.2	5.90	5.27							
7	95.25	109.1	23.52	15.55	13.9	110.8	109.1	6.01	5.90							
8	109.14	120.4	20.136	13.34	11.3	122.5	120.4	5.90	6.01							
9	120.45	125.7	12.72	8.46	5.2	128.9	125.7	5.72	5.90							
10	125.66	132.4	16.86	11.21	6.7	136.9	132.4	4.51	5.72							
11	131.83	122.6	0	0.00		131.8	122.6	2.59	5.08							
12	95.26	88.9	0	0.00		95.3	88.9	0.20	0.39							
13	69.41	65.3	0	0.00		69.4	65.3	0.26	0.31							
Exit	52.09	43.9	0	0.00		52.1	43.9	0.02	0.29							
AB	31.30	0.6	0	0.00		31.3	0.6	0.00	0.00							
	kW	kW	kW	kW	kW	kW	kW									

Appendix E Derivation of entropy generation equation

The entropy generation can be calculated as follows:

$$S_{gen} = \Delta S - \int \frac{dQ}{T}$$

where ΔS is the entropy change and is calculated as follows:

$$\Delta S = mc \ln(T_{final} / T_{initial})$$

And $\int \frac{dQ}{T_s}$ is the entropy flow, which is calculated using respective empirical relations of the model employed.

Materials Processing Model A: (Spatially lumped object)

Let T_i and T_f be the initial and final state point temperatures;

$$T_f = T_\infty + (T_i - T_\infty)[1 - e^{-\frac{t}{\tau_t}}]$$

$$\Rightarrow \frac{t}{\tau_t} = -\ln\left(\frac{T_f - T_\infty}{T_i - T_\infty}\right)$$

$$Q = mc(T_i - T_\infty)[1 - \exp(-\frac{t}{\tau_t})]$$

$$\frac{dQ}{dt} = mc(T_\infty - T_i)[1 - e^{-\frac{t}{\tau_t}}]$$

$$dQ = mc(T_\infty - T_i)(-e^{-\frac{t}{\tau_t}})(-\frac{1}{\tau_t})$$

$$dQ = mc(T_\infty - T_i) \frac{e^{-\frac{t}{\tau_t}}}{\tau_t} dt$$

$$\frac{\theta}{\theta_i} = \frac{T_f - T_\infty}{T_i - T_\infty} = e^{-\frac{t}{\tau_t}}$$

Now,

$$Q = mc (T_i - T_\infty) \left[1 - \frac{\sin \zeta_1}{\zeta_1} C_1 e^{-\zeta_1^2 \alpha \frac{t}{L_c^2}} \right]$$

$$\int \frac{dQ}{T} = mc(T_{\infty} - T_1) \frac{1}{\tau_t} \int \left(\frac{e^{-\frac{t}{\tau_t}}}{T_{\infty} + (T_1 - T_{\infty})[1 - e^{-\frac{t}{\tau_t}}]} \right) dt$$

$$\Rightarrow mc (T_{\infty} - T_1) \frac{1}{\tau_t} \int \left(\frac{1}{T_{\infty} e^{\frac{t}{\tau_t}} - (T_{\infty} - T_1)} \right) dt$$

Note: $\int \frac{dx}{a + be^{mx}} = \frac{1}{ma} [mx - \ln(a + be^{mx})]$

$$\Rightarrow \int \frac{dQ}{T} = mc (T_{\infty} - T_1) \frac{1}{\tau_t} \left(-\frac{\tau_t}{(T_{\infty} - T_1)} \right) \left(\frac{t}{\tau_t} - \ln \left[T_{\infty} e^{\frac{t}{\tau_t}} - (T_{\infty} - T_1) \right] \right) \Bigg|_0^t$$

$$\therefore \int \frac{dQ}{T} = -mc \left[\frac{t}{\tau_t} - \ln \left(\frac{T_{\infty} e^{\frac{t}{\tau_t}} - (T_{\infty} - T_1)}{T_1} \right) \right]$$

Therefore the eventual, entropy generation equation for this case is as follows

$$S_{gen} = mc \ln\left(\frac{T_f}{T_1}\right) + mc \left[\frac{t}{\tau_t} - \ln \left(\frac{T_{\infty} e^{\frac{t}{\tau_t}} - (T_{\infty} - T_1)}{T_1} \right) \right]$$

Materials Processing Model B: (Spatially distributed transient object)

Let T_i and T_f be the initial and final state point temperatures;

$$Q = mc (T_1 - T_{\infty}) \left[1 - \frac{\sin \zeta_1}{\zeta_1} C_1 e^{-\zeta_1^2 \frac{\alpha}{L^2} t} \right]$$

$$\Rightarrow \frac{dQ}{dt} = mc (T_{\infty} - T_1) \frac{\sin \zeta_1}{\zeta_1} C_1 \zeta_1^2 \frac{\alpha}{L^2} e^{-\zeta_1^2 \frac{\alpha}{L^2} t} dt$$

$$\theta^* = C_1 e^{-\zeta_1 \frac{\alpha}{L^2} t \cos \zeta_1} = \frac{T_f - T_\infty}{T_1 - T_\infty}$$

$$T_f = T_\infty + (T_1 - T_\infty) C_1 e^{\zeta_1^2 \frac{\alpha}{L^2} t \cos(\zeta_1)}$$

$$\therefore \int \frac{dQ}{T} = mc(T_\infty - T_1) \frac{\sin \zeta_1}{\zeta_1} C_1 \zeta_1^2 \frac{\alpha}{L^2} \int \left(\frac{e^{-\zeta_1^2 \frac{\alpha}{L^2} t}}{T_\infty + (T_1 - T_\infty) C_1 e^{-\zeta_1^2 \frac{\alpha}{L^2} t} \cos \zeta_1} \right) dt$$

$$mc(T_\infty - T_1) \frac{\sin \zeta_1}{\zeta_1} C_1 \zeta_1^2 \frac{\alpha}{L^2} \int \left(\frac{dt}{T_\infty e^{-\zeta_1^2 \frac{\alpha}{L^2} t} - (T_\infty - T_1) C_1 \cos \zeta_1} \right)$$

Again,

$$\int \frac{dx}{a + be^{mx}} = \frac{1}{ma} [mx - \ln(a + be^{mx})]$$

$$mc(T_\infty - T_1) \frac{\sin \zeta_1}{\zeta_1} C_1 \zeta_1^2 \frac{\alpha}{L^2} \frac{1}{\left(-\zeta_1 \frac{\alpha}{L^2} (T_\infty - T_1) \right)} \left[\zeta_1^2 \frac{\alpha}{L^2} t - \ln \left(T_\infty e^{\zeta_1^2 \frac{\alpha}{L^2} t} - (T_\infty - T_1) \cos \zeta_1 C_1 \right) \right]_0^t$$

$$\Rightarrow \int \frac{dQ}{T} = -mc \frac{\tan \zeta_1}{\zeta_1} \left[\zeta_1^2 \frac{\alpha}{L^2} t - \ln \left(\frac{T_\infty e^{\zeta_1^2 \frac{\alpha}{L^2} t} - (T_\infty - T_1) \cos \zeta_1 C_1}{T_\infty - (T_\infty - T_1) \cos \zeta_1 C_1} \right) \right]$$

$$\therefore S_{gen} = mc \ln \left(\frac{T_f}{T_1} \right) + mc \frac{\tan \zeta_1}{\zeta_1} \left[\zeta_1^2 \frac{\alpha}{L^2} t - \ln \left(\frac{T_\infty e^{\zeta_1^2 \frac{\alpha}{L^2} t} - (T_\infty - T_1) \cos \zeta_1 C_1}{T_\infty - (T_\infty - T_1) \cos \zeta_1 C_1} \right) \right]$$

Appendix F Entropy generation calculation

1. Values used for these calculations

a) Dimensions of Heat exchanger core

$$l = 0.866\text{m},$$

$$b = 0.525\text{m},$$

$$h = 0.054\text{m}.$$

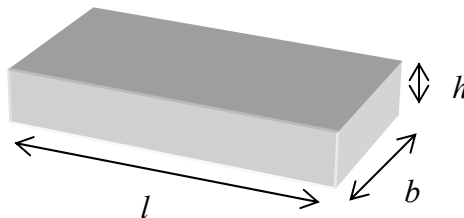


Fig. Heat exchanger core

$$\text{Volume } V = 0.025 \text{ m}^3$$

$$\text{Total C.S.A} = 1.082 \text{ m}^2$$

$$L_c = 0.024 \text{ m}$$

$$\varepsilon = 1 \text{ (perfect emitter assumed)}$$

$$\sigma = 5.67 \times 10^{-8} \text{ W/m}^2\text{K}^4$$

$$\Phi = 0.8 \text{ (Its assumed that only 20\% of structure is filled air)}$$

$$k_o = 250 \text{ W/m.K - Aluminum}$$

$$k_l = 0.05 \text{ W/m.K - Air}$$

$$L = 0.525 \text{ m}$$

b) Temperatures in the last heating zone:

$$T_s = 880 \text{ K}$$

$$T_{surT} = 900 \text{ K}$$

T - Surface temperature

T_o – to be determined

T_i – 300 K

$T_\infty = T_{surr}$

c) Values of Thermo physical properties used:

$$\rho = 2700 \text{ kg/m}^3$$

$$C_p = 10^3 \text{ J/kg.K}$$

$$h = h_r = 160 \text{ W/m}^2\text{K}^4$$

$$k_{eff} = 78.69 \text{ W/m.K (see p.118 for this calculation)}$$

2. Calculation of Biot and Fourier numbers

The following dimensionless numbers are pertinent for the analysis:

- a) **Biot number:** Resistance to conduction over resistance to convection across the fluid boundary layer.

$$Bi = \frac{hL_c}{k} \dots\dots\dots (1)$$

$h = h_r$ Radiative heat transfer coefficient

$$h_r = \varepsilon\sigma(T_s + T_{surr})(T_s^2 + T_{surr}^2) \dots\dots\dots (2)$$

ε = Emissivity

σ = Boltzman constant

T_s = Surface temperature of core

T_{surr} = Surrounding temperature

L_c – Characteristic length

$$L_c = \frac{V}{A} \dots\dots\dots (3)$$

V - Volume of the core

A - Total cross sectional area of the core

$k = k_{\text{eff}}$ Effective thermal conductivity of the porous core

$$k_{\text{eff}} = \frac{k_o}{1 - \phi + \left(\frac{k_1}{k_o \phi} + \frac{4\sigma T^3 L}{k_o} \right)^{-1}} \dots\dots\dots (4)$$

Φ - Volume fraction of the porous structure

k_o - Thermal conductivity of Aluminum alloy

k_1 - Thermal conductivity of Air

L - Thickness in direction of heat conduction

b) **Fourier number**: It is a dimensionless time.

$$Fo = \frac{kt}{C_p \rho L_c^2} \dots\dots\dots (5)$$

where:

C_p = Heat capacity

k = Thermal Conductivity

L_c = Characteristic length

ρ = Density

t = Time

$$\theta_0^* = \frac{T_0 - T_\infty}{T_i - T_\infty} \dots\dots\dots (6)$$

T - Surface temperature

T_o – Midplane temperature

T_i – Initial temperature

T_∞ – Surrounding temperature

From these values Biot number is computed as **0.05** \ll **1**, Hence the assumption of uniform temperature distribution is reasonable and lumped capacitance is valid. This value for the spatially distributed case would much larger than 1.

Materials Processing Model A: (Spatially lumped Object)

Calculations:

Mass of the object $m = 8 \text{ kg}$

Specific Heat $C_p = 900 \text{ J/kg.K}$

Initial state temperature of the object $T_1 = 300\text{K}$

Final state temperature of the object $T_2 = 873 \text{ K}$

$$\therefore \frac{t}{\tau_t} = -\ln(0.045) = 3.1$$

Therefore, $\Delta S = 8*900*\ln(873/300) = 7690.70 \text{ J/K}$

$$\int \frac{dQ}{T} = -8 * 900 \left[3.1 - \ln\left(\frac{900e^{3.1} - 600}{300}\right) \right] = 7690 \frac{J}{K} \quad (\text{Substituting the above values in Eq.5.8})$$

$$S_{\text{gen}} = \Delta S - \int \frac{dQ}{T} = 7690.70 - 7690.45 \approx 0 \text{ J/K}$$

CASE A1 - Spatially lumped object with One heating zone at constant temperature

ENTROPY CHANGE (dS)

$$dS = mC \ln(T_2/T_1)$$

Mass(Kg)	C(J/Kg.K)	T2(K)	T1(K)	dS(J/K)	dS(KJ/K)
8	900	873	300	7690.70	7.6907

ENTROPY FLOW Intg (dQ/T)

$$\text{Int} (dQ/T) = m * C * \{t/T - \ln[(T^\infty - T_i) + e^{(t/T)} * T^\infty / 2T^\infty - T_i]\}$$

$$t/T = \ln[(T^\infty - T_i) / (T^\infty - T)]$$

Mass(Kg)	C(J/Kg.K)	T^∞ (K)	T_i (K)	T (K)	t/T	$T^\infty - T_i$	$e^{t/T}$	Int (dQ/T)	Sgen(J/K)
8	900	900	300	873	3.10	600	22.22	7690.70	0.0000
		950			2.13	650	8.44	7690.70	0.0000
		1000			1.71	700	5.51	7690.70	0.0000
		1050			1.44	750	4.24	7690.70	0.0000
		1100			1.26	800	3.52	7690.70	0.0000
		1150			1.12	850	3.07	7690.70	0.0000

Excel formulae:

$$\begin{aligned}
dS &= A7 * B7 * LN(C7/D7) / 1000 \\
t/T &= -LN(C18 - E\$18) + LN(G18) \\
T_{\infty} - T_i &= C18 - D\$18 \\
e^{t/T} &= EXP(F18) \\
Int (dQ/T) &= -A\$18 * B\$18 * (F18 - LN(-G18 + H18 * C18) + LN(D\$18)) \\
S_{gen}(J/K) &= E\$7 - I18
\end{aligned}$$

Materials processing model B: (Spatially distributed transient object)

Calculations:

Mass of the object $m = 8 \text{ kg}$

Specific Heat $C_p = 900 \text{ J/kg.K}$

Initial state temperature of the object $T_1 = 300\text{K}$

Final state temperature of the object $T_2 = 873 \text{ K}$

The coefficients of the transcendental equation ζ_1 and C_1 are determined by knowing the values of Biot number.

Biot number, $Bi = h_{\text{eff}}L/K$

Heat transfer coefficient (with radiative effect) $h_{\text{eff}} = 180 \text{ W/m}^2\text{K}$

Thermal Conductivity $K = 78.69 \text{ W/m}$

L-cross section across which conduction takes place in the object = 0.024m

Hence $Bi = (180 * 0.024) / 78.69 = 0.05$,

For this $Bi=0.05$, from [73] $\zeta_1 = 0.2217$ and $C_1=1.0082$

$$C_1 e^{-\zeta_1^2 \frac{\alpha}{L^2} t} \cos \zeta_1 = -\ln\left(\frac{T_2 - T_{\infty}}{T_1 - T_{\infty}}\right) = 0.045$$

$$\Rightarrow e^{-\zeta_1^2 \frac{\alpha}{L^2} t} = \frac{0.045}{\cos \zeta_1}$$

$$\Rightarrow \zeta_1^2 \frac{\alpha}{L^2} t = -\ln\left(\frac{0.045}{C_1 \cos \zeta_1}\right) = 3.08$$

$$\therefore \int \frac{dQ}{T} = -8 * 900 * \frac{\tan 0.2217}{0.2217} \left[3.08 - \ln\left(\frac{900e^{3.08} - 600 * 1.0082 * \cos 0.2217}{900 - 600 * 1.0082 * \cos 0.2217}\right) \right]$$

$$\Rightarrow \int \frac{dQ}{T} = 7576.53 \frac{J}{K}$$

$$S_{\text{gen}} = \Delta S - \int \frac{dQ}{T} = 7690.70 - 7576.53 = 114.16 \text{ J/K.}$$

Excel Spreadsheets

ENTROPY CHANGE (dS)												
dS=mCln(T2/T1)												
		B1				B2				Experimental		
Mass(Kg)	C(J/Kg.K)	T2(K)	T1(K)	dS(J/K)	t(min)	T2(K)	T1(K)	dS(J/K)	Tim-Seg	T2(K)	T1(K)	dS(J/K)
8	900	597	492	1396	0	546	492	745	0-1.7	502	492	147
8	900	675	597	885	1.7	591	546	570	1.7-3.4	574	502	965
8	900	733	675	593	3.4	630	591	464	3.4-5.1	649	574	884
8	900	776	733	410	5.1	673	630	479	5.1-6.8	716	649	707
8	900	808	776	290	6.8	716	673	441	6.8-8.5	764	716	467
8	900	832	808	208	8.5	749	716	323	8.5-10.2	813	764	448
8	900	849	832	150	10.2	783	749	326	10.2-11.9	846	813	286
8	900	863	849	110	11.9	810	783	238	11.9-13.6	861	846	127
8	900	872	863	80	13.6	830	810	179	13.6-15.3	877	861	133
8	900	879	872	59	15.3	847	830	145	15.3-17			
8	900					859	847	106	17-18.7			
8	900					870	859	87	18.7-20.4			
8	900					878	870	64	20.4-22.1			

ζ & C constants that depend on Biot number				For Bi=0.	ζ	C
L(m)	ρ(Kg/m3)	k(W/mK)	α		0.2217	1.0082
0.024	2700	78.69	3.2E-05	Sinζ	Cosζ	0.98
				0.22	Tanζ	0.2254

Excel formulae

$$dS(J/K) = A6 * B6 * LN(C6/D6)$$

$$A = -B\$25 * C\$25 * I\$23 / I\$21$$

$$B = -LN(D25 - F25) + LN(D25 - E25) + LN(J\$21 * I\$22)$$

$$C = LN(D25 * EXP(H25) - (D25 - E25) * (I\$22 * J\$21)) - LN(D25 - (D25 - E25) * I\$22 * J\$21)$$

$$\text{Int}(dQ/T) = G25 * (H25 - I25)$$

$$S_{\text{gen}}(J/K) = E6 - J25$$

$$Q(KJ) = B\$25 * C\$25 * (D25 - E25) * (1 - (I\$23 / I\$21) * (D25 - F25) / (D25 - E25)) / 1000$$

Temperature:

e^t		B2					B1				Experimental		
T	t(min)	T∞(K)	T1(K)	T2(K)	t(min)	T∞(K)	T1(K)	T2(K)	dT	T∞(K)	T1(K)	T2(K)	
0.75	1.7	700	492	546	0	900	492	597	208	700	492	492	
0.75	1.7	720	546	591	1.7	900	597	675	174	720	492	550.83	
0.75	1.7	743	591	630	3.4	900	675	733	152	743	492	556.77	
0.75	1.7	798	630	673	5.1	900	733	776	168	798	492	570.96	
0.75	1.7	838	673	716	6.8	900	776	808	165	838	492	581.28	
0.75	1.7	843	716	749	8.5	900	808	832	127	843	492	582.57	
0.75	1.7	883	749	783	10.2	900	832	849	134	883	492	592.9	
0.75	1.7	886	783	810	11.9	900	849	863	102	886	492	593.54	
0.75	1.7	889	810	830	13.6	900	863	872	79	889	492	594.31	
0.75	1.7	896	830	847	15.3	900	872	879	65	896	492	596.12	
0.75	1.7	896	847	859	17	900	879		49	896	492	596.12	
0.75	1.7	900	859	870	18.7				41				
0.75	1.7	900	870	878	20.4				30				
			878		22								

$$e^{-t} = \text{EXP}(-L\$21 * B68 * 60)$$

$$T2(K) = C68 + (D68 - C68) * J\$21 * I\$22 * A68$$

Entropy Generation:

B1

		const Ts		0.22		Tanζ		0.2254			
Mass(Kg)	C(J/Kg.K)	T∞(K)	T1(K)	T2(K)	A	B	C	Int (dQ/T)	Sgen(J/K)	t(min)	Q(KJ)
8	900	900	492	597	-7320	0.28	0.46	1320.15	76.01	0	722
		900	597	675	-7320	0.28	0.40	838.87	46.08	1.7	535
		900	675	733	-7320	0.28	0.36	562.67	30.09	3.4	397
		900	733	776	-7320	0.28	0.34	389.78	20.50	5.1	295
		900	776	808	-7320	0.28	0.32	275.64	14.34	6.8	219
		900	808	832	-7320	0.28	0.31	197.64	10.20	8.5	162
		900	832	849	-7320	0.28	0.30	143.08	7.35	10.2	120
		900	849	863	-7320	0.28	0.30	104.28	5.33	11.9	89
		900	863	872	-7320	0.28	0.29	76.37	3.90	13.6	66
		900	872	879	-7320	0.28	0.29	56.12	2.86	15.3	49

B2

		Var Ts									
Mass(Kg)	C(J/Kg.K)	T∞(K)	T1(K)	T2(K)	A	B	C	Int (dQ/T)	Sgen(J/K)		Q(KJ)
8	900	700	492	546	-7320	0.28	0.38	707.15	38.35		368
		720	546	591	-7320	0.28	0.36	541.45	28.90		308
		743	591	630	-7320	0.28	0.34	440.64	23.29		269
		798	630	673	-7320	0.28	0.34	455.16	24.09		297
		838	673	716	-7320	0.28	0.34	418.55	22.07		291
		843	716	749	-7320	0.28	0.32	306.75	16.00		225
		883	749	783	-7320	0.28	0.32	309.79	16.17		238
		886	783	810	-7320	0.28	0.31	226.66	11.73		181
		889	810	830	-7320	0.28	0.31	169.88	8.75		139
		896	830	847	-7320	0.28	0.30	138.02	7.08		116
		896	847	859	-7320	0.28	0.30	100.65	5.15		86
		900	859	870	-7320	0.28	0.29	82.89	4.23		72
		900	870	878	-7320	0.28	0.29	60.87	3.10		53

		Experimental									
Mass(Kg)	C(J/Kg.K)	T∞(K)	T1(K)	T2(K)	A	B	C	Int (dQ/T)	Sgen(J/K)		Q(KJ)
8	900	700	492	502	-7320	0.03	0.05	98.81	48.41	0.03291	49
		720	502	574	-7320	0.38	0.51	928.95	36.06	0.31908	501
		743	574	649	-7320	0.57	0.69	863.54	20.65	0.43449	529
		798	649	716	-7320	0.58	0.68	691.57	15.82	0.44047	473
		838	716	764	-7320	0.48	0.55	454.48	12.71	0.38331	337
		843	764	813	-7320	0.95	1.01	442.60	4.98	0.61391	349
		883	813	846	-7320	0.62	0.66	280.89	5.59	0.46259	233
		886	846	861	-7320	0.46	0.48	123.03	3.51	0.36938	105
		889	861	877	-7320	0.86	0.87	130.93	1.64	0.57483	114

VITA

Jayasankar Sankara was born in Kakinada, India in 1982. He graduated from Masters Junior College and attended Osmania University. He completed his Bachelors in Mechanical Engineering from Osmania University in 2003, before coming to the United States for attending the graduate program in Mechanical Engineering at the University of Kentucky. As a graduate student, he served as a Research Assistant under Dr. Dusan P. Sekulic in the Metal Joining Laboratory, UK Center for manufacturing. He also presented his research at various conferences both at the national and international level.

Publication and Presentations that resulted from this work (during Masters):

- J. Sankara, F. Bryan and D.P. Sekulic “*Exergy approach for sustainability analysis of a net shape manufacturing processes*” Second Annual Kentucky Innovation and Enterprise Conference March 3, 2004, Louisville, Kentucky –*poster presentation*.
- J. Sankara, D.P. Sekulic “*Irreversibility approach for sustainability analysis of a continuous net shape manufacturing system*”, *AES*, v 44, Proceedings of the ASME Advanced Energy Systems Division, 2004, p 255-261.
- D.P. Sekulic, and J. Sankara, “*Advanced thermodynamics metrics for sustainability assessments of open engineering systems*”, *Thermal Science Journal*-- *to be published*.

Work Experience:

- **Lexmark International, Inc.** Packaging Engineering Lexington, KY
Design Specialist May’05-Present
- **Systems labs**, University of Kentucky Lexington, KY
Engineering workstation/Computer science Lab Consultant Jan’05-May’05
- **Center for Manufacturing**, University of Kentucky Lexington, KY
Research Assistant Jan’04-Jan’05

Other Technical Presentations (during Bachelors):

- J. Sankara, “*Tool Condition Monitoring using Multi-sensor fusion techniques*”; 39th Annual Technical Meeting of Society of Engineering Science (SES2002) October 13-16 2002, Penn State University.
- J. Sankara, K. Kishore “*Performance Evaluation of a Goose necked cutting tool*”; Shaastra 2002, IIT Madras, India.
- J. Sankara, “*Performance Evaluation of a Modified Single point cutting tool*” at a National level technical symposium-Mechmantra 2002, RVR&JC, India.
- J. Sankara, “*IDEAS as a virtual simulator*”, EDS PLM Users conference-2002, Bangalore, India.

Honors and Distinctions:

- Awarded *Kentucky Graduate Scholarship* by University of Kentucky 2003-2005
- Awarded *Travel scholarship award* to present at the ASME International Mechanical Engineering Congress (IMECE-2004) by the University of Kentucky.
- Awarded *Student travel assistance* to present at the 39th Annual Technical Meeting of Society of Engineering Science (SES-2002), Penn State University, USA.
- Awarded *Second prize* for Design Contest-Propositum, Mechanica’02, CBIT, India.
- Awarded *Second prize* for paper titled “*Performance Evaluation of a Modified Single point cutting tool*” at a National level technical symposium-Mechmantra’02, RVR&JC, India.
- Awarded prize for paper titled “*Performance Evaluation of a Goose necked cutting tool*” at a National level technical symposium, Shaastra’02, IIT Madras, India.
- Awarded prize for paper titled “*Eco-friendly Refrigerants*” at a National level technical symposium, Erudition 2003, Naval College of Engineering, INS SHIVAJI, Lonavla.